

**FINAL REPORT ~ FHWA-OK-15-09**

# **INTERPRETATION OF IN SITU TESTS AS AFFECTED BY SOIL SUCTION**

**Gerald A. Miller, Ph.D., P.E.  
Rodney W. Collins, Ph.D. Student  
Kanthasamy K. Muraleetharan, Ph.D., P.E., G.E., F. ASCE  
Amy B. Cerato, Ph.D., P.E.  
Roy Doumet, M.Sc.  
School of Civil Engineering and Environmental Science  
Gallogly College of Engineering  
The University of Oklahoma  
Norman, Oklahoma**

**December 2015**



The contents of this report reflect the views of the author(s) who is responsible for the facts and the accuracy of the data presented herein. The contents do not necessarily reflect the views of the Oklahoma Department of Transportation or the Federal Highway Administration. This report does not constitute a standard, specification, or regulation. While trade names may be used in this report, it is not intended as an endorsement of any machine, contractor, process, or product.

# INTERPRETATION OF IN SITU TESTS AS AFFECTED BY SOIL SUCTION

**FINAL REPORT ~ FHWA-OK-15-09**  
ODOT SP&R ITEM NUMBER 2160

**Submitted to:**

John R. Bowman, P.E.  
Director of Capital Programs  
Oklahoma Department of Transportation

**Submitted by:**

Gerald A. Miller, Ph.D., P.E.  
Rodney w. Collins, Ph.D. Student  
Kanthasamy K. Muraleetharan, Ph.D., P.E., G.E., F. ASCE  
Amy B. Cerato, Ph.D., P.E.  
Roy Doumet, M.S. Student (Graduated)

School of Civil Engineering and Environmental Science (CEES)  
The University of Oklahoma



December 2015

## TECHNICAL REPORT DOCUMENTATION PAGE

1. REPORT NO. <b>FHWA-OK-15-09</b>	2. GOVERNMENT ACCESSION NO.	3. RECIPIENTS CATALOG NO.	
4. TITLE AND SUBTITLE <b>Interpretation of In Situ Tests as Affected by Soil Suction</b>		5. REPORT DATE <b>December 2015</b>	
		6. PERFORMING ORGANIZATION CODE	
7. AUTHOR(S) <b>Gerald A. Miller, Rodney W. Collins, Kanthasamy K. Muraleetharan, Amy B. Cerato, Roy Doumet</b>		8. PERFORMING ORGANIZATION REPORT	
9. PERFORMING ORGANIZATION NAME AND ADDRESS <b>University of Oklahoma, School of Civil Engineering and Environmental Science, 202 West Boyd Street, Room 334 Norman, OK 73019</b>		10. WORK UNIT NO.	
		11. CONTRACT OR GRANT NO. <b>ODOT SP&amp;R Item Number 2160</b>	
12. SPONSORING AGENCY NAME AND ADDRESS <b>Oklahoma Department of Transportation, Materials and Research Division, 200 N.E. 21st Street, Room 3A7 Oklahoma City, OK 73105</b>		13. TYPE OF REPORT AND PERIOD COVERED <b>Final Report Oct. 2011-Dec. 2015</b>	
		14. SPONSORING AGENCY CODE	
15. SUPPLEMENTARY NOTES			
16. ABSTRACT In situ testing of soil with invasive methods such as the Cone Penetration Test (CPT) are increasingly used in geotechnical engineering practice. However, there has been very little work to develop methods for interpreting results of these tests when performed in unsaturated soil. It is important to develop such methods because the in situ test results in unsaturated soil will depend on the moisture conditions at the time of testing and may not reflect the soil behavior corresponding to the moisture conditions during the life of supported structures. Research described in this report involved conducting in situ tests at two test sites, containing lean to fat clayey soils, at various times of the year. The purpose was to investigate the influence of changes in moisture conditions and soil suction on the test response. In situ testing included the Cone Penetration Test (CPT), Standard Penetration Test (SPT) and Pre-bored Pressuremeter Test (PMT). Test sites were characterized by sampling and laboratory testing to determine important soil properties and moisture content profiles. Additionally, test sites were instrumented with weather monitoring equipment and sensors to measure temporal variations in soil moisture with depth. Another goal was to evaluate two commercially available computer programs to evaluate their predictive ability with respect to soil moisture change. The PMT, CPT and SPT parameters determined from standard interpretation of the results were compared to total suction measured at corresponding depths obtained from measurements on samples obtained in the field using a chilled mirror hygrometer. At both sites, the suction had a profound impact on the in situ test parameters, especially at total suction in excess of approximately 150 psi, which generally corresponded to shallow test depths. At both sites, for the shallow depths there was a noticeable trend of increasing magnitude of in situ test parameters with increasing suction, as expected. Plots of normalized in situ test parameters against suction show expected, albeit weak, correlations for the two test sites. These correlations give a sense of the variation of in situ parameters that might be expected for similar soils under changing suction conditions. It was demonstrated how correlations for PMT, CPT and SPT parameters with suction can be used to roughly predict possible changes in these parameters as a result of suction changes. Unsaturated seepage modeling was found to provide reasonable comparisons to measured soil moisture profiles; however, significant effort was required to define the various input parameters through calibration procedures.			
17. KEY WORDS <b>in situ testing, pressuremeter, cone penetrometer, suction, unsaturated seepage, weather, climate</b>		18. DISTRIBUTION STATEMENT <b>No restrictions. This publication is available from the Materials and Research Div., Oklahoma DOT.</b>	
19. SECURITY CLASSIF. (OF THIS REPORT) <b>Unclassified</b>	20. SECURITY CLASSIF. (OF THIS PAGE) <b>Unclassified</b>	21. NO. OF PAGES <b>182</b>	22. PRICE <b>N/A</b>

## SI\* (MODERN METRIC) CONVERSION FACTORS

APPROXIMATE CONVERSIONS TO SI UNITS				
SYMBOL	WHEN YOU KNOW	MULTIPLY BY	TO FIND	SYMBOL
<b>LENGTH</b>				
<b>in</b>	inches	25.4	millimeters	mm
<b>ft</b>	feet	0.305	meters	m
<b>yd</b>	yards	0.914	meters	m
<b>mi</b>	miles	1.61	kilometers	km
<b>AREA</b>				
<b>in<sup>2</sup></b>	square inches	645.2	square millimeters	mm <sup>2</sup>
<b>ft<sup>2</sup></b>	square feet	0.093	square meters	m <sup>2</sup>
<b>yd<sup>2</sup></b>	square yard	0.836	square meters	m <sup>2</sup>
<b>ac</b>	acres	0.405	hectares	ha
<b>mi<sup>2</sup></b>	square miles	2.59	square kilometers	km <sup>2</sup>
<b>VOLUME</b>				
<b>fl oz</b>	fluid ounces	29.57	milliliters	mL
<b>gal</b>	gallons	3.785	liters	L
<b>ft<sup>3</sup></b>	cubic feet	0.028	cubic meters	m <sup>3</sup>
<b>yd<sup>3</sup></b>	cubic yards	0.765	cubic meters	m <sup>3</sup>
NOTE: volumes greater than 1000 L shall be shown in m <sup>3</sup>				
<b>MASS</b>				
<b>oz</b>	ounces	28.35	grams	g
<b>lb</b>	pounds	0.454	kilograms	kg
<b>T</b>	short tons (2000 lb)	0.907	megagrams (or "metric ton")	Mg (or "t")
<b>TEMPERATURE (exact degrees)</b>				
<b>°F</b>	Fahrenheit	5 (F-32)/9 or (F-32)/1.8	Celsius	°C
<b>ILLUMINATION</b>				
<b>fc</b>	foot-candles	10.76	lux	lx
<b>fl</b>	foot-Lamberts	3.426	candela/m <sup>2</sup>	cd/m <sup>2</sup>
<b>FORCE and PRESSURE or STRESS</b>				
<b>lbf</b>	poundforce	4.45	newtons	N
<b>lbf/in<sup>2</sup></b>	poundforce per square inch	6.89	kilopascals	kPa

APPROXIMATE CONVERSIONS FROM SI UNITS				
SYMBOL	WHEN YOU KNOW	MULTIPLY BY	TO FIND	SYMBOL
<b>LENGTH</b>				
mm	millimeters	0.039	inches	in
m	meters	3.28	feet	ft
m	meters	1.09	yards	yd
km	kilometers	0.621	miles	mi
<b>AREA</b>				
mm <sup>2</sup>	square millimeters	0.0016	square inches	in <sup>2</sup>
m <sup>2</sup>	square meters	10.764	square feet	ft <sup>2</sup>
m <sup>2</sup>	square meters	1.195	square yards	yd <sup>2</sup>
ha	hectares	2.47	acres	ac
km <sup>2</sup>	square kilometers	0.386	square miles	mi <sup>2</sup>
<b>VOLUME</b>				
mL	milliliters	0.034	fluid ounces	fl oz
L	liters	0.264	gallons	gal
m <sup>3</sup>	cubic meters	35.314	cubic feet	ft <sup>3</sup>
m <sup>3</sup>	cubic meters	1.307	cubic yards	yd <sup>3</sup>
<b>MASS</b>				
g	grams	0.035	ounces	oz
kg	kilograms	2.202	pounds	lb
Mg (or "t")	megagrams (or "metric ton")	1.103	short tons (2000 lb)	T
<b>TEMPERATURE (exact degrees)</b>				
°C	Celsius	1.8C+32	Fahrenheit	°F
<b>ILLUMINATION</b>				
lx	lux	0.0929	foot-candles	fc
cd/m <sup>2</sup>	candela/m <sup>2</sup>	0.2919	foot-Lamberts	fl
<b>FORCE and PRESSURE or STRESS</b>				
N	newtons	0.225	poundforce	lbf
kPa	kilopascals	0.145	poundforce per square inch	lbf/in <sup>2</sup>

\*SI is the symbol for the International System of Units. Appropriate rounding should be made to comply with Section 4 of ASTM E380.

## Table of Contents

Disclaimer.....	i
Title Page.....	ii
Technical Report Documentation Page.....	iii
SI* (Modern Metric) Conversion Factors.....	iv
Table of Contents.....	vi
List of Tables.....	ix
List of Figures.....	ix
Summary.....	xiv
Chapter 1 INTRODUCTION.....	1
1.1 Problem Statement.....	1
1.2 Overview of Research.....	2
1.3 Research Objectives and Tasks.....	4
1.4 Organization of Report.....	5
Chapter 2 LITERATURE REVIEW.....	7
2.1 Introduction.....	7
2.2 In Situ Tests.....	7
2.2.1 Pressuremeter Test (PMT).....	7
2.2.2 Cone Penetration Test (CPT).....	10
2.2.3 Standard Penetration Test (SPT).....	11
2.3 In Situ Testing in Unsaturated Soil.....	11
2.4 Modeling Moisture Variation in Unsaturated Soil Profiles.....	15
Chapter 3 FIELD, LABORATORY AND ANALYSIS METHODS.....	24
3.1 Test Sites.....	24
3.2 Test Site Field Instrumentation for Monitoring Weather and Soil Moisture.....	25
3.3 Soil Sampling.....	25
3.4 Laboratory Testing Methods.....	26
3.4.1 Basic Soil Properties.....	26
3.4.2 Soil Water Characteristic Curve (SWCC) Testing.....	27
3.4.3 Shear Strength.....	27
3.4.4 Hydraulic Conductivity.....	28

3.5 In Situ Testing Methods.....	28
3.5.1 Pressuremeter Testing (PMT) .....	29
3.5.2 Cone Penetration Testing (CPT) .....	30
3.5.3 Standard Penetration Testing (SPT) .....	30
3.6 Modeling Soil Moisture Changes in Response to Weather .....	31
Chapter 4 RESULTS OF LABORATORY TESTING .....	40
4.1 Basic Soil Properties .....	40
4.2 SWCC Test Results .....	42
4.3 Saturated Hydraulic Conductivity Results and Unsaturated Functions.....	43
4.4 CIUC Triaxial Test Results .....	43
Chapter 5 RESULTS FROM FIELD WEATHER INSTRUMENTATION AND SOIL MOISTURE MONITORING .....	51
5.1 Weather Data from the North Base Site .....	51
5.2 Weather Data from the Goldsby Site.....	53
Chapter 6 MODELING MOISTURE VARIATIONS IN SOIL PROFILES.....	67
6.1 Introduction .....	67
6.2 Moisture Modeling, Goldsby.....	67
6.3 Material Properties and Property Functions, Goldsby .....	69
6.4 Top and Bottom Soil Boundary Conditions and FEM Mesh Control for Goldsby and North Base .....	71
6.5 Ground-Atmosphere Interaction Predictions, Goldsby, VADOSE/W .....	72
6.6 VADOSE/W Predictions using Modified Ksat, Goldsby .....	74
6.7 Ground-Atmosphere Interaction Predictions, Goldsby, SVFlux.....	76
6.8 Sensitivity Analyses.....	77
6.9 Moisture Modeling, North Base .....	78
6.10 Ground-Atmosphere Interaction Predictions, North Base, VADOSE/W .....	79
6.11 VADOSE/W Predictions using Modified Ksat, North Base .....	80
6.12 Results of Model Predictions, North Base, SVFlux.....	81
Chapter 7 IN SITU TESTING RESULTS AND INTERPRETATION .....	104
7.1 Introduction .....	104
7.2 Pressuremeter Test (PMT) Results .....	104
7.2.1 Influence of soil suction on PMT Results.....	105
7.2.1.1 North Base PMT Results .....	106

7.2.1.2 Goldsby PMT Results.....	110
7.3 Cone Penetration Test (CPT) Results .....	112
7.3.1 Influence of soil suction on CPT Results .....	112
7.3.1.1 North Base CPT Results .....	112
7.3.1.2 Goldsby CPT Results .....	114
7.4 Standard Penetration Test (SPT) Results .....	116
7.4.1 Influence of soil suction on SPT Results .....	116
7.5 A Methodology to Interpret In Situ Test Results in Unsaturated Soil .....	117
7.5.1 Introduction .....	117
7.5.2 Estimating the Influence of Suction on PMT Limit Pressure and Moduli .....	118
7.5.3 Estimating the Influence of Suction on CPT Tip Resistance .....	120
7.5.4 Estimating the Influence of Suction on SPT N-Values.....	121
Chapter 8 CONCLUSIONS AND RECOMMENDATIONS.....	152
8.1 Summary.....	152
8.2 Conclusions Regarding Influence of Suction on In Situ Test Results.....	153
8.3 Conclusions Regarding Numerical Modeling of Soil Moisture Variations .....	155
8.4 Recommendations.....	158
ACKNOWLEDGEMENTS .....	162
REFERENCES.....	162

## LIST OF TABLES

Table 3. 1. Summary of multistage triaxial compression test conditions for thin-walled tube samples for Goldsby and North Base sites. ....	34
Table 3. 2. Summary of Pressuremeter Tests from Goldsby and North Base sites. ....	35
Table 3. 3. Summary of Cone Penetration Tests from Goldsby and North Base sites. .	36
Table 3. 4. Summary of methods to define input parameters.....	36
Table 3. 5. Differences and similarities between computational method used in SVFlux and VADOSE/W.....	37
Table 4. 1. Specific gravity of North Base and Goldsby soil.....	45
Table 4. 2. Cation Exchange Capacity Results North Base and Goldsby. ....	45
Table 4. 3. Goldsby: saturated, flexible wall hydraulic conductivity test results.....	45
Table 4. 4. North Base: saturated, flexible wall hydraulic conductivity test results. ....	46
Table 4. 5. Summary of triaxial results for North Base and Goldsby.....	46
Table 5. 1. Total monthly rainfall during the monitoring period recorded at the North Base test site.....	55
Table 6. 1. Units and phase change related values. ....	82
Table 6. 2. Key in analysis input parameters.....	82
Table 6. 3. Advanced options for ponding and vegetation.....	82
Table 6. 4. Goldsby material input parameters.....	83
Table 6. 5. Climate and vegetation boundary conditions.....	84
Table 6. 6. Mesh properties.....	84
Table 6. 7. North Base material input parameters.....	85
Table 7. 1. North Base: summary of PMT Data for 3 ft depth.....	123
Table 7. 2. North Base: summary of PMT data for 5 ft depth. ....	123
Table 7. 3. North Base: summary of PMT data for 7 ft depth. ....	124
Table 7. 4. Goldsby: summary of PMT Data for 3 ft depth. ....	124
Table 7. 5. Goldsby: summary of PMT Data for 6 ft depth. ....	125
Table 7. 6. Goldsby: summary of PMT Data for 9 ft depth. ....	125

## LIST OF FIGURES

Figure 2. 1: Pressuremeter curve showing different test phases.....	22
Figure 2. 2. Pressuremeter limit pressure ( $P_L$ ), reload modulus ( $E_r$ ) and pressuremeter modulus ( $E_p$ ) versus matric suction ( $u_a-u_w$ ) from field tests in Minco Silt (from Miller and Muraleetharan, 2000). ....	22

Figure 2. 3. a) Limit pressure (PL) versus matric suction ( $u_a-u_w$ ) from PMTs in Minco Silt in a calibration chamber, b) average dry unit weight ( $\rho_d$ ) of the soil bed versus matric suction (after Tan and Miller 2005).....	23
Figure 2. 4. Tip resistance ( $q_c$ ) versus matric suction ( $u_a-u_w$ ) from cone penetration tests in Minco Silt in a calibration chamber (from Tan et al. 2003).....	23
Figure 3. 1. Test sites used for this study with North Base indicated with B and Goldsby with A (image from Google).....	38
Figure 3. 2. Weather station installed at North Base test site. ODOT cone truck in background. ....	38
Figure 3. 3. Type of sensors and their corresponding range of measurements. ....	39
Figure 4. 1. Goldsby: soil profile, Atterberg limits, and percent fines.....	47
Figure 4. 2. North Base: soil profile, Atterberg limits and percent of fines.....	48
Figure 4. 3. Goldsby: measured and fitted SWCCs.....	49
Figure 4. 4. North Base: measured and fitted SWCCs.....	49
Figure 4. 5. Goldsby: hydraulic conductivity-suction curves. ....	50
Figure 4. 6. North Base: hydraulic conductivity-suction curves. ....	50
Figure 5. 1. North Base: maximum and minimum daily temperature, total rainfall, and volumetric water content at the test site. ....	56
Figure 5. 2. North Base: daily average temperature, total solar radiation, and subsurface soil temperature at the test site. ....	57
Figure 5. 3. North Base: daily maximum relative humidity and average wind speed at the test site.....	58
Figure 5. 4. North Base: total daily solar radiation data from the test site and nearest Mesonet station.....	58
Figure 5. 5. North Base: total daily precipitation and air temperature from the test site and nearest Mesonet station. ....	59
Figure 5. 6. North Base: average daily relative humidity and wind speed from the test site and nearest Mesonet station. ....	60
Figure 5. 7. Goldsby: daily maximum and minimum temperature, total rainfall, and volumetric water content at the test site. ....	61
Figure 5. 8. Goldsby: daily average temperature, total solar radiation, and subsurface soil temperature at the test site. ....	62
Figure 5. 9. Goldsby: daily maximum relative humidity and average wind speed at the test site.....	63
Figure 5. 10. Goldsby: average daily relative humidity and wind speed from the test site and nearest Mesonet station. ....	64

Figure 5. 11. Goldsby: total daily solar radiation data from the test site and nearest Mesonet station.....	65
Figure 5. 12. Goldsby: total daily precipitation and air temperature from the test site and nearest Mesonet station.....	66
Figure 6. 1. Initial soil profile volumetric water contents.....	86
Figure 6. 2. Initial soil profiles pressure head.....	86
Figure 6. 3. Goldsby: VADOSE/W soil column.....	87
Figure 6. 4 Goldsby: estimated thermal conductivity curves.....	87
Figure 6. 5. Goldsby: estimated volumetric heat capacity functions.....	88
Figure 6. 6. Estimated LAI function for both sites.....	88
Figure 6. 7. Typical plant moisture limiting function for most types of grasses.....	89
Figure 6. 8. Estimated root depth function.....	89
Figure 6. 9. Goldsby: predicted vs. measured VWC values at 1 ft depth.....	90
Figure 6. 10. Goldsby: predicted vs. measured VWC values at 3 ft depth.....	90
Figure 6. 11. Goldsby: predicted vs. measured VWC values at 6 ft depth.....	91
Figure 6. 12. Goldsby: measured vs. predicted VWC values using the modified $K_{sat}$ value for 1 ft depth.....	91
Figure 6. 13. Goldsby: measured vs. predicted VWC values using the modified $K_{sat}$ value for 3 ft depth.....	92
Figure 6. 14. Goldsby: measured vs. predicted VWC values using the modified $K_{sat}$ value for 6 ft, depth.....	92
Figure 6. 15. Goldsby: SVFlux soil column.....	93
Figure 6. 16. Goldsby: predicted vs. measured VWC values using SVFlux and VADOSE/W for 1ft depth.....	93
Figure 6. 17. Goldsby: predicted vs. measured VWC values using SVFlux and VADOSE/W for 3ft depth.....	94
Figure 6. 18. Goldsby: predicted vs. measured VWC values using SVFlux and VADOSE/W for 6 ft depth.....	94
Figure 6. 19. Goldsby: sensitivity analysis.....	95
Figure 6. 20. North Base: VADOSE/W soil column.....	96
Figure 6. 21. North Base: estimated thermal conductivity function curves.....	96
Figure 6. 22. North Base: estimated volumetric heat capacity curves.....	97
Figure 6. 23. North Base: predicted vs. measured VWC values at 1 ft depth.....	98
Figure 6. 24. North Base: predicted vs. measured VWC values at 3 ft depth.....	98
Figure 6. 25. North Base: predicted vs. measured VWC values at 6 ft depth.....	99

Figure 6. 26. North Base: measured vs. predicted VWC values using a modified $K_{sat}$ for 1 ft depth. ....	99
Figure 6. 27. North Base: measured vs. predicted VWC values using a modified $K_{sat}$ for 3 ft depth. ....	100
Figure 6. 28. North Base: measured and predicted VWC values using a modified $K_{sat}$ for 6 ft depth. ....	100
Figure 6. 29. North Base: sensitivity analysis. ....	101
Figure 6. 30. North Base: SVFlux soil column. ....	102
Figure 6. 31. North Base: predicted vs. measured VWC values using SVFlux and VADOSE/W for 1 ft depth. ....	102
Figure 6. 32. North Base: predicted vs. measured VWC values using SVFlux and VADOSE/W for 3 ft depth. ....	103
Figure 6. 33. North Base: predicted vs. measured VWC values using SVFlux and VADOSE/W for 6 ft depth. ....	103
Figure 7. 1. North Base: PMT location map. ....	126
Figure 7. 2. Goldsby: PMT location map. ....	126
Figure 7. 3. North Base: PMT stress-strain curves for 3 ft depth. ....	127
Figure 7. 4. North Base: limit pressure versus suction for 3 ft depth. ....	127
Figure 7. 5. North Base: PMT modulus versus suction for 3 ft depth. ....	128
Figure 7. 6. North Base: unload-reload modulus versus suction for 3 ft depth. ....	128
Figure 7. 7. North Base: PMT stress-strain curves for 5 ft depth. ....	129
Figure 7. 8. North Base: limit pressure versus suction for 5 ft depth. ....	129
Figure 7. 9. North Base PMT modulus versus suction for 5 ft depth. ....	130
Figure 7. 10. North Base: unload-reload modulus versus suction for 5 ft depth. ....	130
Figure 7. 11. North Base: PMT stress-strain curves for 7 ft depth. ....	131
Figure 7. 12. North Base: limit pressure versus suction for 7 ft depth. ....	131
Figure 7. 13. North Base: PMT modulus versus suction for 7 ft depth. ....	132
Figure 7. 14. North Base: unload-reload modulus versus suction for 7 ft depth. ....	132
Figure 7. 15. Goldsby: PMT stress-strain curves for 3 ft depth. ....	133
Figure 7. 16. Goldsby: limit pressure versus suction for 3 ft depth. ....	133
Figure 7. 17. Goldsby: PMT modulus versus suction for 3 ft depth. ....	134
Figure 7. 18. Goldsby: unload-reload modulus versus suction for 3 ft depth. ....	134
Figure 7. 19. Goldsby: PMT stress-strain curves for 6 ft depth. ....	135
Figure 7. 20. Goldsby: limit pressure versus suction for 6 ft depth. ....	135

Figure 7. 21. Goldsby: PMT modulus versus suction for 6 ft depth. ....	136
Figure 7. 22. Goldsby: unload-reload modulus versus suction for 6 ft depth. ....	136
Figure 7. 23. Goldsby: PMT stress-strain curves for 9 ft depth. ....	137
Figure 7. 24. Goldsby: limit pressure versus suction for 9 ft depth. ....	137
Figure 7. 25. Goldsby: PMT modulus versus suction for 9 ft depth. ....	138
Figure 7. 26. Goldsby: unload-reload modulus versus suction for 9 ft depth. ....	138
Figure 7. 27. North Base: CPT location map. ....	139
Figure 7. 28. Goldsby: CPT location map. ....	139
Figure 7. 29. North Base: tip resistance and suction versus depth. ....	140
Figure 7. 30. North Base: sleeve friction and suction versus depth. ....	140
Figure 7. 31. North Base: CPT parameters during test period at 1 ft and 3 ft depths. .	141
Figure 7. 32. North Base: CPT parameters versus suction at 1 ft and 3 ft depths. ....	141
Figure 7. 33. Goldsby: tip resistance and suction versus depth. ....	142
Figure 7. 34. Goldsby: skin friction and suction versus depth. ....	142
Figure 7. 35. Goldsby: CPT parameters during test period for 1 ft and 3 ft depths. ....	143
Figure 7. 36. Goldsby: CPT parameters versus suction for 1 ft and 3 ft depths. ....	143
Figure 7. 37. North Base: SPT location map. ....	144
Figure 7. 38. Goldsby: SPT location map. ....	144
Figure 7. 39. North Base: SPT N-value and suction versus depth. ....	145
Figure 7. 40. Goldsby: SPT N-value and suction versus depth. ....	146
Figure 7. 41. North Base: Normalized PMT limit pressure and moduli versus suction. ....	147
Figure 7. 42. Goldsby: Normalized PMT limit pressure and moduli versus suction. ....	148
Figure 7. 43. Normalized limit pressure versus suction for North Base and Goldsby test sites and data from Tan (2005). ....	149
Figure 7. 44. Normalized PMT modulus versus suction for North Base and Goldsby test sites and data from Tan (2005). ....	149
Figure 7. 45. Normalized unload-reload modulus versus suction for North Base and Goldsby test sites and data from Tan (2005). ....	150
Figure 7. 46. Normalized cone tip resistance versus suction for North Base and Goldsby test sites. ....	150
Figure 7. 47. Normalized cone tip resistance versus suction for North Base and Goldsby test sites and data from the literature (Lehane et al. 2004, Tan 2005, Yang and Russell 2015). ....	151
Figure 7. 48. Normalized SPT versus suction. ....	151

## **SUMMARY**

In situ testing of soil with invasive methods such as the Cone Penetration Test (CPT) are increasingly used in geotechnical engineering practice. However, there has been very little work to develop methods for interpreting results of these tests when performed in unsaturated soil. In addition, while reliance on the Standard Penetration Test (SPT) remains at the forefront of geotechnical practice, very little research has been done on the influence of partial saturation on the SPT blow counts or “N-values” used in design. It is important to develop such methods because the in situ test results in unsaturated soil will depend on the moisture conditions at the time of testing. If these conditions change, as they frequently do in near surface soils, the interpreted soil properties may not reflect the soil behavior corresponding to the moisture conditions existing during construction or over the life of supported structures. Research described in this report involved conducting in situ tests at two test sites, containing lean to fat clayey soils, at various times of the year. The purpose was to investigate the influence of changes in moisture conditions and soil suction on the test response.

In situ testing included the Cone Penetration Test (CPT), Standard Penetration Test (SPT) and Pre-bored Pressuremeter Test (PMT). Test sites were characterized by sampling and laboratory testing to determine soil properties and moisture content profiles. Additionally, test sites were instrumented with weather monitoring equipment and sensors to measure temporal variations in soil moisture with depth. Another goal was to evaluate two commercially available computer programs in their predictive ability with respect to soil moisture change. The PMT, CPT and SPT parameters determined from standard interpretation of the results were compared to total suction measured using a chilled mirror hygrometer for samples obtained in the field at corresponding

depths. At both sites, the suction had a profound impact on the in situ test parameters, especially at total suction in excess of approximately 150 psi, which generally corresponded to shallow test depths. At both sites, for the shallow depths there was a noticeable trend of increasing magnitude of in situ test parameters with increasing suction, as expected. Plots of normalized in situ test parameters against suction show expected correlations for the two test sites. These correlations give a sense of the variation of in situ parameters that might be expected for similar soils under changing suction conditions. It was demonstrated how empirical relationships for PMT, CPT and SPT parameters with suction can be used to roughly predict possible changes in these parameters as a result of suction changes. While these correlations should not be used to determine design parameters, they do allow engineers to develop insight regarding the importance of suction changes. Unsaturated seepage modeling was found to provide reasonable comparisons to measured soil moisture profiles; however, significant effort was required to define the various input parameters through calibration procedures.

## **Chapter 1 INTRODUCTION**

### **1.1 Problem Statement**

In situ testing of soil with invasive methods such as the Cone Penetration Test (CPT) and Pre-bored Pressuremeter Test (PMT), for example, are increasingly being used in geotechnical engineering practice in the United States to estimate soil property profiles. In Oklahoma, the Materials and Research Division of the Department of Transportation (ODOT) has led the way in the use of in situ testing, and relies heavily on the CPT and in practice. However, there has been very little work to develop methods for interpreting results of these tests when performed in unsaturated soil. In addition, while reliance on the Standard Penetration Test (SPT) remains at the forefront of geotechnical practice, very little research has been done on the influence of partial saturation on the SPT blow counts or “N-values” used in design.

During a subsurface exploration, a zone of unsaturated soil is often encountered, sometimes extending to considerable depth. This is particularly true when tests are conducted through highway embankments. It is generally understood that the behavior of unsaturated soil is different from the commonly assumed saturated-undrained or drained soil behavior; yet there are no proven methods for interpreting in situ test results that account for these differences. A great deal of research has been devoted to the interpretation of these tests in saturated cohesive and cohesionless soils; however, there are currently no reliable comprehensive methods for interpreting in situ test results from unsaturated soils. It is important to develop such methods because the in situ test results in unsaturated soil will depend on the moisture conditions at the time of testing. If these conditions change, as they frequently do in near surface soils, the interpreted soil

properties may not reflect the soil behavior corresponding to the moisture conditions existing during construction or over the life of supported structures. The research described in this report built upon prior work of the investigators to work towards developing a method for interpreting in situ test results in light of expected changes in soil moisture condition and suction.

## **1.2 Overview of Research**

Research involved conducting in situ tests at two test sites at various times of the year to investigate the influence of changes in moisture conditions and soil suction on the test response. In situ testing included the Cone Penetration Test (CPT), Standard Penetration Test (SPT) and Pre-bored Pressuremeter Test (PMT). The CPT and SPT tests were conducted by the Oklahoma Department of Transportation (ODOT) Materials Division personnel in cooperation with University of Oklahoma (OU) personnel, while the PMT was conducted by OU personnel. One test site located in Goldsby, OK consists primarily of low to moderately plastic fine-grained soil while the other site in Norman, OK consists of moderate to highly plastic fine-grained soils. Test sites were characterized by sampling and laboratory testing to determine soil properties and moisture content profiles.

Additionally, test sites were instrumented with weather monitoring equipment and sensors to measure variations in soil moisture. The purpose was to examine the variations in soil moisture content as a function of time and depth. A primary goal was to evaluate two commercially available computer programs in their ability to predict soil moisture changes due to weather. Understanding how soil moisture changes in

response to weather is critical to predicting the influence of matric suction changes on in situ test results.

Laboratory testing focused on basic soil characterization, evaluating shear strength, hydraulic conductivity and soil water characteristic behavior of the soil. The purpose was to provide the necessary parameters to populate models for predicting climate variations in soil moisture and in situ test response under various moisture conditions.

Modeling was conducted using software to predict variations in soil moisture content as a function of weather. Two commercially available programs were used for soil moisture modeling: Vadose/W and SV-Flux. The analysis and modeling of results had two major components: first to study the temporal changes in moisture content and soil suction resulting from weather changes; and second to study the influence of changes in moisture content and soil suction on in situ test results.

A primary goal of this research was to gain important knowledge about the influence of matric suction on in situ test results. In accomplishing this goal a valuable set of experimental data was established in an area of soil mechanics where information is scarce. Empirical models were used to enhance the interpretation of in situ test results obtained in unsaturated soils. Results of this work are important in that they provide engineers with better understanding of, and approaches to addressing, the influence of moisture conditions and matric suction on results from in situ tests.

### **1.3 Research Objectives and Tasks**

Three primary objectives of the research include: 1) obtaining data that reveals the influence of soil moisture conditions, and suction, on results of CPT, SPT and PMT tests; 2) developing recommendations for conducting and interpreting results of in situ tests in unsaturated soil including predicting how the in situ test results and interpreted soil parameters would change if the suction changes; and 3) to provide geotechnical engineers guidance for predicting changes in soil moisture conditions and suction as a function of climate changes so that a proper “design moisture condition” can be selected for a given site.

In achieving these objectives, the variation of in situ test results can be predicted as a function of expected soil moisture changes due to climate changes and ground water conditions. To achieve the project objectives many tasks were completed as follows.

- 1) An extensive search of the literature was conducted to gather published information relevant to in situ testing in unsaturated soil, and modeling of soil moisture variations in the vadose zone.
- 2) Two test sites were identified with assistance of ODOT personnel. Instrumentation was installed to monitor primary weather parameters and soil moisture content at different depths. Instruments were monitored for about two years while numerous site visits occurred to conduct in situ tests, collect soil samples, make observations, download data and conduct site maintenance.
- 3) In situ testing was conducted at various times of the year over the course of two years and included CPT, SPT and PMT tests.

- 4) Basic soil testing was conducted to determine engineering properties of the soils needed for classification and phase relationship calculations. Testing was also conducted to determine the mechanical and hydraulic properties of the soil.
- 5) Soil Water Characteristic Curve Testing was performed to determine the relationship between suction and water content for samples from different depths at each test site.
- 6) Moisture flow testing via one dimensional diffusion and back-pressure saturated flexible wall hydraulic conductivity testing was carried out.
- 7) Extensive modeling of soil moisture profiles using weather data as input was conducted to evaluate the predictive capability of two commercially available software programs Vadose/W and SV-Flux.
- 8) Extensive analysis of the data was conducted to examine relationships between soil moisture content and matric suction and various in situ testing parameters of interest.
- 9) Recommendations for conducting and interpreting in situ tests in unsaturated soil were developed.

#### **1.4 Organization of Report**

In Chapter 2, results of the literature review are presented. Chapter 3 contains descriptions of the two tests sites, instrumentation installed to monitor weather and soil moisture, soil sampling and field measurements, in situ testing procedures, laboratory testing methods and software used to model soil moisture variations. In Chapter 4, results of laboratory testing are presented. Chapter 5 is used to present the weather

and soil moisture instrumentation data obtained during the nearly two years of monitoring at each test site. Chapter 6 presents the results of soil moisture modeling using the unsaturated seepage programs, SVFlux and Vadose/W. Chapter 7 presents the results of in situ testing as related to field soil suctions and moisture contents, as well as, the interpretation and analysis of in situ test results. Chapter 8 provides conclusions and recommendations for practice.

## **Chapter 2 LITERATURE REVIEW**

### **2.1 Introduction**

The literature presented in this chapter focuses on in situ tests including the Pressuremeter Test (PMT), Cone Penetration Test (CPT), and Standard Penetration Test (SPT), as well as work conducted on in situ testing in unsaturated soil. In addition, moisture flux modeling, or unsaturated seepage modelling, is also addressed. The PMT, CPT, and SPT are well studied and available reference materials are abundant. However, published work on in situ testing in unsaturated soil is relatively scarce and so the literature review presented here is somewhat limited in this regard. This observations stresses the importance of the current study described in this report.

### **2.2 In Situ Tests**

In situ testing in combination with a thorough laboratory investigation is a useful tool and vital part of any geotechnical investigation. The ultimate goal in any geotechnical investigation is to understand the soil in intricate detail including: soil type, layering, plasticity, shear strength, and compressibility behavior. There are many approaches to obtain this type of information from a site of interest. The most common method is to use a combination of field sampling with laboratory tests, and some in situ tests.

#### **2.2.1 Pressuremeter Test (PMT)**

The pressuremeter is a device that can be placed into a soil layer to determine mechanical properties of the given soil. The pressuremeter consists of an aluminum

body with a rubber sheath covering it. Fluid is pumped into the rubber sheathing causing it to expand. The pressure and volume needed to inflate the probe is regulated by the user so that determinations of stress and strain in soil next to the probe can be made. There are several ways to insert the pressuremeter into the soil at the desired depth. The prebored borehole method was used in this research. This method consists of excavating a borehole, in this case with a hand auger, and inserting the pressuremeter into the hole. The borehole should be no greater than 1.2 times the diameter of the uninflated probe and no less than 1.03 times the diameter of the uninflated probe (Briaud 1992). This minimizes the inaccuracy during testing from overinflating the probe or problems with placement.

The pressuremeter test (PMT) is based on theory in which the probe is modeled by the expansion of an infinitely long cylinder in an infinite soil mass. Results from a PMT test are presented in terms of corrected volume versus corrected pressure, as shown in Figure 1. These corrected values represent the actual change in volume of the soil and actual pressure applied to the soil surrounding the probe. Corrected volume represents the volume of liquid injected into the probe at a given pressure, corrected for the system compressibility. Corrected pressure represents the pressure measured above the ground surface, corrected for the resistance of the membrane surrounding the probe and includes the additional pressure that result from fluid head between the measuring point and the center depth of the probe. The pressuremeter expansion curve can be used to create an in situ stress and strain curve for the soil. The radial stress is obtained from the probe pressure. The hoop strain is obtained from the initial probe radius and the expansion of the borehole from the probe. From the in situ stress and

strain curve, or the corrected pressure-volume curve, several soil parameters can be determined.

As shown in Figure 1, there are 3 phases associated with the PMT expansion curve. In the first phase, the probe is expanding to fill the borehole cavity and is assumed to reload the soil to the in situ state of stress. The second phase is the pseudo-elastic region of the expansion where the soil response is assumed to be primarily elastic. However, an unload-reload procedure is assumed to provide a truer estimate of the elastic response as the pseudo-linear initial loading behavior is believed to be influenced by soil disturbance. The third and final phase of the test begins with soil yielding and development of a failed plastic zone of soil around the expanding cavity. The transition points between these phases and soil response within Phases II and III are used to determine soil parameters of interest.

The first parameter is the at rest total earth pressure,  $P_{oh}$ , which can be estimated from the transition point between Phase I and II. The pressuremeter modulus,  $E_p$ , and unload-reload modulus,  $E_r$ , represent the Young's modulus of elasticity. These parameters are found by fitting a straight line to the initial linear portion in Phase II, and a secant line to the unload-reload portion in an unload-reload loop, respectively. The yield pressure shown in Figure 1 represents the transition from elastic to plastic behavior while the limit pressure corresponds to the ultimate resistance when the plastic zone surrounding the probe is fully mobilized. Practically, the limit pressure is determined as the radial soil stress corresponding to a soil cavity that has been inflated to twice its initial volume. The limit pressure is usually not obtained during field

measurements, and so it is found by extrapolating the pressure-volume response to estimate the pressure at two times the initial soil cavity volume.

### **2.2.2 Cone Penetration Test (CPT)**

The cone penetration test (CPT) is one of the most useful in situ tests commonly used in geotechnical testing. Its usefulness comes from its ability to “rapidly” test to great depth and provide near continuous indications of soil stratigraphy. This makes it possible to know site stratigraphy in detail and obtain a basic knowledge of the soil properties at the site rather quickly. The drawbacks of the CPT are that one must have a fully functional truck and specialized equipment to perform the test, and thus it is relatively expensive. In addition, the test does not allow for subsurface sampling and so must accompany standard field sampling methods. Field testing with an electric friction cone penetrometer involves pushing an instrumented probe into the ground at a standard rate of 2 cm/sec, while simultaneously measuring the force exerted by the soil on the tip and on a separate friction sleeve just behind the tip. These forces are converted to the tip resistance and sleeve friction by dividing by the projected area of the tip and sleeve area, respectively.

As indicated by Yu and Mitchell (1998), the tip resistance can be used to predict soil properties by employing theoretically based empirical correlations or by using calibration chamber based correlations. Yu and Mitchell (1998) suggest that the use of cavity expansion theory for predicting cone resistance is one of the better approaches, as it allows for elastic and plastic deformations around the probe, and to some extent can account for the buildup of stress around the cone shaft during penetration. Use of

cavity expansion theory involves development of theoretical relationships between cavity limit pressures and cone resistance. Since, the limit pressures are a function of soil properties, the theoretically derived cone resistance can be compared to soil properties such as strength and stiffness. Thus, one can compare values of cone resistance from the field with theoretically derived values of cone resistance and obtain an estimate of soil properties such as undrained shear strength or friction angle, depending on soil type.

### **2.2.3 Standard Penetration Test (SPT)**

The standard penetration test (SPT) is the most common in situ test performed at a site of interest in a geotechnical investigation. The test is dynamic and consists of a split spoon sampler attached to drill rod stem that is driven by a hammer. The hammer hits an anvil on top of the drill rods which in turn drives the split spoon sampler into the ground. The number of blows per six inches of penetration are counted until a total depth of eighteen inches is obtained. The SPT “N” value is the number of blows obtained for the last 12 inches of penetration. There are a number of correlations between SPT test results and soil parameters. These correlations include relative density (Kulhawy and Mayne, 1990), shear strength (Demello, 1971), and newer studies to assess seismic soil liquefaction potential (Cetin et al., 2004).

### **2.3 In Situ Testing in Unsaturated Soil**

For unsaturated soils, there are no proven methods of interpretation for the cone penetrometer, pressuremeter, or standard penetration tests. Observations from cone

penetration testing and pressuremeter testing in unsaturated soils by the principal investigators, show that the soil response to CPT penetration and PMT expansion is influenced significantly by the matric suction, as shown in Figure 2.2 (Miller and Muraleetharan 2000), Figure 2.3 (Tan and Miller 2005) and Figure 2.4 (Tan et al. 2003). In addition, observations from PMT results (Figure 2.3) show that the dry unit weight has a significant influence on some PMT results.

Provided the length to diameter ratio of the probe is sufficient, a pressuremeter test closely approximates the plane strain expansion of a cylindrical cavity. Therefore, cavity expansion theory provides a theoretical basis for interpretation of PMT results. In Section 2.3, a cylindrical cavity expansion theory is presented for unsaturated soils (Muraleetharan et al. 1998). Application of this theory to the PMT was introduced by Miller and Muraleetharan (1998 and 2000).

At the University of Oklahoma, Miller and Muraleetharan (1998, 2000) presented a framework for interpretation of pressuremeter tests in unsaturated soil. This framework is built around a cylindrical cavity expansion model developed by Muraleetharan et al. (1998). This model extends the original model developed by Vesic (1972) to include unsaturated soil behavior. The cavity expressions developed by Vesic (1972) and methods of interpretation of pressuremeter test results hinge on the assumption of soil behavior defined by completely drained or undrained behavior. Implicit in these assumptions is that the soil behavior depends on a single independent stress-state variable, i.e., the effective stress. For unsaturated soil, it is suggested that the soil behavior can be described using two stress-state variables, the net normal stress, defined as the difference between the total stress and pore air pressure ( $\sigma_n - u_a$ )

and the matric suction, defined as the difference between the pore air and pore water pressure ( $u_a - u_w$ ) (Fredlund and Rahardjo 1993). To accurately describe the expansion of a cylindrical cavity in unsaturated soil, these two stress-state variables should be incorporated into the derivation of the ultimate cavity pressure.

Miller and Muraleetharan (2000) demonstrated that the cavity expansion theory for unsaturated soils might be used to interpret pressuremeter test results in unsaturated soils. They performed a series of field tests at a site in Oklahoma at different times of the year and monitored the soil suction using tensiometers (Figure 2.2). While the cavity expansion predictions were reasonably good, there are a number of issues with this method that make it relatively difficult to employ in practice. Generally, the method in its current form is somewhat cumbersome because there are a large number of unknown variables in the cavity expansion equations. Some of these unknown variables can be assumed with reasonable accuracy while others can be estimated using the actual pressuremeter measurements. Current research is focused on developing a streamlined semi-empirical approach to analysis.

Pereira et al. (2003) numerically modeled the pressuremeter in unsaturated soil. Three separate conditions were modeled including unsaturated undrained, unsaturated with constant suction, and saturated undrained. A constitutive model was developed based on effective stress. Suction is accounted for in the model using the parameter,  $\pi$ , which is variable depending whether the suction value is above or below the air entry value. The model was used in a finite element simulation. The model constructed by Pereira et al. (2003) appears to be a reasonable representation of pressuremeter behavior in unsaturated soil. However, in presenting the model, there is little mention of

some of the basic characteristics used by geotechnical engineers to describe soil such as, soil type, plasticity, and grain size. In addition, experimental verification of the model is not included. Verifying the results experimentally also becomes difficult because critical soil details are not included.

Tan et al. (2003) showed through a study at the University of Oklahoma that similarly developed equations for spherical cavity expansion in unsaturated soil could be applied to results of cone penetration tests in unsaturated soils. Again, there are unresolved issues in the application of the theory for practical interpretation of CPT results. Thus, current research has focused on developing a sound semi-empirical approach to interpreting cone penetration test results in unsaturated soils.

Russell et al. (2011) worked to develop of a framework of interpretation for the CPT in unsaturated sand. The framework is based on power law proportionality between the initial effective stress present in a soil and cavity expansion pressure. The authors worked with poorly graded sand in a calibration chamber to develop the method. The calibration chamber was capable of applying various confining pressure and suctions. Experimental results from other experimental investigation were used to verify the CPT interpretation method.

Generally, cone penetration testing in unsaturated soils is not very well explored in the literature. There are notable studies where researchers have explored the CPT in sand, such as described earlier (Russell et al. 2011). In another limited study, Lehane et al. (2004), evaluated a discrepancy in CPT measurements from two separate contractors. The CPT results showed one contractor's results to be nearly double of another's at the same location. This fluctuation in results was attributed to nearby trees

causing high suction in the soil during the dry season. While the study was limited, it demonstrates the importance of considering matric suction in the interpretation of in situ tests in all types of unsaturated soils from sands to clays.

## **2.4 Modeling Moisture Variation in Unsaturated Soil Profiles**

The prediction of soil moisture content due to changes in weather conditions is generally important in areas where highly plastic clayey soils are abundant. These types of soil are greatly affected by seasonal changes in soil moisture, and the costs to repair the damages caused by soil shrinkage and swelling are significant compared to preventative measures. In addition, even for non-reactive soils, it is important to realize that variations in soil moisture will have a strong influence on in situ tests in unsaturated soil. Therefore, having methods of analysis and related software that allows for the prediction of site variations in soil water content and suction in response to weather is a useful component in the analysis of in situ test results.

Vadose/W is one of eight 2-D finite element models that are part of GeoStudio 2007. This software combines water, heat and vapor flow through unsaturated and saturated soil, to provide predictions of water content and suction in the vadose zone and soil cover (Park, 2006). Vadose/W accounts for the surface-atmosphere boundary conditions such as: vegetation and root transpiration, surface evaporation, solar radiation, humidity, wind speed, precipitation, infiltration and surface runoff. It also requires information about the soil thermal properties such as the thermal conductivity and volumetric heat capacity. Vadose/W also allows the application of runoff ponding, gas diffusion and ground freezing (Zamara, 2013). The analysis is based on Darcy's law

for the saturated flow, Richard's Equation, and heat conduction equations for unsaturated soil layers in response to atmospheric conditions. It relates permeability with soil suction and volumetric water content, to produce realistic pore water pressure distributions.

Several research projects have involved Vadose/W, such as Gofar et al. (2006), who investigated a case of a rainfall-induced landslide using a transient seepage and slope stability analyses. Others like Overton et al. (2006), studied the time rate of heave prediction for expansive soils. Adem and Vanapalli (2013) used Vadose/W to predict vertical movements of expansive soils over a period of one year. They used a fully coupled transient analysis to model a soil profile that consists mostly of expansive clay, and the predicted values of soil suction were then compared to published results. They observed that soil suction variations correlated well with environmental conditions on the surface boundary, such that these fluctuations decreased with depth. They concluded that the model solved with a total mass error of less than 1.5%.

Chao et al. (2010) used Vadose/W to study the effect of precipitation, irrigation and deep underground water sources on the migration of water in soils and bedrock. They used the software to predict the free-field heave of a constructed building over the period of 50 years. The obtained results showed a good agreement between the predicted water content distribution and the measured data.

Jayarathne et al. (2012) used Vadose/W to create a hydrological model that simulates an on-site soil absorption system of domestic wastewater. The obtained soil moisture content predictions were compared to recorded field data. The results showed a fair to good agreement between these two sets of data, and specifically at depths

between 0.5 and 2 meters (1.6 to 6.5 ft.). However, they found greater discrepancies at the top surface layer that is covered by vegetation. According to Jayarathne et al. (2012) the reasons behind these discrepancies could be the readings obtained from the moisture probes that are located close to the soil's surface. They explain that these readings could have been affected by the presence of organic material in the top-soil, and that these sensors are near the boundary layer which is most influenced by short-term weather variations.

Benson et al. (2005) conducted several analyses in Vadose/W to verify and calibrate the model against in situ measured data. They found limited agreement between the data and noted that Vadose/W does not predict percolation accurately because it fails to simulate the evapotranspiration pattern and phenology changes with changes in weather conditions. They also found that the predicted quantity of drainage was much higher than the in situ flow. On the other hand, Chao et al. (2010) stressed the importance of identifying deep water bearing strata and irrigation sources because they greatly affect the model predictions.

In their research project, Benson et al. (2005), studied the limitations associated with modelling a single rainfall event. They explained that Vadose/W does not allow modelling of several rainfall events with different intensities during a single day; it only allows one event per day and one type of rainfall distribution: average, sinusoidal, or dropping, which does not represent actual field conditions.

Gitirana et al. (2006), used SVFlux and Vadose/W in their numerical modelling of the soil-atmosphere interaction for unsaturated surfaces. They found out that Vadose/W overestimates runoff values and therefore underestimates the amount of water entering

the system. They explained that the reduced amount of water entering the system resulted in higher soil suctions and lower evaporation rates compared to SVFlux results. Zamara (2013) noted that runoff can be disabled in the Vadose/W analysis, but this would result in loss of water infiltration in further time steps of the analysis. (Runoff= precipitation-infiltration-evapotranspiration–change in storage)

Fredlund and Zhang (2011) found that SVFlux software over-predicts evaporation from a soil column, when compared to actual evaporation. They explain that this comes from the over-prediction of relative humidity at the soil surface. They explain that to improve stability in the numerical solution, SVFlux introduced an adjustment factor to compensate for the vapor pressure calculations at the ground surface. The adjustment factor ranges from 0 to -2; it varies for different soils with the most negative values for coarse-grained soils.

Park (2006) performed a sensitivity analysis to determine which input parameters had the greatest influence on Vadose/W predictions. He found that the hydraulic conductivity function had the largest impact on the predicted values; however, he noted that the saturated hydraulic conductivities of the soil cover and bedrock had a very small effect on the yearly flux rates. Zamara (2013) also reached the same conclusion, that factors such as precipitation intensity and hydraulic properties are the most important.

Kang and Chao (2014), compared 1-D, 2-D, and 3-D water migration studies in expansive soils. The 1-D and 2-D seepage analyses were conducted using Vadose/W and the 3-D analyses by using SVFlux. Field investigation and laboratory testing were conducted to characterize the subsurface soil profile such as plasticity index, water content, percentage passing #200 sieve, the saturated hydraulic conductivity, and depth

of the ground water table based on regional groundwater maps. As to the boundary conditions, the minimum and maximum temperature, precipitation, maximum relative humidity, and wind speed values were obtained from nearby weather stations for the years of 2002 through 2007. They also used a weather generating software called ClimGen to generate daily climate data for a period of one hundred years. The model was then calibrated by using the initial water content profile obtained from the Vadose/W output. The results showed that the 1-D and 2-D modeling had a similar depth of wetting and migration pattern to that obtained with the 3-D modelling approach. Kang and Chao (2014) also note that when the influence of lateral flow like surface runoff, is minimal, the seepage model can be simplified using a 1-D model instead of the other two, since it provides a cheaper and reasonable approach to estimate the depth and degree of wetting of the subsoil.

Zamara (2013) discussed about the need to consider spatial variability such as cracks, preferential flow paths, and various rainfall distributions throughout one day in future software development. Zamara (2013) recommended not to use Vadose/W in commercial field applications unless several design functions were adjusted. For instance, it was shown that the quantity of the infiltrated water modelled in unsaturated soil is usually underestimated at the beginning of precipitation, when desiccation cracks are still open.

It is important to consider limitations of field moisture sensor measurements since these are often the basis for judging the accuracy of numerical predictions. It is important to recognize that discrepancies between the predicted soil moisture values and the in situ determinations may be due in part to limitations with the field

measurements. Generally, moisture sensors are used to estimate the volumetric water content based on the measurement of the dielectric constant of the tested soil, which increases with increasing water content. This is due to the fact that dielectric constant of water is much larger than the dielectric constant of soil (Friedman, 1998). Thus, water contents are determined via calibration of the sensor output to the water content of a given soil. However, introducing certain substances, such organic material in the surface layer, might alter the soil moisture readings (Jayarathne et al. 2012). Furthermore, in the current research, concern has been raised about the possibility that desiccation cracks and non-uniform macro-features introduced into the soil profile during installation of the sensors can produce localized increases in water content near the sensors. Thus, a particular sensor location may not provide a reasonable representation of average moisture conditions at a particular depth depending on, for example, its proximity to a desiccation crack.

The soil temperature is an important factor that influences the soil's water content. It depends on the thermodynamic heat exchange between the soil surface and the atmosphere. Heat is absorbed when liquid water is transformed to water vapor, and then released during condensation into cooler locations. In Vadose/W two of the primary input parameters are the frozen and unfrozen volumetric heat capacities, and thermal conductivity. Assuming that the soil is homogeneous, Hillel (2004) suggests it is acceptable to assume that the soil volumetric heat capacity is independent of depth. Thermal conductivity in soil increases with the increase of the soil's bulk density. The thermal conductivity also increases with increasing water content Farouki (1982); therefore, when soil approaches saturated, the thermal conductivity increases. The soil

temperature changes with the presence or absence of clouds, warm and cold weather fluctuations, precipitation and other factors (Lakshmi, 2003). For example, when the sky is clear, the heat absorbed by the soil surface will radiate back into space, but when the sky is cloudy the heat loss will be lower. Heat produced by solar radiation travels down the soil profile and decreases with depth due to the fact that it takes time to travel, this phenomenon is called amplitude damping. Lakshmi (2003), explains that a time lag is needed for the temperature cycle to reach a given point in the soil. He adds that it is a common assumption that the soil surface temperature oscillates as a sinusoidal function of time about some mean value of temperature. Therefore, the maximum and minimum daily temperatures are needed as input parameter in Vadose/W.

Zamara (2013) discussed the need to address spatial variability, such as crack formation in soil surface layers, in numerical models such as Vadose/W. Measurements of soil suction can be used to estimate the effective stresses between soil particles and to detect the presence of desiccation cracks (Krahn et al. 1989). To incorporate desiccation cracks in Vadose/W, one might assign higher permeability values during the dry seasons.

To understand the soil–moisture prediction results during the different seasons, there is a need to understand the relationship between surface vegetation and water storage. For instance, vegetative has an insulating effect, and thus retains surface heat. This can be observed in Vadose/W modelling where the vegetation cover increased the water storage of soil. However, Versegby (1991) explains that soil-moisture evaporation due to solar radiation has an effect that overcomes the presence of surface vegetation, and decreases the surface temperature.

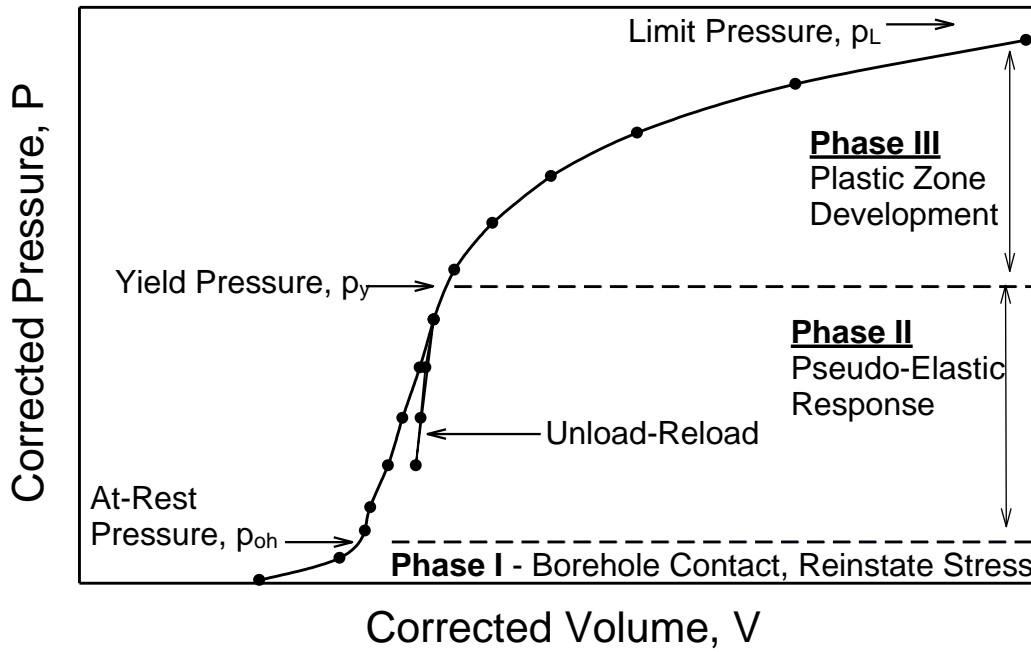


Figure 2. 1: Pressuremeter curve showing different test phases.

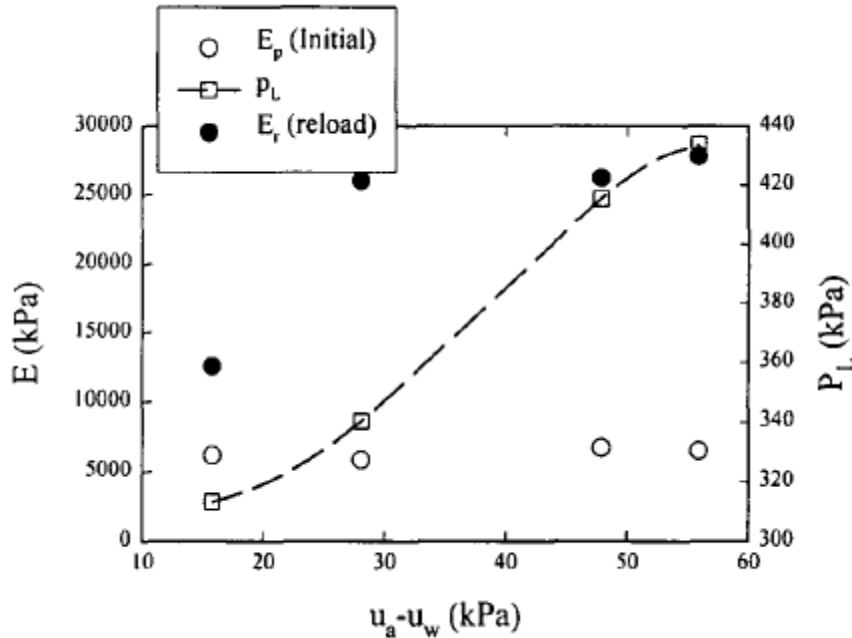


Figure 2. 2. Pressuremeter limit pressure ( $P_L$ ), reload modulus ( $E_r$ ) and pressuremeter modulus ( $E_p$ ) versus matric suction ( $u_a - u_w$ ) from field tests in Minco Silt (from Miller and Muraleetharan, 2000).

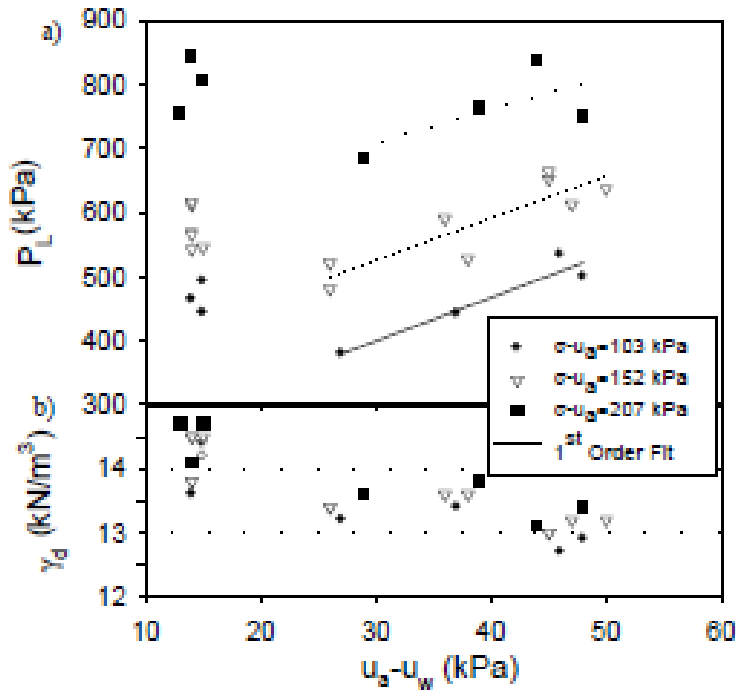


Figure 2. 3. a) Limit pressure (PL) versus matric suction ( $u_a - u_w$ ) from PMTs in Minco Silt in a calibration chamber, b) average dry unit weight ( $\gamma_d$ ) of the soil bed versus matric suction (after Tan and Miller 2005).

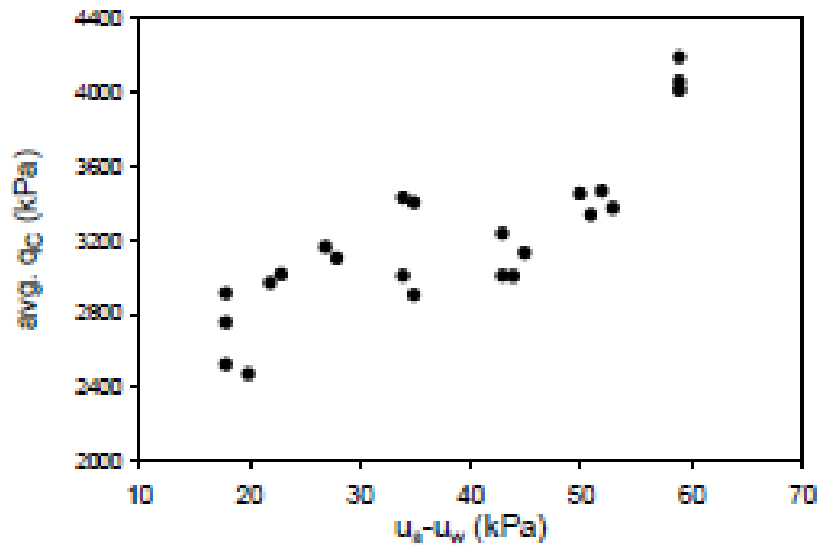


Figure 2. 4. Tip resistance ( $q_c$ ) versus matric suction ( $u_a - u_w$ ) from cone penetration tests in Minco Silt in a calibration chamber (from Tan et al. 2003).

## Chapter 3 FIELD, LABORATORY AND ANALYSIS METHODS

### 3.1 Test Sites

Two sites were chosen for this project referred to as the North Base and Goldsby sites. The sites chosen for installation of weather stations and in situ testing have several specific characteristics that make them desirable. Both sites were chosen reasonably close to the university campus to accommodate relatively frequent site visits.

The North Base site is located west of the Max Westheimer Airport in Norman, OK (latitude: 35°14'6.58"N, longitude: 97°27'46.39"W). The soil profile at the site contains low and high plasticity soil with soil plasticity greater near the surface. A water table was found to fluctuate between depths of 8 to 9 feet. The majority of material found at North Base is considered fine grained; however there were some rock inclusions found at depths near bedrock. The soil appears to be part of the Kirkland-Pawhuska complex soil series having parent material consisting of clayey alluvium over clayey residuum weathered from calcareous shale (NRCS soil survey website), and appears to overly shales of the Hennessey geologic unit (OHD 1969).

The Goldsby site is located near Goldsby, OK approximately 5 miles south of the University of Oklahoma (latitude: 35° 9'20.61"N, longitude: 97°28'40.04"W). The soil profile contains low plasticity clay for at least ten feet, which was the depth of interest for this investigation. There was no bedrock or a water table encountered during the research. The soil is mapped as part of the Minco Silt soil series that is a terrace deposit associated with the Canadian River and with parent material consisting of Eolian sediments (NRCS soil survey website). The unconsolidated terrace deposits appear to overly the Hennessey geologic unit (OHD 1969).

### **3.2 Test Site Field Instrumentation for Monitoring Weather and Soil Moisture**

Initial field work at the Goldsby site began in June, 2012 and the fully functional weather station was installed and began collecting data at the same time. The weather station manufactured by Campbell Scientific instruments includes sensors to quantify rainfall, air temperature, relative humidity, wind speed, wind direction, solar radiation, and volumetric water content at three depths in the soil profile.

A similar weather station was installed at the North Base site in August, 2012 at which time data collection began. A photograph of the weather station installed at North Base is shown in Figure 3.2. A list of sensors and measurement ranges is provided in Figure 3.3.

### **3.3 Soil Sampling**

Initial soil sampling started in August of 2012. Initial sampling of the field sites was done using a 3-inch diameter hand auger. Moisture content samples were collected in 6-inch increments to the final sampling depth. Samples collected for moisture content determination were placed in moisture tins and sealed with electrical tape around the rim to limit moisture loss. Representative samples from each foot of depth were collected in plastic bags for laboratory testing. Additional in situ samples were collected using Shelby tubes. The Shelby tubes were pushed into the ground using an ODOT drilling truck. Shelby tube samples were then sealed on top and bottom using a combination of rubber caps and duct tape. Samples were brought to the laboratory as quickly as possible for extrusion. Once extruded, samples were measured and weighed,

then sealed in plastic wrap and stored in a moisture room until they were required for testing.

Numerous field samples were obtained for both determinations of moisture content and suction. These samples were generally collected during in situ testing events. Samples were sealed and brought to the laboratory for testing.

### **3.4 Laboratory Testing Methods**

#### **3.4.1 Basic Soil Properties**

Laboratory testing was conducted to determine basic physical and index properties. Grain-size distribution and liquid and plastic limit tests were conducted in general accordance with ASTM standards (D422, D4318) on samples obtained at depths encompassing the locations of in situ tests (0 to 10 ft.). Results of these tests were used to classify the soils at each test site. Specific gravity was determined on selected samples in accordance with ASTM Standard D854.

In addition, Cation Exchange Capacity (CEC) was determined for selected samples by a commercial laboratory, Agsource, in Lincoln Nebraska. The summation of cations method was used to determine the amount of exchangeable cations. This method involves measuring the amounts of available calcium, magnesium, potassium, and sodium; the method used by Agsource is described in detail in Brown and Warncke (1988).

### **3.4.2 Soil Water Characteristic Curve (SWCC) Testing**

The WP4 Dew Point Potentiometer manufactured by Decagon was the primary method for determining the SWCC. The WP4 measures total water potential (total suction) using the chilled mirror method to determine the relative humidity of the air above a sample in a closed chamber. The relative humidity above the sample is assumed to be at equilibrium with the air in the sample. At temperature equilibrium, relative humidity is directly related to water potential. Total suctions up to about 300 MPa (43,500 psi) can be determined with a resolution of about 0.1 MPa. The method followed was consistent with that provided by Decagon.

### **3.4.3 Shear Strength**

Shear strength testing was conducted to determine saturated strength parameters from thin-walled samples obtained in situ. Thin-walled tube samples were tested in a conventional triaxial compression device. Samples were subjected to multi-stage isotropically consolidated undrained compression (CIUC) tests incorporating pore water pressure measurements. This test allows for the determination of both undrained shear strength and effective stress-strength (drained strength) parameters. However, it is noted that drained and undrained testing may not produce identical effective stress-strength envelopes.

Table 3.1 presents the site name, borehole number and sample depth as well as the cell pressure and back pressure used for each test. The same effective pressure range was used for each sample during multistage tests. The triaxial tests were conducted with measurement of pore-water pressure to assess both drained and

undrained strength parameters, as prescribed by ASTM D4767. Samples were saturated under back pressure. The triaxial tests were run on specimens corresponding to in situ testing depths. As it is difficult to obtain identical specimens to run several tests, multistage test were conducted under confining pressures of 3, 7, and 15 psi. The cell pressure in each stage is shown in Table 3.1.

#### **3.4.4 Hydraulic Conductivity**

To determine the saturated hydraulic conductivity of the soil located at the test sites, Shelby tube samples were collected at different times during the project as described previously. After extruding, the soil samples were wrapped with plastic film and stored in a moisture room. The standard test method for measurement of hydraulic conductivity of saturated materials with a flexible wall permeameter was used as described in ASTM D5084 -10. Samples were back pressure saturated and tested under effective confining pressures of 3 to 6 psi. The goal was to simulate the in situ effective stress while maintaining sufficient cell pressure to counter the head pressure while achieving the desired gradient. For soil with very low hydraulic conductivity, necessitating high gradients, it is impractical to use confining pressures less than about 5 psi.

#### **3.5 In Situ Testing Methods**

The in situ tests used in this research included the Pressuremeter Test (PMT), Cone Penetration Test (CPT) and Standard Penetration Test (SPT). Pressuremeter tests were performed by University of Oklahoma (OU) personnel (authors) while the CPTs and SPTs were performed by the Oklahoma Department of Transportation (ODOT) with

assistance from OU personnel. Data interpretation of all in situ tests was conducted by OU personnel.

### **3.5.1 Pressuremeter Testing (PMT)**

The pressuremeter probe used was a Roctest Texam NX long probe with a rubber membrane. The rubber membrane was desired compared to the more common metal sheathed membrane because the soils tested were relatively soft, so a flexible membrane provides better contact and more uniform cavity expansion in this case. Stress-controlled tests were conducted according to ASTM D4719-09 Procedure A, whereby expansion pressure is increased incrementally while monitoring volume injected into the probe during a 60-second interval for each pressure increment. Regulated nitrogen was used to force fluid into the pressuremeter probe and injected volume was measured with a site glass on the fluid standpipe.

Prior to PMT testing, a borehole was created using a hand auger. The testing hole was advanced to a depth such that the probe center was at the desired test depth, the probe was in place at the bottom of the borehole and testing started. Relatively small pressure increments were used in an attempt to produce well-defined expansion curves and in most cases an unload-reload sequence was used. To capture an unload-reload loop the soil was loaded until the soil showed slight yield behavior. The pressure was then decreased and the soil was allowed to rebound for five minutes prior to reloading. When reloading commenced the probe inflation continued until the injected volume reached the safe limit. The probe was then deflated and retracted from the earth. The hand auger was then advanced to the next test depth and the process was

repeated. Moisture tins were used to collect samples from each test depth. These samples were brought to the laboratory to determine suctions using the WP4 device and corresponding gravimetric moisture contents. A summary of test PMT tests conducted during this study is presented in Table 3.2, including test dates, test depths, and measured suction and water content obtained at each test depth.

### **3.5.2 Cone Penetration Testing (CPT)**

The Oklahoma Department of Transportation (ODOT) performed cone penetration tests at both Goldsby and North Base with assistance from OU Personnel. Three test soundings were obtained per site visit. As with the PMT, after cone testing the test locations were mapped so that subsequent tests would not be in the same location. The cone was pushed to a depth of 10 feet for each sounding. A total of 39 cone soundings were conducted over the course of the research, as summarized in Table 3.3.

The CPT was run in general accordance with ASTM Standard D5778-12, with a penetration rate of approximately 2 cm/sec using a standard cone with a 60 degree apex conical point having a projected tip area of 10 cm<sup>2</sup> (1.55 in.<sup>2</sup>) and a friction sleeve just behind the cone with an area of 150 cm<sup>2</sup> (23.3 in.<sup>2</sup>). Electronic signals from the tip and sleeve load cells were collected with a data acquisition system and used to compute the tip resistance and skin friction.

### **3.5.3 Standard Penetration Testing (SPT)**

Standard penetration testing (SPT) was performed by the Oklahoma Department of Transportation (ODOT). An automatic hammer was used attached to a drill rig. A split

spoon sampler was used to perform the test and collect soil samples. One SPT test was performed per test date in general accordance with ASTM D1586-11.

### **3.6 Modeling Soil Moisture Changes in Response to Weather**

Two computer programs were used to model the variation in soil moisture profiles over time at the test sites. Vadose/W and SVFlux are two computer programs used to model transient flow of water, heat, and vapor in unsaturated soil. The programs are built around fundamental equations governing the exchange of water between the soil and atmosphere at the ground surface (e.g. Penman 1948, Wilson et al. 1994) and can account for variations in the soil state (dry, frozen, saturated, unsaturated), soil type, soil temperature, and extent and type of vegetative cover, among other things.

Basically, the user is required to input a number of different parameters that govern the movement and storage of heat and water (in liquid and vapor forms) within a soil profile as well as information about the type and temporal variation of vegetative cover at the site. In addition, the initial soil moisture conditions in the profile are required. Once the basic soil and vegetative material parameters are input, the desired climate data defining weather variations over some defined time period are provided as input. The program is then run and the output generated provides predicted moisture (and suction) profiles as a function of time.

In this research, Vadose/W and SVFlux were used to predict the variations in moisture content in the soil profiles at each test site for comparison to the actual moisture content variations observed. In addition, the variations in moisture content and suction on different testing dates were used in the analysis of in situ test results. The

purpose of this modeling was to evaluate and compare the predictive capability of these programs for predicting moisture variations soil profiles due to seasonal weather changes.

The required input parameters and methods used to define the parameters with respect to Vadose/W and SVFlux are summarized in Table 3.4. These parameters are divided into categories of climate data, vegetation data, and soil data. As indicated in Table 3.4, the required input data and methods used to model variations in the input parameters varies somewhat between the two programs. As for the output, the programs were used to provide variations in volumetric water content over time at specific depths in the soil profiles.

Aside from the similarities in the required input and output parameters, the primary differences between these two programs are as follows:

- 1- VADOSE/W (2007) solves 1D and 2D problems, whereas SVFlux (2009) solves 1D, 2D and 3D problems.
- 2- In VADOSE/W mesh properties are manually defined, whereas in SVFlux mesh properties are automatically defined.
- 3- Different infiltration rates are computed by SVFlux and VADOSE/W for high precipitation rates. For instance, VADOSE/W does not respond well to high positive pressure gradients. In fact, infiltration is underestimated, and runoff values are overestimated when compared to those predicted by SVFlux (Gitrana et al. 2005).
- 4- VADOSE/W predicts lower actual evaporation rates (AE) when compared to SVFlux (Gitrana et al. 2005).

- 5- VADOSE/W couples the thermal fluxes within the soil whereas SVFlux does not.
- 6- VADOSE/W (2007) has a feature that allows runoff to pond at the ground surface, and then infiltrate in the following time steps. To predict the surface infiltration and actual evaporation VADOSE/W requires adding a thin surface layer above the ground surface to deal with high changes in flow gradients. The solver computes the seepage flow through this layer, and allows the water that does not infiltrate immediately into the soil profile to build-up and become a positive head pressure in subsequent steps. This situation happens specifically whenever the soil goes from being very dry to very wet.
- 7- Table 3.5 summarizes the type of methods used by both programs to compute the potential and actual evaporation, transpiration, runoff and infiltration. The main differences between VADOSE/W and SVFlux are in the way the amount of runoff is calculated during a wetting period, and the meshing properties when high positive gradients are applied on the system.

**Table 3. 1. Summary of multistage triaxial compression test conditions for thin-walled tube samples for Goldsby and North Base sites.**

Site	Sample Date	Sample Depth (in)	Back pressure (psi)	Cell Press. (psi) Stage 1	Cell Press. (psi) Stage 2	Cell Press. (psi) Stage 3
Goldsby	12/8/2014	30-37.5	61	64	68	76
Goldsby	5/10/2014	71-81	50	52	57	79
Goldsby	9/20/2014	113-120	50	58	72	80
North Base	9/3/2013	48-54	50	53	57	65
North Base	11/21/2014	85-96	24	62	65	x

**Table 3. 2. Summary of Pressuremeter Tests from Goldsby and North Base sites.**

Site	Test Date	3 ft. Suction (psi)	3 ft. Water Content (%)	5 ft. Suction (psi)	5 ft. Water Content (%)	7 ft. Suction (psi)	7 ft. Water Content (%)
NB	2/1/2012	463.4	14.8	95.7	17.2	-	-
NB	3/11/2013	302.4	14.5	72.5	16.2	-	-
NB	4/12/2013	359.7	14.7	117.5	13.8	45.0	19.5
NB	4/30/2013	378.1	15.8	168.2	16.1	59.5	18.2
NB	10/11/2013	427.9	16.2	103.0	21.0	84.1	21.0
NB	1/7/2014	224.8	23.5	121.8	19.5	113.1	26.1
NB	3/31/2014	223.4	21.6	71.1	22.9	-	-
NB	7/25/2014	91.4	20.6	46.4	20.8	7.25	20.3
NB	8/22/2014	245.1	20.0	100.1	20.4	53.7	22.6
NB	10/31/2014	226.3	18.0	110.2	18.5	76.9	19.2
NB	10/31/2014	269.8	19.0	76.9	17.8	15.9	19.9
G	2/1/2013	306.5	13.5	73.5	15.6	89.9	17.8
G	3/13/2013	310.4	10.6	103.7	12.2	46.4	16.9
G	4/15/2013	62.4	20.4	53.7	14.3	46.4	18.1
G	5/2/2013	81.2	20.3	90.4	13.8	74.9	17.2
G	6/10/2013	87.0	21.4	130.5	12.7	87.0	17.1
G	10/16/2013	124.7	13.5	63.8	18.5	72.5	20.3
G	1/8/2014	81.2	19.2	85.6	17.6	110.2	21.8
G	3/31/2014	46.4	18.8	34.8	21.2	8.7	20.5
G	7/23/2014	103.0	15.1	85.6	16.2	66.7	18.1
G	8/22/2014	174.0	13.7	92.8	14.8	81.2	17.2
G	10/17/2014	195.8	10.5	84.1	15.1	78.3	18.0
G	10/17/2014	339.4	9.8	89.9	13.8	68.2	17.6

**Table 3. 3. Summary of Cone Penetration Tests from Goldsby and North Base sites.**

Site	Test Date	Number of Soundings	Average Site Moisture Content
North Base	2/1/2013	3	16.6
North Base	5/6/2013	3	20.5
North Base	9/3/2013	3	17.7
North Base	11/21/2013	3	20.2
North Base	2/18/2014	3	22.6
North Base	9/10/2014	3	18.9
North Base	12/30/2014	3	20.4
Goldsby	2/1/2013	3	15.1
Goldsby	5/6/2013	3	16.7
Goldsby	7/29/2013	3	16.8
Goldsby	11/21/2013	3	16.8
Goldsby	2/18/2014	3	18.5
Goldsby	9/10/2014	3	13.9

**Table 3. 4. Summary of methods to define input parameters.**

Input Parameters	SVFlux	Vadose/W
$m_v$ (Coefficient of compressibility)	measured or estimated	measured or estimated
Unsaturated permeability function	van Genuchten & Mualem function	Fredlund & Xing
SWCC fitting curve	van Genuchten & Mualem fitting estimation	Spline Function
Actual evaporation method	Wilson Limiting Equation (1997)	Penman-Wilson (1990-1994)
Leaf Area Index	Constant	Tratch (1996)
Plant Limiting Factor	SVFlux database	User Input
Root depth (ft.)	estimated based on vegetation and climate	estimated based on vegetation and climate

**Table 3. 5. Differences and similarities between computational method used in SVFlux and VADOSE/W.**

<b>Parameter</b>	<b>SVFlux (SoilVision Ltd.,2009)</b>	<b>VADOSE/W (GeoSlope, 2007)</b>
<b>Transpiration</b>	Tratch (1995)	Tratch (1996)
<b>Potential Evaporation (PE)</b>	Modified Penman method Wilson (1990) and Gitrana (2005)	Penman-Wilson (1990,1994)
<b>Actual Evaporation</b>	Improved Fredlund-Wilson Penman method (1990) and Gitrana (2005)	Penman-Wilson (1990)
<b>Infiltration</b>	Mansell (2002) Based on the Theory of Soil Cover	If Precipitation-AE < 0 then: Infiltration = Precipitation- AE
<b>Runoff</b>	Gitrana (2005)	If Precipitation - AE > 0 * Runoff = Precipitation - AE - Infiltration
<b>Precipitation Intensity Application and Distribution</b>	Flexible Step-function	Fixed Sinusoidal
<b>Mesh Properties</b>	Automatic adaptive mesh refinement	Manual and remains fixed
<b>Time Stepping</b>	Automatic time refinement	Adaptive time steps

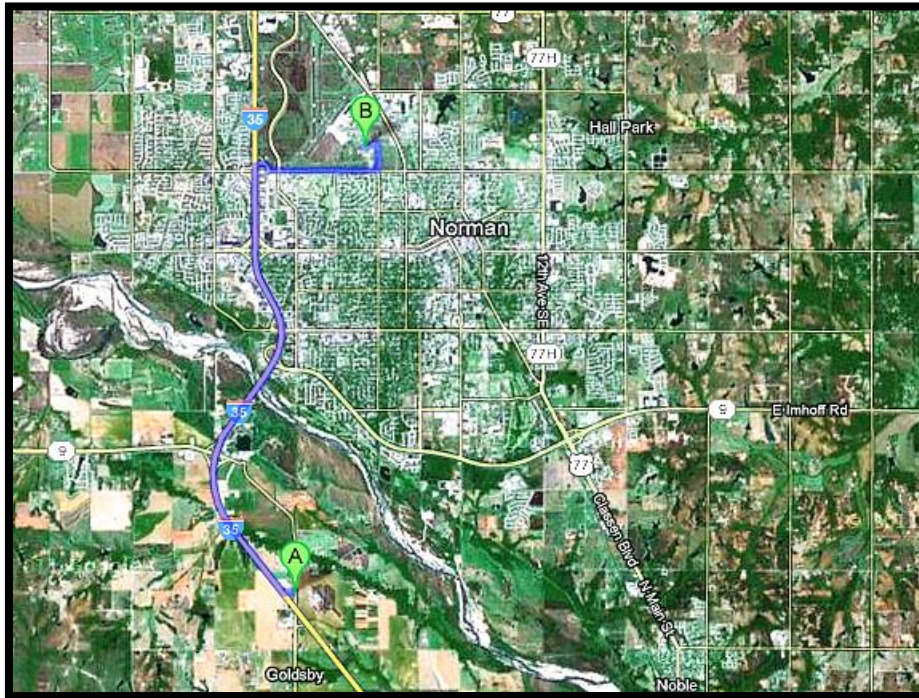


**Figure 3. 1. Test sites used for this study with North Base indicated with B and Goldsby with A (image from Google).**



**Figure 3. 2. Weather station installed at North Base test site. ODOT cone truck in background.**



Figure 3. 3. Type of sensors and their corresponding range of measurements.

## Chapter 4 RESULTS OF LABORATORY TESTING

### 4.1 Basic Soil Properties

Basic soil testing was performed to categorize and identify the soil profiles at each field site. Soils were tested following the earlier described ASTM standards and classified according to the Unified Soil Classification System. Particle size distribution was the first test performed on soil returned from the test site. The majority of material from the field sites was fine grained. To determine the fine grained particle size, two tests were performed. First, one sample from each foot of depth was wet washed through a No.200 sieve to determine percent of fines. Second, for selected depths a hydrometer analysis was used to determine actual particle size distribution of the fines. The percent of material passing a No. 200 sieve for Goldsby is shown in Figure 4.1. Above 5 feet, over 90% of material passed through a No.200 sieve and below this depth there was more sand present in the samples. The percent of fines for all samples is 75% or above indicating a mostly fine grained soil profile. Grain-size distribution and liquid and plastic limit tests were conducted in general accordance with ASTM standards (D422, D4318), on samples obtained at depths down to 10 ft.

The percentage of material passing the #200 sieve for North Base soil is shown in Figure 4.2. The majority of material from this site passed through a No. 200 sieve, which classifies it as fine grained. The average percent of material passing the No. 200 sieve is around 85%.

Atterberg limits were determined for each foot of soil at both sites. At Goldsby, the plasticity indices through 10 feet of depth are relatively uniform with an average PI of 11 as shown in Figure 4.1. There is an increase in plasticity around 4 feet where the

PI reaches 14, but then returns to nearly average below this depth. The PI at North Base is not as uniform as Goldsby. The Atterberg limits for North Base soil are shown in Figure 4.2. There are two distinct layers of soil at North Base. With the exception of the first foot of soil at North Base the PI in the top 5 feet of soil is above 40. Below 5 feet the average PI drops to around 14. Other visual/manual tests were also done to characterize the soil at both sites including the dry strength test and acid reaction tests. It was noted that soil from both sites form strong casts; however, Goldsby soil was more reactant to HCL and therefore had generally more calcium carbonate. The only significant reaction to HCL at North Base was on samples collected at a depth of 10 ft, where the bedrock layer was encountered.

Specific gravity was measured for three depths at each site following the ASTM standard test method of specific gravity of soil solids by water pycnometers, designation D854–14. The specific gravities for North Base and Goldsby are presented in Table 4.1. For both sites shallow depths had lower specific gravities. Soils at both sites had specific gravities consistent with clay, silt and sandy soils.

Cation exchange capacity (CEC) was measured for both sites for all depths. Cation exchange capacity is typically measured in milliequivalents per 100g of soil (meq/100g). A higher CEC corresponds to a higher ability for the soil to hold exchangeable cations. This becomes a measure of a soils attraction to water which results in greater shrink/swell characteristics and soil plasticity. Soils with high CEC typically exhibit behavior that makes construction with them more challenging. They are useful in situations where absorption of water is a desirable feature such as liners in landfills. The results of CEC testing are shown in Table 4.2. Generally, Goldsby soils

show lower CEC than North Base. The CEC for Goldsby is lower for the top four feet of soil and then increases for depths of 5 to 8 feet followed by a decrease at 9 feet. North Base soil shows especially high CEC at 3 feet and then decreases with increased depth.

## **4.2 SWCC Test Results**

Soil Water Characteristic Curve testing for North Base and Goldsby was performed for the depths of interest for each site. The measured SWCC data and interpreted SWCC curves of Goldsby and North Base are shown in Figures 4.3 and 4.4, respectively. The curves represent different layers identified within the soil profile. Layer boundaries were estimated based on variations in soil properties. As noted, the curves for Goldsby from different depths are relatively similar, reflecting the somewhat uniform character of the soil stratigraphy. At North Base the curves are different consistent with the variations in stratigraphy and the higher PI soils at the mid-depths.

In this project, only the drying SWCC was determined because of the difficulty in determining the wetting SWCC. It was assumed for modeling that the hysteresis effect for fine grained soils that have undergone several wetting and drying cycles is very small and negligible. The model SWCC curves shown in Figures 4.3 and 4.4 were obtained using the Fredlund and Xing (1994) equation. The slope of the curve is gentle, which is typical for fine grained soils. For the unsaturated seepage modeling, modifications to the fitted curve included increasing the saturated volumetric water content (VWC) and air entry value (AEV) to better match the maximum values of VWC measured in the field.

### **4.3 Saturated Hydraulic Conductivity Results and Unsaturated Functions**

As soil dries, eventually the suction exceeds the air entry value (AEV) and air enters the soil pores. Air in the voids causes the flow of water between the soil particles to become slower with time and a corresponding decrease in hydraulic conductivity. The relationship between hydraulic conductivity and suction can be modeled with an unsaturated permeability function developed using the SWCC and the saturated hydraulic conductivity. Such functions are shown in Figures 4.5 and 4.6 for Goldsby and North Base. Tables 4.3 and 4.4 provide a summary of hydraulic conductivity test results on saturated samples for Goldsby and North Base, respectively. The range of reported values is consistent with the silty to clayey soils encountered at the test sites.

The unsaturated seepage modeling programs, Vadose/W and SVFlux allow the user to select between the unsaturated hydraulic conductivity estimation functions developed by Van Genuchten (1980) or Fredlund and Xing (1994). It was noticed by Chan et al. (2012), that both methods are less accurate for fine grained soil than sandy soils. For this project, the Fredlund and Xing (1994) method was used because it doesn't require information about the residual water content values for different layers.

### **4.4 CIUC Triaxial Test Results**

Isotropically consolidated undrained compression (CIUC) triaxial tests were performed for Goldsby and North Base soils at depths of interest at each test site. A summary of triaxial results is presented in Table 4.5. The test results show that both sites have soil with increasing friction angles with greater depths. On the other hand, effective stress cohesion intercepts tend to decrease with depth. These observations are consistent

with a soil profile that is more overconsolidated near the ground surface and less so with depth. In this case, apparent overconsolidation of the soil profile is influenced by weathering due to atmospheric interactions, which are greatest in the near surface soils.

**Table 4. 1. Specific gravity of North Base and Goldsby soil.**

<b>Goldsby Depth (ft)</b>	<b>Goldsby G<sub>s</sub></b>	<b>North Base Depth (ft)</b>	<b>North Base G<sub>s</sub></b>
3	2.66	3	2.66
6	2.79	5	2.75
9	2.69	7	2.74

**Table 4. 2. Cation Exchange Capacity Results North Base and Goldsby.**

<b>Goldsby Depth (ft)</b>	<b>Goldsby CEC (meq/100g)</b>	<b>North Base Depth (ft)</b>	<b>North Base CEC (meq/100g)</b>
1	11.0	2	20.6
2	11.9	3	38.2
3	10.7	4	29.7
4	13.3	5	21.6
5	19.4	6	18.1
6	21.6	7	15.3
7	20.3		
8	16.9		
9	12.1		

**Table 4. 3. Goldsby: saturated, flexible wall hydraulic conductivity test results.**

<b>Sample No.</b>	1	2	3	4	5	6	7
<b>Depth (ft)</b>	0 - 2	2 - 2.5	3-3.5	4 - 5.5	5.5 - 6.5	6.5 - 7.5	8 - 9.5
<b><math>\gamma_d</math> (pcf)</b>	73.4	98.0	80.7	78.9	72.3	80.0	95.4
<b>Effective Confining Stress (psi)</b>	1.5	2	2	4	4.5	6	7.5
<b>Corrected Hydraulic Conductivity, <math>k_{20}</math> (ft/hr)</b>	4.40E-02	1.35E-02	2.46E-03	2.17E-02	4.57E-03	2.48E-02	1.26E-03

**Table 4. 4. North Base: saturated, flexible wall hydraulic conductivity test results.**

Sample No.	1	2	3	4	5	6	7
Depth (ft)	0 - 1	1.5-2.5	2.5-3.0	3.0-4.0	4.5-5.0	5.0-6.0	6.0-7.0
$\gamma_d$ (pcf)	---	95.7	96.6	98.9	103.9	110.6	98.3
Effective Confining Stress (psi)	1	2	2	3	4	4.5	5
Corrected Hydraulic Conductivity, $k_{20}$ (ft/hr)	2.45E-02	9.99E-04	3.51E-05	1.23E-05	3.93E-03	8.51E-02	3.75E-03

**Table 4. 5. Summary of triaxial results for North Base and Goldsby.**

Test Site	Goldsby	Goldsby	Goldsby	North Base	North Base	North Base
Depth (ft)	3	6	9	3	5	7
Moisture Content (%)	19.1	24.2	18.3	20.2	23.9	15.6
Wet Unit Weight (pcf)	122.7	134.7	111.3	121.8	124.6	136.3
Dry Unit Weight (pcf)	103.0	108.5	94.1	101.3	100.6	117.9
$c'$ (psi)	2.5	2.0	1.0	10.0	1.0	1.0
$\phi'$ (°)	25.4	31.0	42.0	26.0	31.0	41.6

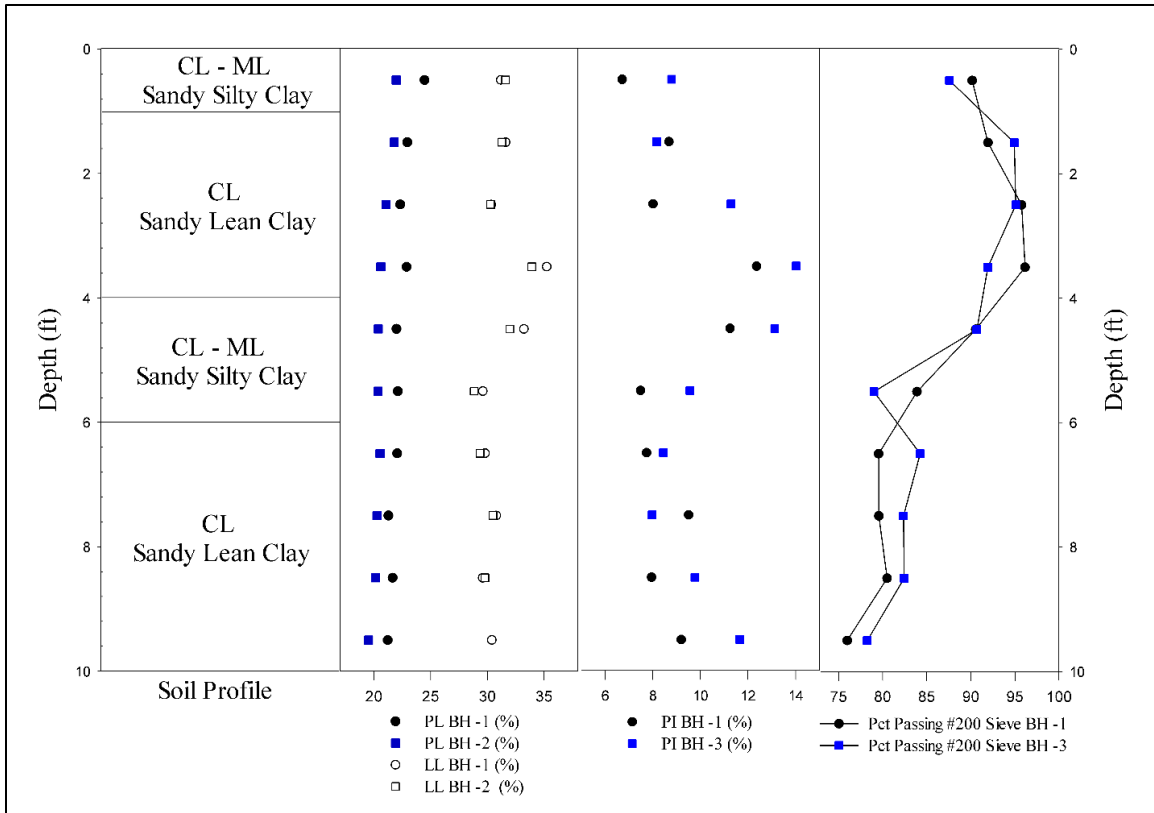


Figure 4. 1. Goldsby: soil profile, Atterberg limits, and percent fines.

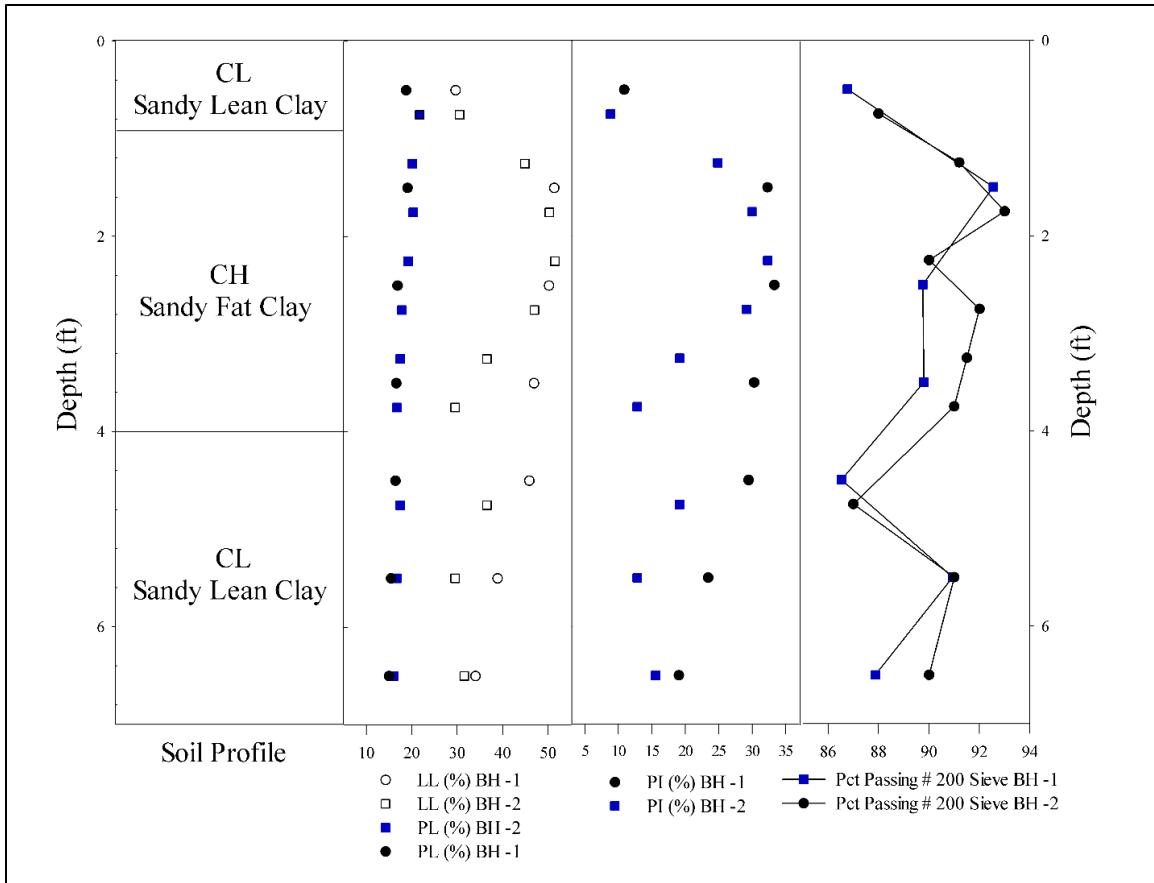
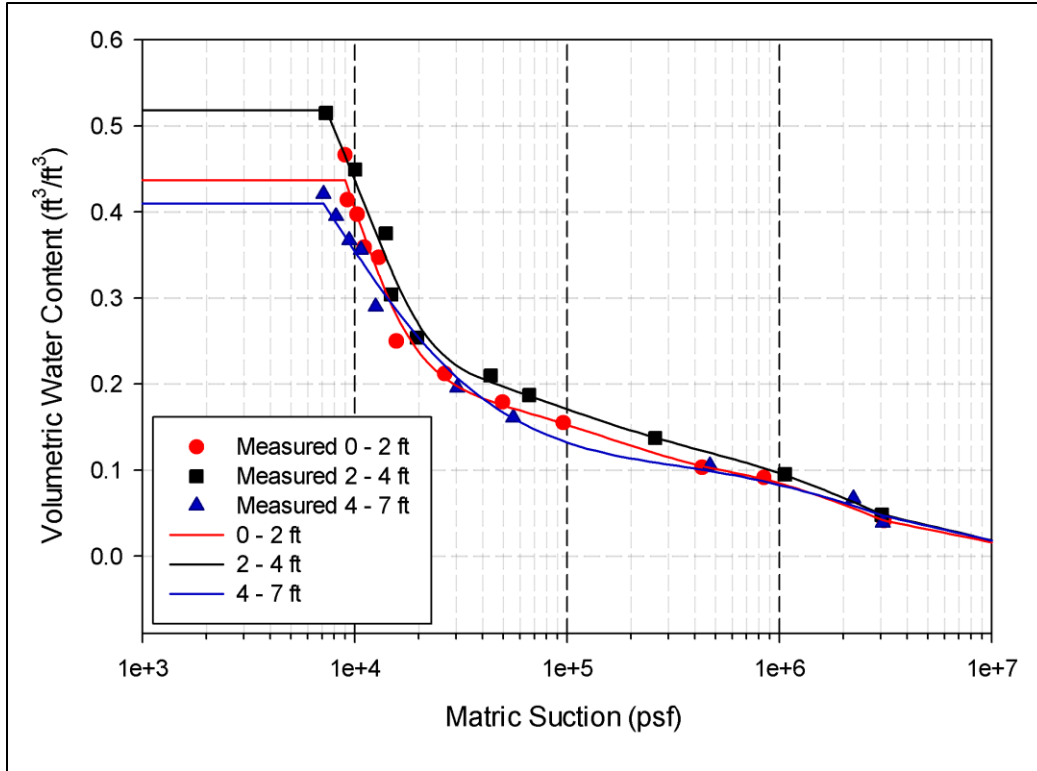
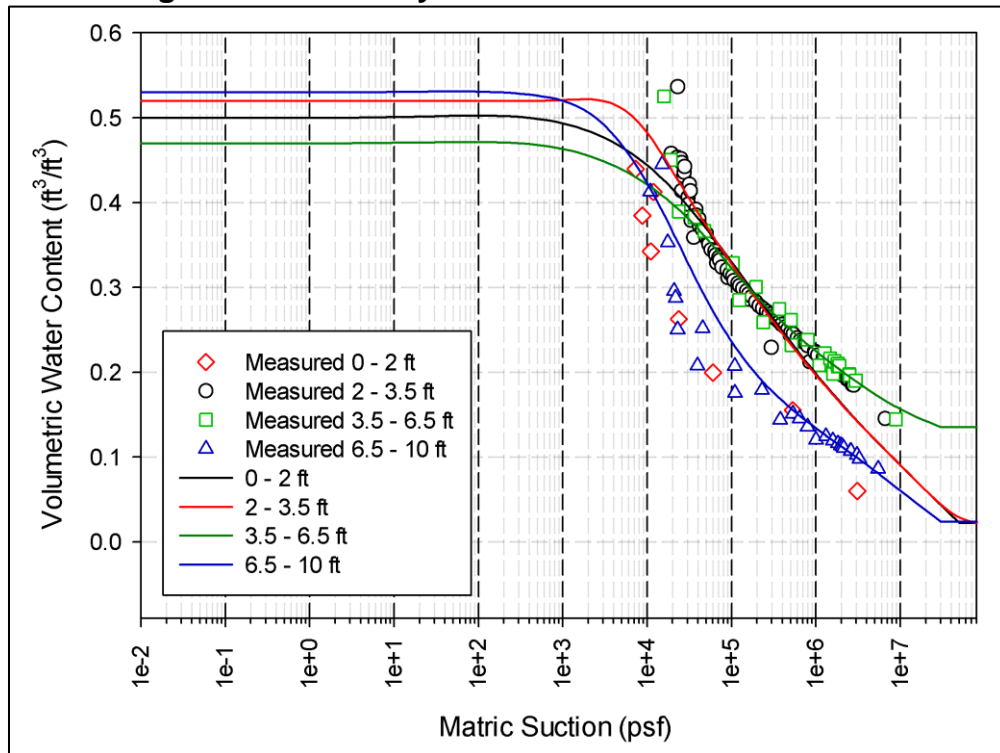


Figure 4. 2. North Base: soil profile, Atterberg limits and percent of fines.



**Figure 4. 3. Goldsby: measured and fitted SWCCs.**



**Figure 4. 4. North Base: measured and fitted SWCCs.**

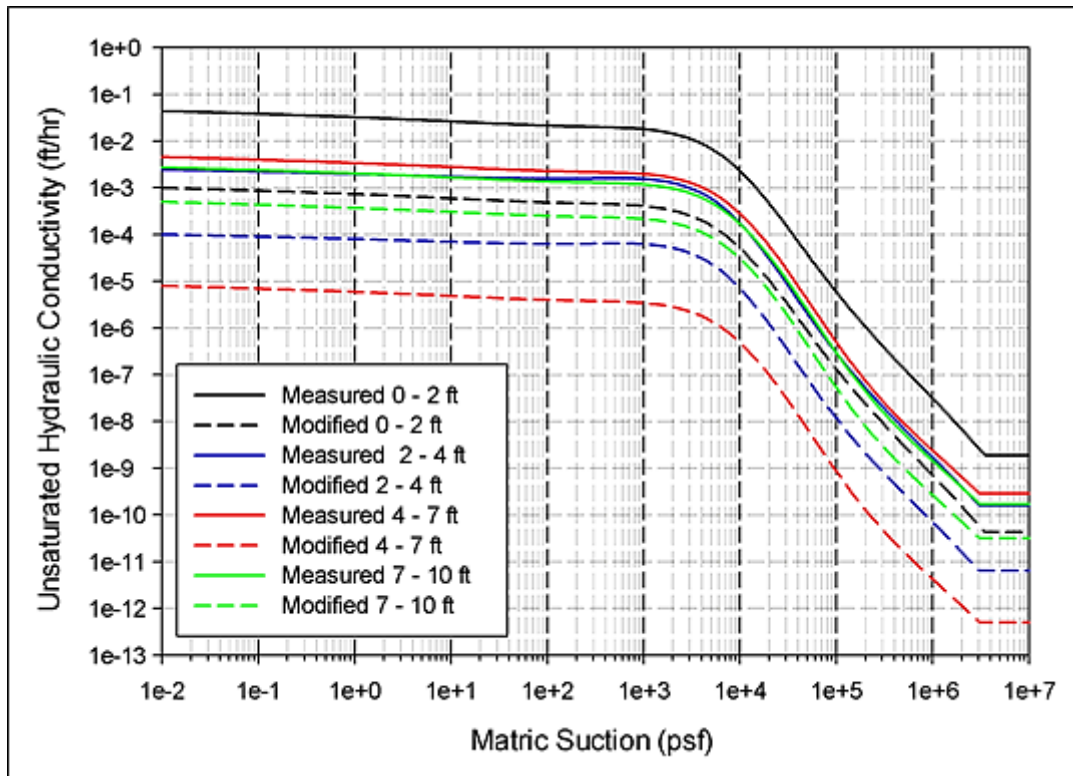


Figure 4. 5. Goldsby: hydraulic conductivity-suction curves.

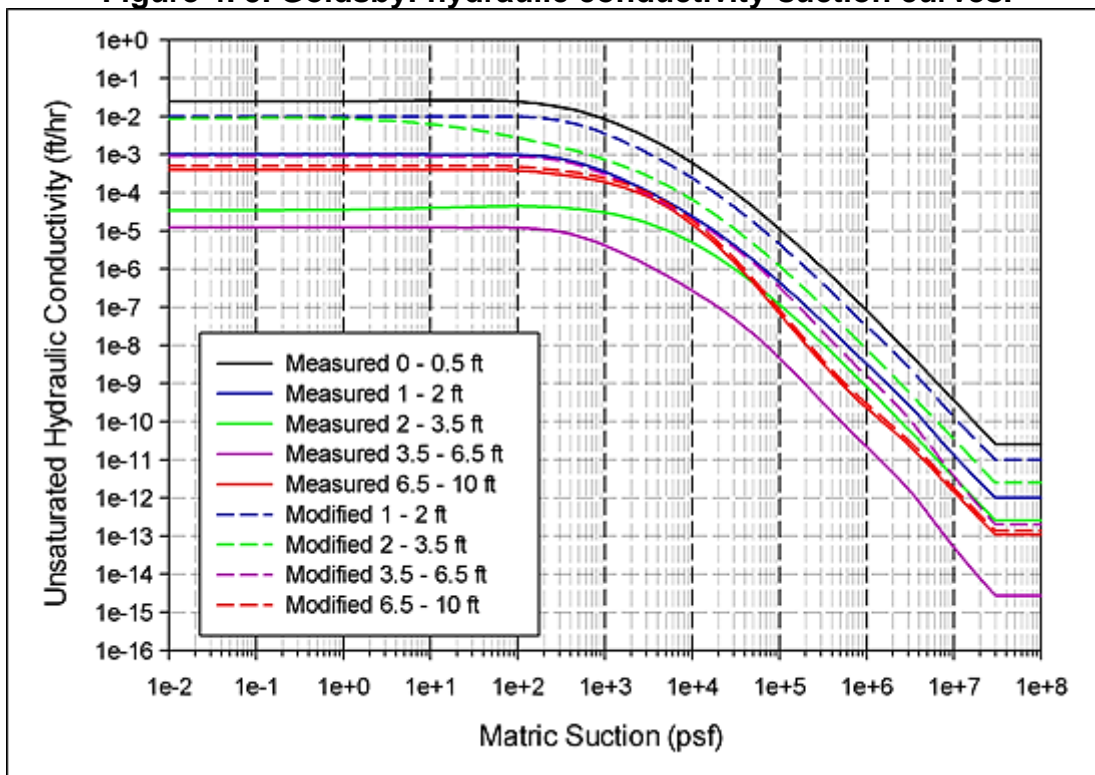


Figure 4. 6. North Base: hydraulic conductivity-suction curves.

## **Chapter 5 RESULTS FROM FIELD WEATHER INSTRUMENTATION AND SOIL MOISTURE MONITORING**

### **5.1 Weather Data from the North Base Site**

Data were collected from the weather monitoring station located at the North Base site in Norman, Oklahoma between August 24, 2012 and October 20, 2014. Figures 5.1, 5.2 and 5.3 show plots of the following information: 1) average daily air temperature, 2) wind speed, 3) maximum daily relative humidity, 4) maximum and minimum air temperature, 5) total daily solar radiation, 6) precipitation, and 7) average daily soil volumetric moisture content and temperature at depths of at 1, 3 and 6 ft.

The factors that most affect the air temperature are: the latitude, altitude and cloud coverage. The city of Norman is located at 35.22° North of the equator and at an elevation of about 1,171 ft above sea level. The average temperature ranges between a maximum of 105°F to a minimum of 5°F. Between December and January, it was noticed that the average air temperature drops to the minimum, and then increases gradually to its maximum between July and August. Similar factors also influence the total solar radiation. In fact, the highest value of solar radiation was recorded during the longest day in a calendar year which happens to be in June when the duration of solar radiation is the longest and the solar angle of incidence is the greatest. Interestingly, the maximum recorded value of solar radiation equal to 2,581 BTU/ft<sup>2</sup> corresponds to June and not July or August when the atmospheric temperature is the highest. This is due to the fact that the amount of precipitation and water vapor increase at the end of the summer thus keeping the air temperature high but with reduced intensity of the solar radiation.

The soil temperature was measured at 1, 3 and 6 ft. The maximum soil temperatures recorded at each depth were from 84°F at 1 ft. on September 6, 2012, 80°F at 3 ft. two days later, and 73°F at 6 ft. four days later. This time lag corresponds to the time needed for the soil to dissipate solar energy. The observed annual variation follows the pattern for air temperature rather than the solar radiation as shown in Figure 5.2. The highest recorded soil temperatures were between July and September, and the lowest were in between January and March. These values are mostly influenced by the soil moisture content, rainfall, net solar radiation, vegetation cover, soil texture, soil thermal conductivity and heat capacity.

The rainfall distribution during the monitoring period is shown in Figure 5.1 and tabulated for in Table 5.1. As the relative humidity increases in warm weather conditions, the chances for rainfall also increase. In fact, high precipitation occurred in spring and summer months and generally lower in fall and winter. Relative humidity is influenced mostly by air temperature and latitude.

The daily pattern of soil moisture content is not complete for portions of the record for all depths due to some equipment limitations. However, a reasonably good picture of moisture variations can be extrapolated from the data. For a depth of 1 ft., the soil moisture content profile shows the seasonal variation with weather conditions. It can be noted that relatively rapid drying at shallow depth can occur during summer and fall months when temperatures and solar radiation are high. Desiccation cracks likely enhance the rate of drying and wetting during these months. Soil moisture changes at a depth of 3 ft. are significant but not as sensitive to shorter, intense drying and wetting

events compared to the shallower depth. Soil moisture changes at a depth of 6 ft. are gradual and not very large compared to measurement locations at 1 and 3 ft.

Similar types of weather data were also collected from the Oklahoma Mesonet monitoring station located in Norman, through the [daily data retrieval website tool](http://www.mesonet.org/index.php/weather/daily_data_retrieval) ([http://www.mesonet.org/index.php/weather/daily\\_data\\_retrieval](http://www.mesonet.org/index.php/weather/daily_data_retrieval)). The data were collected for the same period corresponding to the dates of monitoring at the test sites. Comparisons of data obtained from the test sites and Mesonet stations are shown in Figures 5.4 to 5.6. The comparison between the two sets of data indicates some differences between the total daily solar radiation, wind speed, and relative humidity; however, general trends and magnitude of values are in reasonable agreement. Measured average air temperature and total amount of rainfall are relatively close at the two sites.

## **5.2 Weather Data from the Goldsby Site**

Similar weather data was collected from the weather station installed at the second test site located in Goldsby, McClain County, Oklahoma. Weather data for the Goldsby site are presented in Figures 5.7, 5.8 and 5.9. The general wetting and drying patterns at both sites are similar and specifically between March 2013 and August 2014. This is due to the fact that the test site weather stations are 5.5 miles away from each other. At Goldsby, the moisture sensors at depths of 3 feet and particularly 6 feet seem slightly more responsive to weather changes than for similar depths at North Base. This may be due to greater permeability of the lower plasticity soils at Goldsby.

The comparisons between the weather data obtained from the Goldsby site and the nearest Mesonet station are shown in Figures 5.10, 5.11 and 5.12. The comparisons indicate similarities in the various measurements. There appears to be some slight differences between the amount of precipitation and average wind speed at the two sites. This might be explained by the fact that the Mesonet station used for comparison is located in Norman, approximately 5.5 miles north of the Goldsby site. Additionally, the Goldsby site measurements may be slightly affected by the highway embankment approximately 80 yds to the south and the RV dealership 125 yds to north of the weather station.

**Table 5. 1. Total monthly rainfall during the monitoring period recorded at the North Base test site.**

<b>Month</b>	<b>Year</b>	<b>Rainfall (inches)</b>
September	2012	1.18
October	2012	0.37
November	2012	0.9
December	2012	0.34
January	2012	0.32
February	2012	1.16
March	2012	0.61
April	2012	1.85
May	2012	1.98
June	2012	1.15
July	2012	3.73
August	2012	1.02
September	2013	1.31
October	2013	0.7
November	2013	1.56
December	2013	0.4
January	2013	0.02
February	2013	0.13
March	2013	0.73
April	2013	0.25
May	2013	0.24
June	2013	1.36
July	2013	0.8
August	2013	0.71

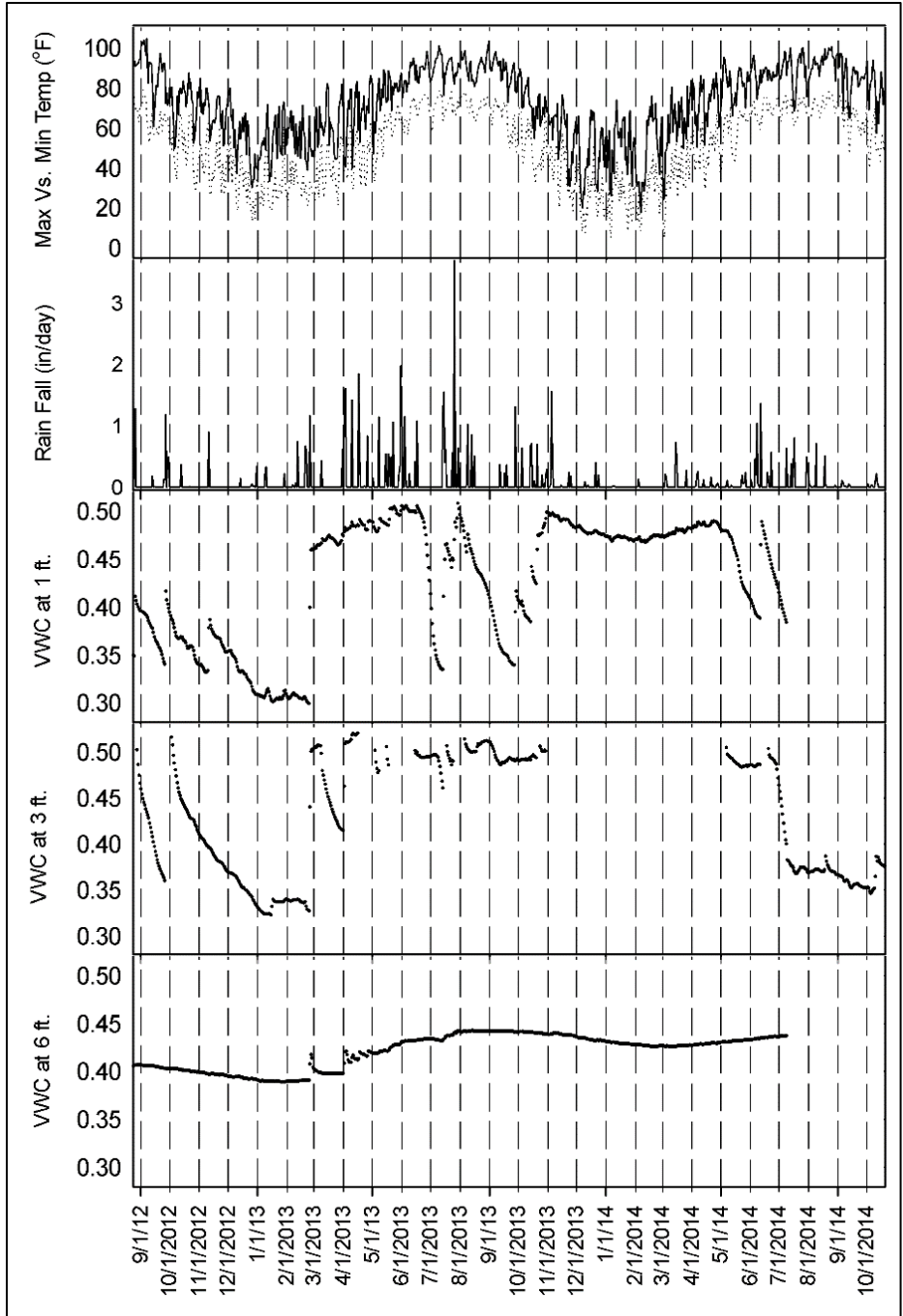


**Figure 5. 1. North Base: maximum and minimum daily temperature, total rainfall, and volumetric water content at the test site.**

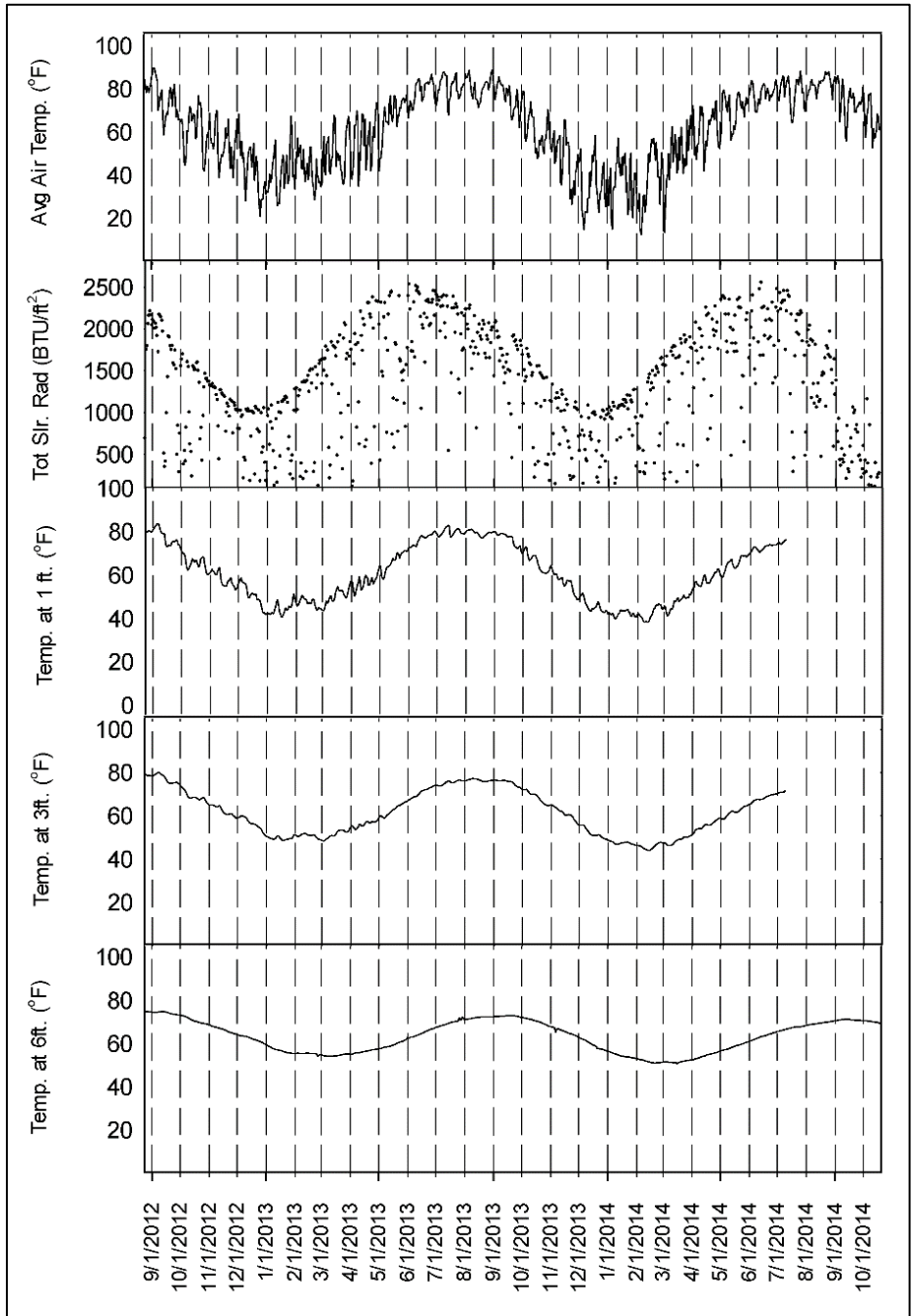


**Figure 5. 2. North Base: daily average temperature, total solar radiation, and subsurface soil temperature at the test site.**

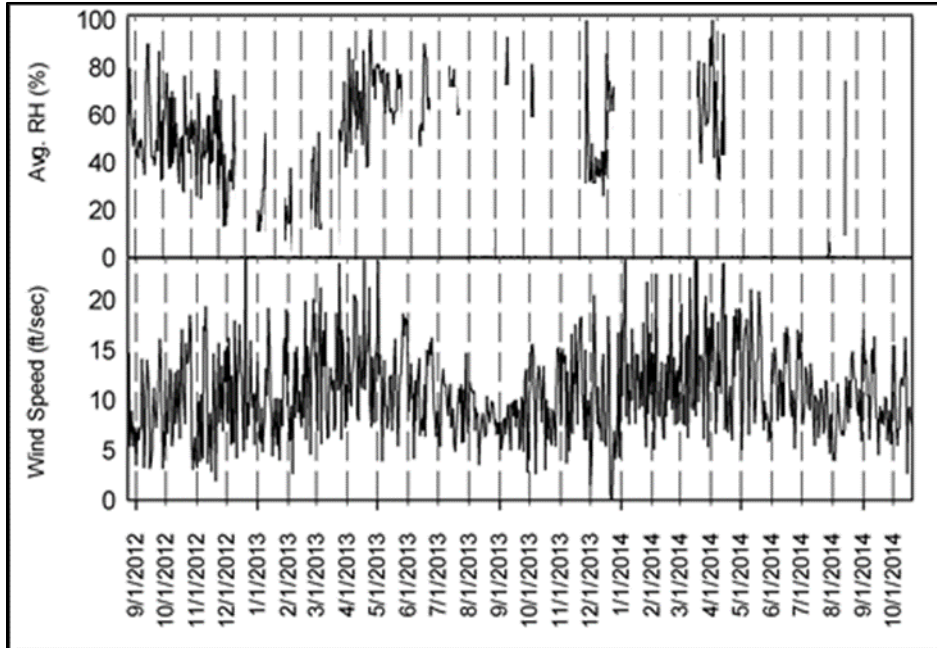


Figure 5. 3. North Base: Daily average relative humidity and average wind speed at the test site.

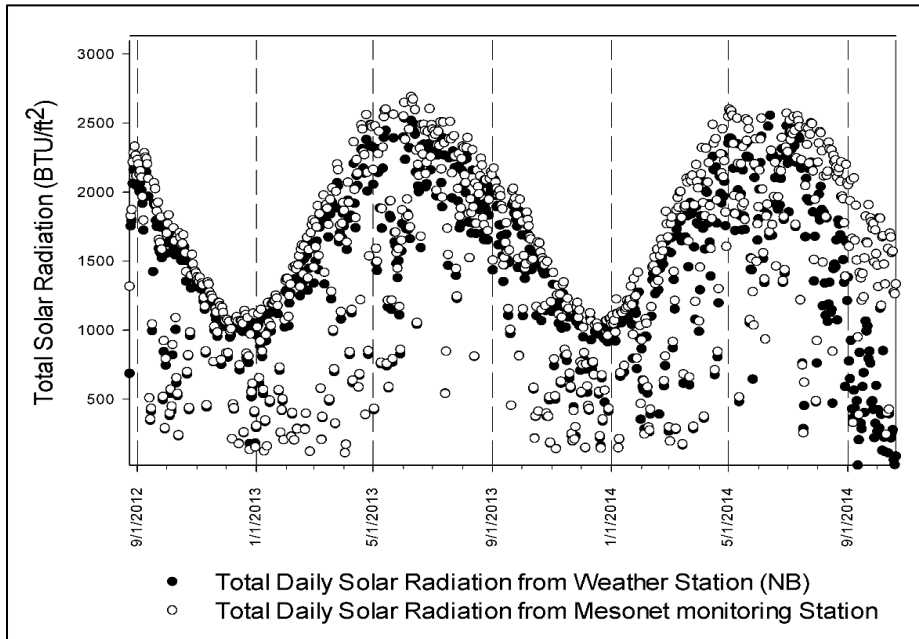
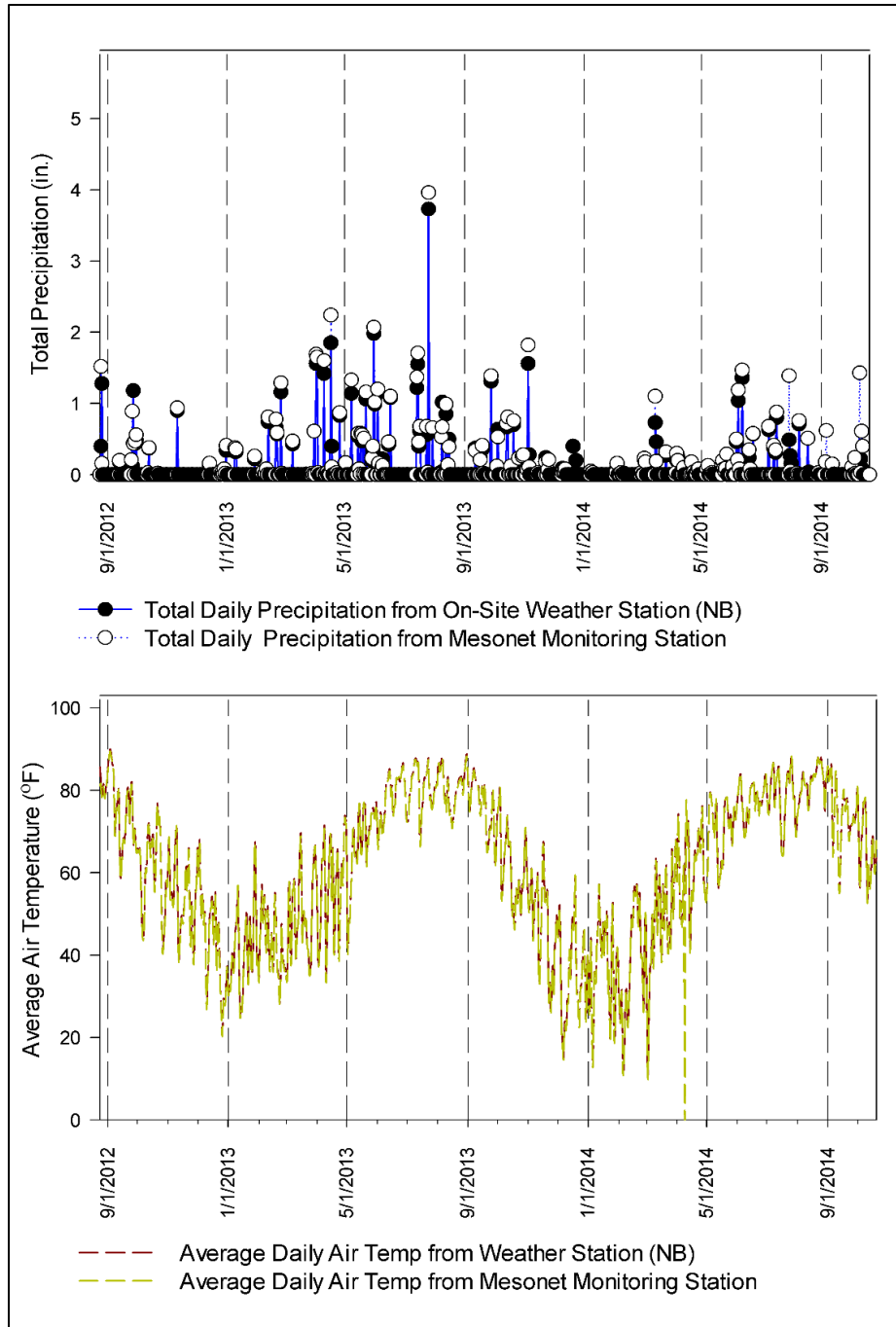
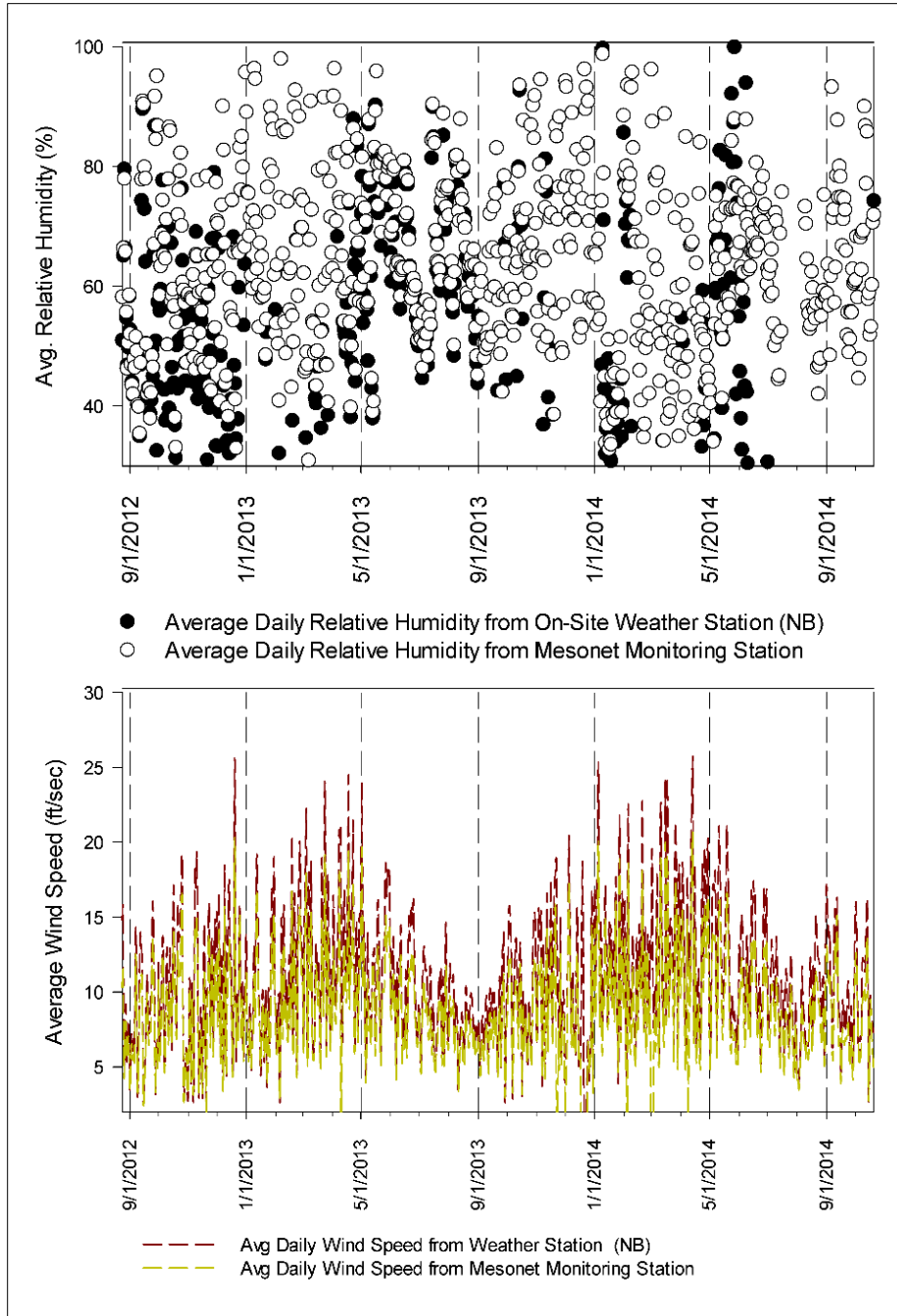


Figure 5. 4. North Base: total daily solar radiation data from the test site and nearest Mesonet station.



**Figure 5. 5. North Base: total daily precipitation and air temperature from the test site and nearest Mesonet station.**



**Figure 5. 6. North Base: average daily relative humidity and wind speed from the test site and nearest Mesonet station.**

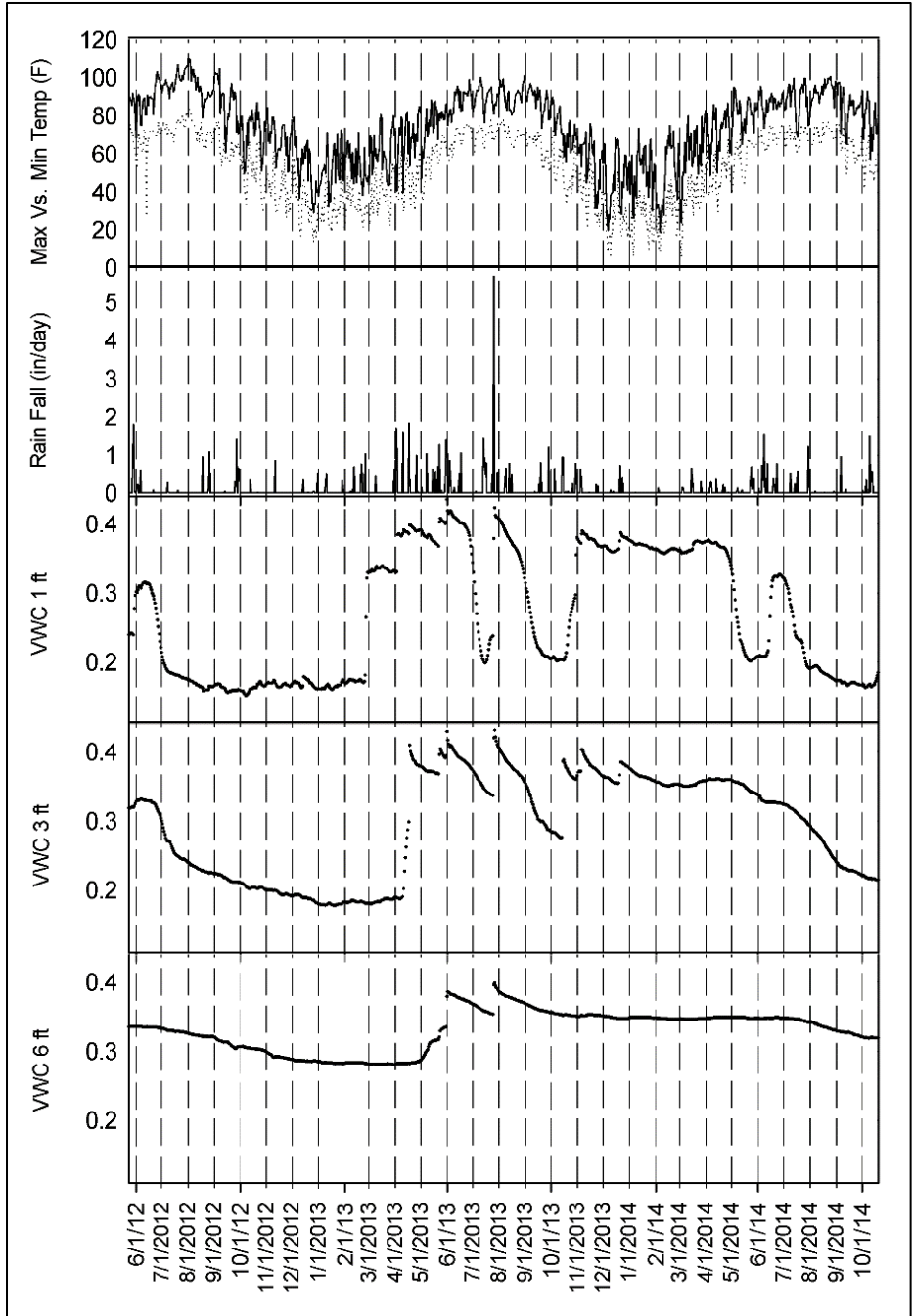


**Figure 5. 7. Goldsby: daily maximum and minimum temperature, total rainfall, and volumetric water content at the test site.**

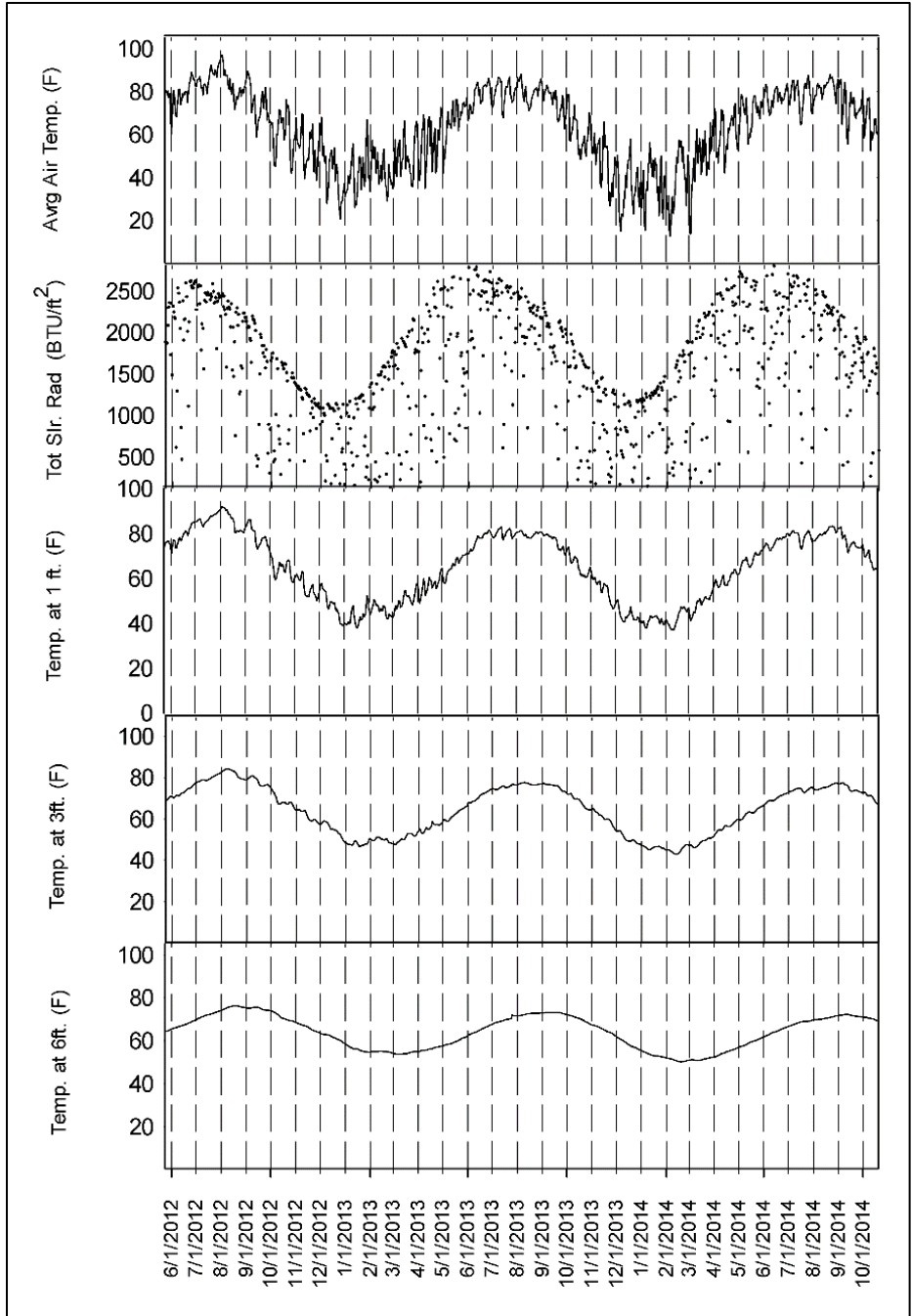


**Figure 5. 8. Goldsby: daily average temperature, total solar radiation, and subsurface soil temperature at the test site.**

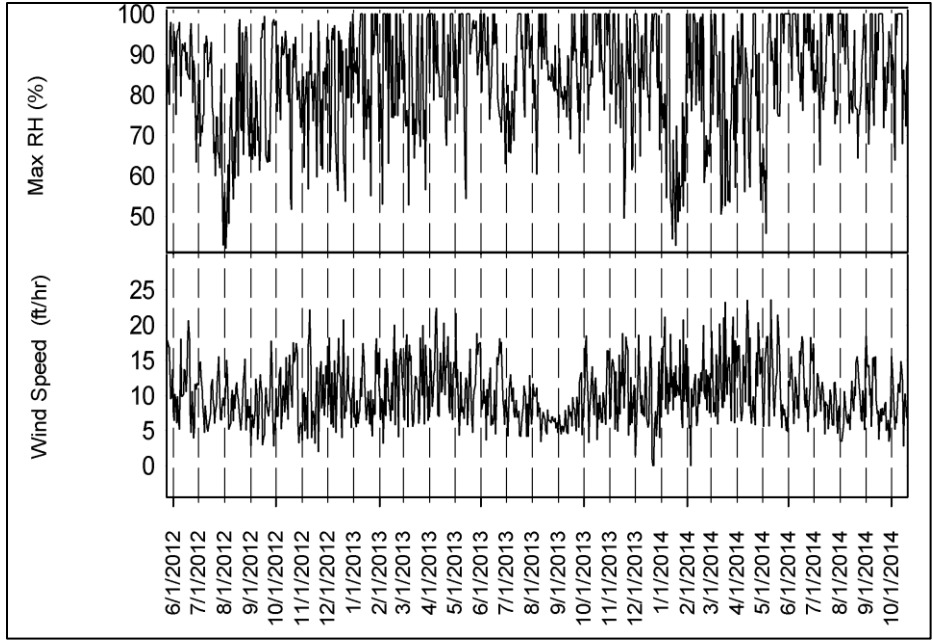


**Figure 5. 9. Goldsby: daily maximum relative humidity and average wind speed at the test site.**

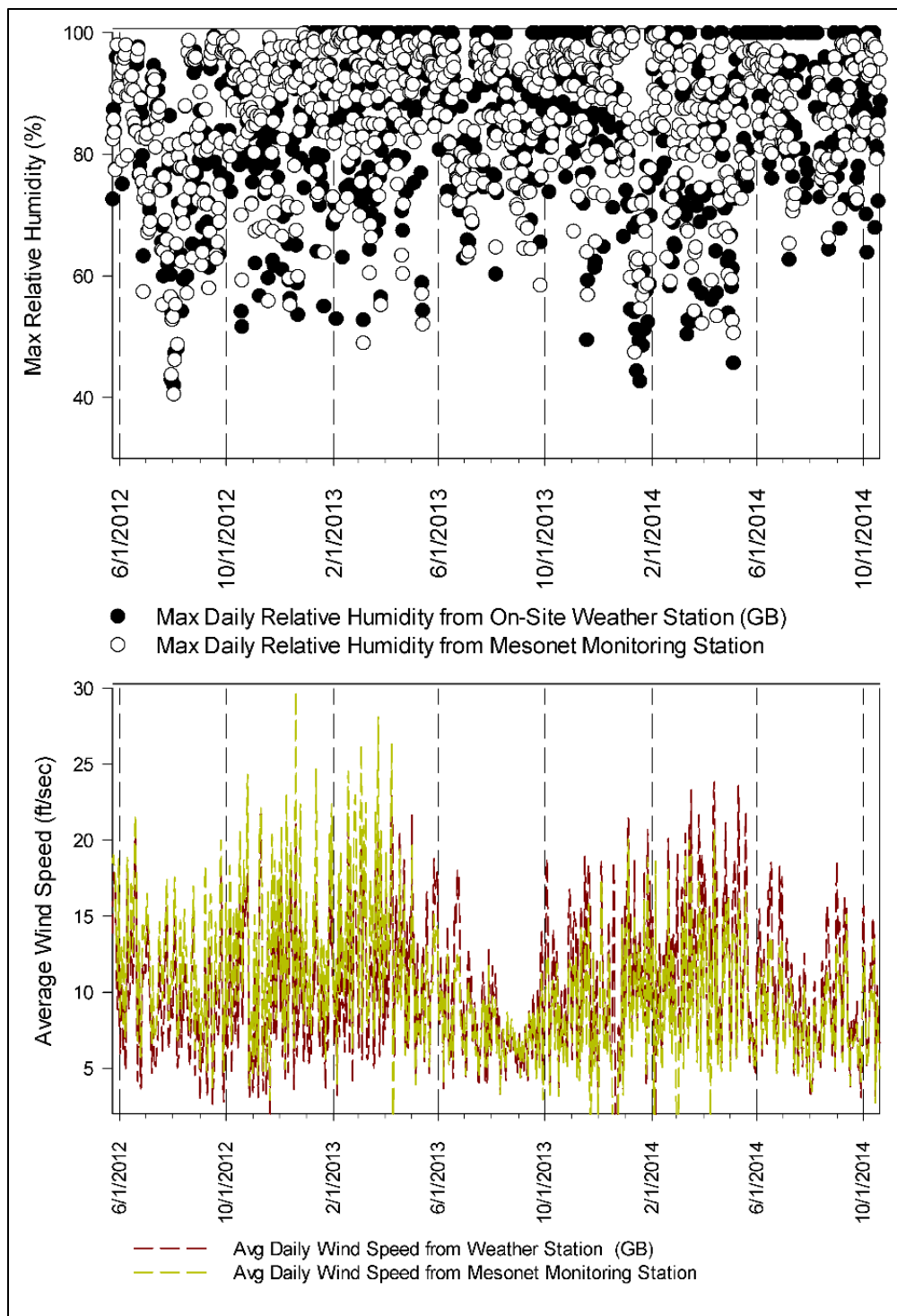


**Figure 5. 10. Goldsby: average daily relative humidity and wind speed from the test site and nearest Mesonet station.**

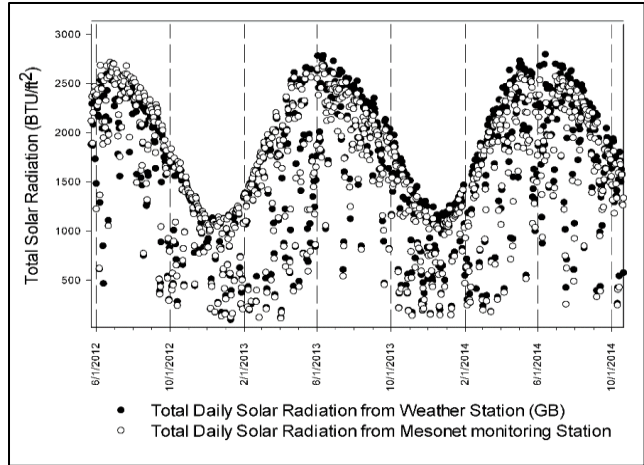


**Figure 5. 11. Goldsby: total daily solar radiation data from the test site and nearest Mesonet station.**

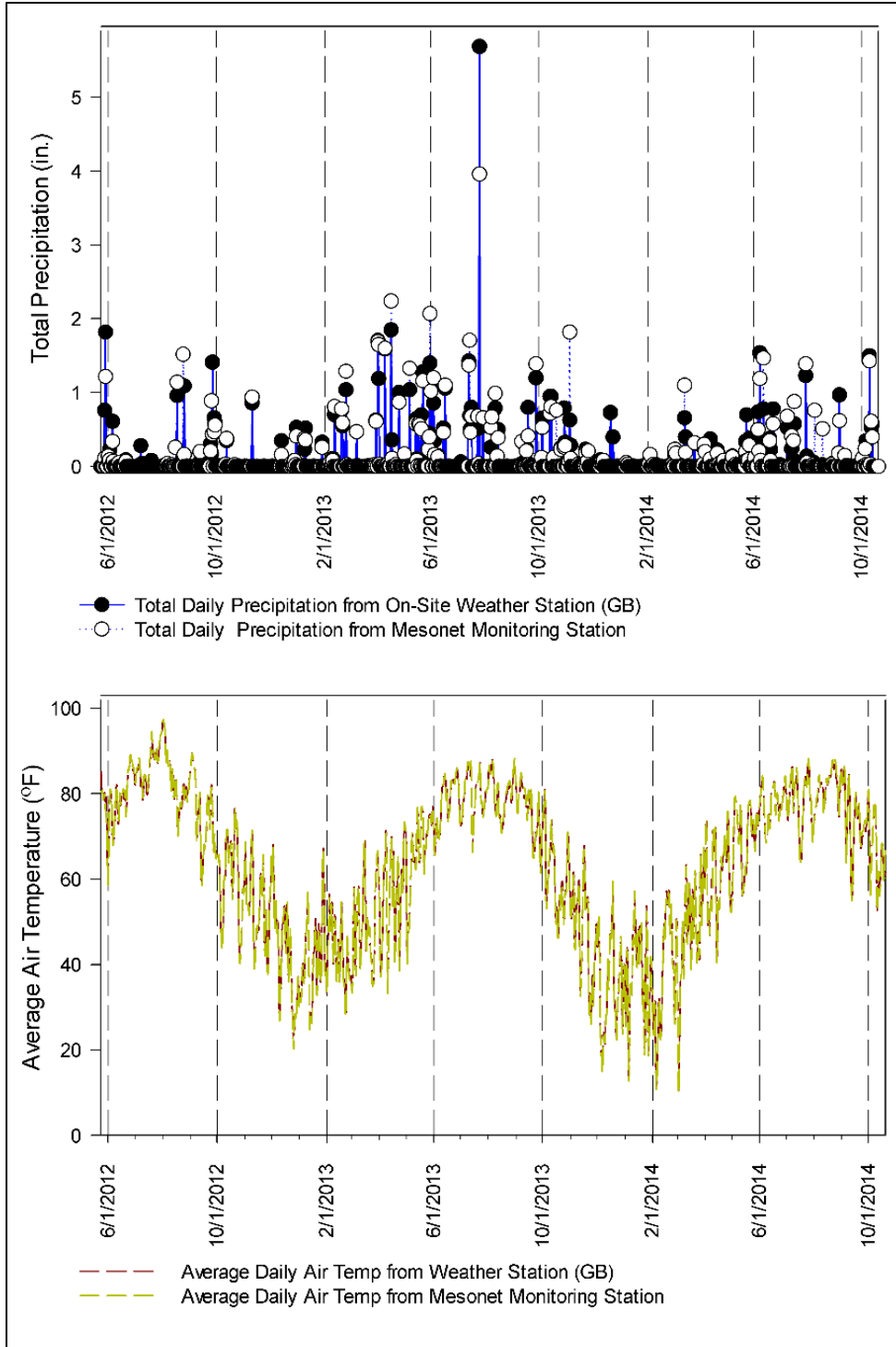


**Figure 5. 12. Goldsby: total daily precipitation and air temperature from the test site and nearest Mesonet station.**

## **Chapter 6 MODELING MOISTURE VARIATIONS IN SOIL PROFILES**

### **6.1 Introduction**

In this project, the volumetric water content at test depths is predicted for the two test sites using two computer programs that model the interaction between the ground and the atmosphere. This chapter describes the results of the modeling as well as the basic soil input parameters and initial conditions at both sites. The simulation of the ground-atmosphere interaction requires information about the initial soil suction and temperature profile in addition to other boundary conditions related to the weather and flow conditions at the top and bottom boundaries of the soil column, respectively. For both sites, a zero total flow boundary condition was assigned to the deepest layer at both sites. This is due to the fact that at 10ft a hard layer was encountered at North Base, and relatively little soil moisture variation was encountered at Goldsby below a depth of 6 feet.

### **6.2 Moisture Modeling, Goldsby**

To design a 1-D model with an element thickness of 1 it is necessary to first set units to imperial and then the page scale. VADOSE/W simplifies this step by calculating automatically maximum extents from scale and origin values. The units set for both programs are shown in Table 6.1.

The type of finite element seepage analysis that is selected is a transient analysis, since water pressures and flow rates are always changing with weather conditions. The boundary conditions are changing with time, therefore selecting a

steady state analysis would be incorrect. The general input parameters are shown in Table 6.2.

A transient analysis requires information about the initial soil pressure conditions (at  $t = 0$  hours). There are several options available to set the initial water pressures including: special function, water table, or input from another analysis method. In this transient analysis, the initial soil water content (Figure 6.1) and VWC function shown in Figure 4.3 and Figure 4.4 were used to define the pressure head functions (Figure 6.2).

The initial head pressure profile was determined from soil suction and moisture content measurements from soil samples collected from test sites when the weather stations were first installed. Figures 6.1 and Figure 6.2 show the initial pressure head values used in the model for North Base and Goldsby. The solvers interpolate between these measured values to have a complete pressure head profile.

These models were run for a total duration of 2 years and 41 days or 21,120 hours. The total running time that would be expected would range between 5 to 7 hours, which depends on the type of computer that is being used. The time steps go hour by hour to capture the changes in moisture and temperature conditions. It is recommended to use one day-time steps or less while solving a climate boundary condition using VADOSE/W. The head pressure is allowed to change by only 5% between successive steps. Also, VADOSE/W allows the use of adaptive time steps that give additional time steps when the solution is not converging. The allowable time steps range was set to be between 9 seconds, and 1 hour.

VADOSE/W recommends to calculate the change in hydraulic head from nodal heads in a 1-D model where there are sharp drying and wetting fronts. SVflux on the

other hand defines the time steps automatically, which is considered a good advantage for the user and the analysis in general.

It is very important to enable the vegetation option, as it will affect greatly the predicted values of the soil's volumetric water content. This will be explained in more detail in the following sections. There is also an option to turn on or off the ponding at the ground surface as a climate boundary condition as shown in Table 6.3. Since the ground surface that is modeled is flat, ponding allows water to infiltrate and is not lost from the system.

Figure 6.3, shows the sketch of the soil column of 4 layers and one additional surface layer used in the analysis for soil-atmosphere interaction. The depth of each layer was determined based on identified soil characteristics and depths of interest, namely at 1 ft, 3 ft and 6 ft.

### **6.3 Material Properties and Property Functions, Goldsby**

Four main functions were determined before assigning them to the corresponding layers. First, the volumetric water content data point function that defines VWC ( $\text{ft}^3/\text{ft}^3$ ) versus matric suction (psf). The 'curve fit' and 'curve segments' are two tools that were used for curve fitting. The coefficient of volume compressibility ( $m_v$ ) is a measure of volume change per unit increase in soil effective stress in saturated conditions (Soil-Vison, 2009). In VADOSE/W it is suggested to use a small value of  $1.0\text{e-}5 \text{ kPa}^{-1}$  ( $4.78\text{e-}7 \text{ psf}^{-1}$ ); however, in SVFlux this value is relatively critical to the analysis for some types of soils.

To estimate an unsaturated hydraulic conductivity function for soils at different depths, the model requires a corresponding volumetric water content function. There are two options to find  $K_{\text{usat}}$ , either an estimation function by Van Genuchten or by Fredlund and Xing, with the only difference that the first requires some data related to the residual water content value. It is recommended to define  $K_{\text{usat}}$  over the full pressure range from zero to -20,800,000 psf. The corresponding  $K_{\text{ratio}}$  that was used is equal to 1, such that  $K_y = K_x * K_{\text{ratio}} = K_x$ . This assumes the hydraulic conductivity is isotropic with respect to flow in different directions.

VADOSE/W uses two different estimation methods to determine the thermal conductivity (Figure 6.4) and volumetric specific heat functions (Figure 6.5). Typical values of thermal conductivity and volumetric specific heat for the materials are based on soil mineralogy. The Johansen method requires a material mineral thermal conductivity. Therefore, a value of 3.35 BTU/hr/ft/°F was used, and that corresponds to sandstone and shale type minerals most commonly found at both sites. In addition, a volumetric water content function and activation temperature were also defined. Activation values correspond to the initial soil temperatures measured at both test sites. The solver uses the activation values as initial values at the start of the analysis.

Similarly, to define the volumetric heat capacity it is required to determine a mass specific heat function for soil minerals. This value is equal to 0.17 Btu/ (lb\*°F) and along with the determined activation temperature value, the De Vries method (1952) was used to determine the volumetric heat capacity functions as shown in Figure 6.5. In Table 6.4 a summary of the material property parameters used in the moisture flux modeling are presented.

## 6.4 Top and Bottom Soil Boundary Conditions and FEM Mesh Control for Goldsby and North Base

After setting up material properties as shown in Table 6.4, and assigning them to geometrical regions, the boundary conditions at the top and bottom of the soil profile should be specified. To specify the climate boundary condition, VADOSE/W and SVFlux require information about the latitude of the site location to estimate the net radiation. Also for VADOSE/W the user has to specify a sinusoidal daily rainfall distribution, where the maximum amount of rainfall would occur in the middle of the day. On the other hand, SVFlux, distributes the total amount of rainfall evenly throughout the day.

Other parameters that are required are the average wind speed, maximum and minimum relative humidity, temperature as well as vegetation. The input data related to the vegetation parameters are the leaf area index (LAI), root depth (RD), and plant moisture limit (PML). The LAI function determines the amount of solar energy that is intercepted by the grass cover. As the area covered by grass is larger, more solar energy is absorbed by the plants rather than the soil. To determine the LAI function, the first day of the grass growing season was set to 60 days and the last day to 365 as shown in Figure 6.6. The growing season corresponds to the time between the first and last frost in the fall and the spring, respectively (VADOSE/W, 2007).

VADOSE/W uses built-in functions that allows the user to set the quality of leaf coverage to excellent, good or poor; in addition to other parameters such as the root depth (Figure 6.8). As to the plant moisture limiting function, a spline data point function was defined based on past research studies related to the plants wilting point and transpiration demands. Figure 6.7 shows the plant moisture limiting (PML) factor versus

matric suction; it can be observed that for suctions higher than 3000 psf the PML factor decreases to zero.

The layers were subdivided into smaller pieces or finite elements; this process is called meshing. To properly model the ground surface process, it is recommended in VADOSE/W to use quadrilateral elements rather than triangular, because the initial unknown hydraulic gradients are steep in the vertical direction compared to other directions. Table 6.6 shows the input parameters used to define the regional mesh. SVFlux, on the other hand, uses an automatic meshing system that changes with the rate of change in the hydraulic gradient.

VADOSE/W has an advanced surface layering system that tries to take care of the cyclic soil shrinkage and swelling. Setting a surface layer mesh allows the activation of the surface ponding option; thus, water that does not immediately infiltrate is allowed to pond.

### **6.5 Ground-Atmosphere Interaction Predictions, Goldsby, VADOSE/W**

The analysis was conducted by using the actual saturated hydraulic conductivity values and soil-water pressure characteristic properties determined by laboratory testing. The predicted and measured values of volumetric water content are shown in Figures 6.9 to 6.11, along with the amount of rainfall precipitation with time. The predicted volumetric water content curve follows a trend similar to measured values, but the magnitude of changes is different. The predicted soil moisture doesn't build-up as much nor decrease as drastically as the measured values; specifically between the periods of July and

August 2013, in addition to May 2014. This is especially true for results of modeling for the 1 foot and 3-foot depths shown in Figures 6.9 and 6.10.

The predicted results in Figure 6.9 (1 ft) show a steep drop in the initial 80 days, during which the amount of water leaving and entering the ground surface is high. This might be due to the high measured hydraulic conductivity value for the upper layer. That is, the predicted water content does not build-up with time, whereas the actual-measured values gradually increase with successive rainfall events. The change in volumetric water content between the cycles of wetting and drying is not well predicted; however, by adjusting the hydraulic conductivity functions the model can be calibrated to provide better predictions. In a practical situation this would not be possible without measured data and so it may be preferable to test the hydraulic conductivity in the field specifically for the upper layer in addition to using the flex-wall method.

A sensitivity analysis was conducted to determine the hydraulic conductivity value that would produce the best fit prediction compared to actual measured values. It was found that the saturated hydraulic permeability had to be decreased by two orders of magnitudes. Other factors might also apply such as the model does not take into account the soil desiccation cracks, or overestimates the amount of evapotranspiration during the summer.

Rainfall infiltrates through the top layer reaching the second layer and the atmospheric influences decrease with depth, which can be seen for the 3-ft depth predictions in Figure 6.10. The predicted water content significantly increases during the summer of 2013 where it reaches a value of  $0.4 \text{ ft}^3/\text{ft}^3$ . However, the percent increase is not considerably high compared to the measured results. On the other hand, the

predicted values also decrease significantly during the first 120 days, which might be due to the fact that the first layer has a higher permeability value and thus releases water-vapor easily to the atmosphere, under a strong negative head pressure.

It can be observed from Figure 6.11 for a depth of 6 ft, that the changes in soil moisture content in deep soil layers are mostly indicative of seasonal variations rather than atmospheric forcing. In fact, it can be seen that in all three summers or 2012, 2013, and 2014, the soil moisture content starts decreasing to reach the minimum VWC during the fall (October 2012, October 2014). Starting November or December the soil moisture starts to increase or reach a steady state condition. In fact, it was observed that the soil samples collected from 6 ft deep were warm and moist and had high amount of water vapor that condensed once the sample was put in a plastic bag.

Looking at the predicted results, it is evident that the solver overestimates the atmospheric influences on deep layers same as it does for surface layers. There are several possible reasons for these discrepancies including: 1) the model does not pick-up the high rate of percolation during the summer possibly caused by desiccation cracks, 2) rainfall events that happened before June 2012 (the start date of the analysis) had contributed to an increase in VWC values, 3) there are problems with the field measurements, 4) the model permeabilities were too high compared to actual permeabilities.

## **6.6 VADOSE/W Predictions using Modified Ksat, Goldsby**

Several modeling sequences have been performed using VADOSE/W to determine the parameters that have the greatest effect on predicted values. The factors that change

the predicted values significantly when compared to actual-measured values are as follows: initial pressure head values, saturated hydraulic permeability, VWC function, and vegetation.

In this section, only the hydraulic conductivity function was changed while keeping all other parameters the same. Figure 6.12, shows the results obtained after decreasing the saturated permeability for the first layer from  $4.40 \times 10^{-2}$  ft/hr to  $1.00 \times 10^{-3}$  ft/hr. The predicted curve matches well the measured values; however, the new predictions do not match adequately the consecutive rainfall events that occurred in June and July 2014. This is probably due to the fact that desiccation cracks are not properly considered in the analysis process. It should be also noted that decreasing the permeability has increased the predicted values corresponding to the fall and winter season of 2012 (120 days till 280 days). Therefore, decreasing the permeability almost solved the discrepancy issue between the measured and predicted values specifically during the summer, but created another issue during the winter. The added increase in soil moisture between October 2012 and March 2012 contributed to the increase in the predicted values for the summer of June 2013 and August 2013. However, this increase was minimal during the summer of 2014 where soil evaporation, and low permeability were more significant compared to soil-water characteristics. It can be seen that there is a compromise between trying to match the measured winter and summer VWC. On one hand, we want the moisture content to rise during the summer, and on the other hand to remain within the measured range of VWC during the winter.

Figure 6.13, shows a very good correlation between the measured and predicted values, but this does not completely apply to the period between October 2012 and April

2013 where the soil water accumulation is more noticeable compared to the results obtained from the surface layer.

Figure 6.14, shows the predicted values of the volumetric water content at 6 ft. The changes that were done include the adjustment of the saturated permeability for the soil in the layers 1 to 4. The corresponding values were decreased to a point where the soil is capable of retaining the infiltrated rainwater and condensed water vapor; however, this has reduced the sensitivity of the soil to rainfall events and specifically between April and May 2013.

### **6.7 Ground-Atmosphere Interaction Predictions, Goldsby, SVFlux**

The soil properties and boundary conditions were assigned to the soil column using SVFlux. The soil column for Goldsby is shown in Figure 6.15. The results of SVFlux soil moisture predictions are shown alongside the VADOSE/W predictions and measured values in Figure 6.16, 6.17 and 6.18 for the corresponding depths of 1 ft, 3 ft, and 6 ft. The comparison between the results obtained from the two solvers and the field data showed that SVFlux generally better predicts the moisture variation due to weather conditions compared to VADOSE/W. However, discrepancies between the predicted and measured values are mainly observed during the summer. This is specifically the case in June when solar radiation is the highest and ending in August or October during in which several consecutive rainfall events were recorded but not picked-up well by the model. The fact that the soil moisture content is not “recharged” during the summer, causes an under-prediction during the winter.

Figure 6.17, shows that throughout the monitoring time, the total-measured VWC at 3 ft is generally higher than the measured VWC at 1 ft. The predicted values at 3 ft are higher than those predicted at 1 ft.

Figure 6.18, shows that the soil water at 6 ft is not highly affected by the atmospheric forcing. VWC values exhibit a cyclic change in the measured volumetric water content values over a period of two years. In fact, there is a long time lag between several rainfall events and the increase in a volumetric water content at this depth. These values do not vary significantly between June 2012 and April 2013, as well as between October 2013 and July 2014, which contradicts what was predicted by both models where the soil water content seems to be affected somehow by weather changes.

## **6.8 Sensitivity Analyses**

Figure 6.19 shows the results obtained from VADOSE/W after changing the hydraulic conductivity values of the surface layer. As the permeability increases the soil becomes more sensitive to rainfall events and loses water and vapor much easier. In fact, for a permeability value of  $5 \times 10^{-4}$  ft/hr the predicted soil moisture content decreases 20% a few days after the rainfall event that happened on June 7, 2012, whereas the actual-measured values decreased only by 6%. The effect of the atmospheric forcing is not well adjusted in the two solvers even when an excellent grass cover system (LAI of 3) was used. Therefore, as the hydraulic conductivity increases the soil moisture content does not build-up over time, but the time lag between a certain rainfall events and an increase in VWC decreases. On the other hand, it was noticed that using a low

permeability of about  $1.5 \times 10^{-5}$  ft/hr would not “allow” soil-water to build-up efficiently because the surface runoff would be high as rainfall is not able to infiltrate.

## **6.9 Moisture Modeling, North Base**

VADOSE/W allows the user to select between simplified thermal and full thermal soil properties, which makes soil moisture predictions less or more accurate. Many factors influence the soil moisture and water vapor flux within a soil column, including head pressure and temperature gradients. Therefore several full-thermal soil materials were defined and assigned to the soil layers shown in Figure 6.20, which corresponds to a modeled soil column at North Base.

VADOSE/W uses several estimation functions developed by Johansen (1975) to define the thermal conductivity and volumetric heat capacity functions shown in Figure 6.21 and Figure 6.22, respectively. It can be seen that as the soil moisture increases, temperature increases too. Therefore, the soil temperature in unsaturated soils should decrease, when soil moisture decreases. This was observed from the measured soil temperature, where the lowest soil temperatures were an indication of a significant decrease in soil moisture. In general, the amount of soil moisture is larger in North Base than in Goldsby, which might be related to several factors explained in the following sections.

Figure 6.22, shows that as soil becomes more saturated it is more difficult to raise the soil temperature by one degree. This implies that the migration water vapor towards colder areas would mostly happen when there is a significant temperature gradient between the deepest layer in the vadose zone and the surface layer.

Table 6.7, shows all the input parameters that were used to define the material properties. These parameters are similar to both solvers with the exception of the coefficient of compressibility and the function for fitting the SWCC curve. Such as the Van Genuchten and Mualem functions (1980) used in SVFlux, versus Fredlund and Xing's (1994) functions in VADOSE/W. The other parameter differences between the two models are related to the root depth and leaf area index function definition. The LAI in SVFlux is a constant value, while that in VADOSE/W is a changing function similar to the one used for Goldsby.

### **6.10 Ground-Atmosphere Interaction Predictions, North Base, VADOSE/W**

The soil at North Base has more sand at the surface layer compared to the soil at Goldsby. In fact, about 90% to 95% passes sieve No. 200 at GB versus 85% at NB. As to the lower layers, the soil becomes sandier at Goldsby and finer at North Base where the percent of fine grained soils is about 85% to 91%. Figure 6.23, shows a more significant change in the soil moisture content at North Base than Goldsby. In fact, water infiltrates easily through the surface layer and percolates slowly to the deeper layers. VADOSE/W was able to predict well the change in the volumetric water content with the increase in weather conditions except for the period between December 2013 and May 2014. This might be possibly due to the fact that VADOSE/W did not take into account the desiccation cracks that have developed during the summer.

Similar to the results obtained at Goldsby, the volumetric water content measured at 3 ft is higher than that measured at 1 ft. Also, the volumetric water content at NB reaches a maximum of  $0.52 \text{ ft}^3/\text{ft}^3$  (Figure-24) versus  $0.42 \text{ ft}^3/\text{ft}^3$  for GB.

Both the negative head pressure gradients that develop during the summer at the top layer, as well as the cold soil temperature at the same location, forces the water vapor and water to flow from the lowest layers towards the surface. Figure 6.25 for the 5-foot depth shows a small decrease in the volumetric water content during the winter (January and February 2012) and a small increase during the summer (August 2013). The predicted results show a good agreement with the measured values at this location.

### **6.11 VADOSE/W Predictions using Modified Ksat, North Base**

The model predictions using the modified saturated conductivity has not caused a significant improvement in the predictions as shown in Figure 6.26, Figure 6.27, and Figure 6.28. Decreasing the saturated conductivity has made the soil more sensitive to rainfall precipitation, but at the same time caused an over prediction of the VWC values at 1 ft, and 3 ft, and a little improvement during the 2012 and 2013 winter seasons.

Figure 6.28 showed that when the hydraulic conductivity was increased, the predicted values were a little better during the summer but the soil is influenced more by weather conditions rather than seasonal changes. Therefore, keeping the measured hydraulic conductivity is generally better than the modified value.

Figure 6.29 shows a set of several sensitivity analyses that were conducted where the permeability function was increased to try to obtain better predictions. It was noticed that the saturated hydraulic permeability for both Goldsby and North Base had the greatest influence on the results, along with other parameters like the SWCC function, vegetation, and compressibility coefficients (SVFlux).

## 6.12 Results of Model Predictions, North Base, SVFlux

Figure 6.29, shows a sketch of a soil column at North Base having a similar layer distribution as the one drawn using VADOSE/W. Also, the exact same input parameters used to model the soil atmosphere interaction in VADOSE/W, were used in SVFlux without change to the unsaturated permeability function, coefficient of compressibility and leaf area index.

SVFlux uses the volume compressibility value ( $m_v$ ) to adjust the change in the volume of voids between low and high gradients; however, this does not compensate for the presence of desiccation cracks between dry and wet cycles. On the other hand, it was noted in VADOSE/W software's manual that the coefficient of volume compressibility does not need to be accurately defined for most unsaturated soil seepage problems, and it was suggested to use a small value. Figure 6.31, 6.32, and 6.33 showed that the low amount of water infiltrated through the first layer affected the predictions of all subsurface layers.

**Table 6. 1. Units and phase change related values.**

<b>Engineering Units</b>	<b>Latent Heat of Water (Btu)</b>	<b>Phase Change Temp. (°F)</b>	<b>Unit Weight of Water</b>
Imperial: Btu, days, feet, °F, lbs	8,975	32	62.4 lb/ft <sup>3</sup>

**Table 6. 2. Key in analysis input parameters.**

<b>Analysis Type</b>	Transient Coupled
<b>Initial Water Pressures from:</b>	Pressure Head Spatial Function
<b>Initial Temperature</b>	None
<b>Starting Time (hr)</b>	0
<b>Duration (hr)</b>	21,120
<b>Number of Steps</b>	21,120
<b>Adaptive Time Steps</b>	Calculate from nodal heads
<b>Maximum percent change in head per step</b>	5
<b>Allowable Minimum Time Step</b>	0.0024
<b>Allowable Maximum Time Step</b>	1

**Table 6. 3. Advanced options for ponding and vegetation.**

<b>Include Vegetation</b>	Yes
<b>Allow Surface Water to Pond on Ground Surface</b>	Yes

**Table 6. 4. Goldsby material input parameters.**

<b>Material Property or Program Setting</b>	<b>Layer 1: Depth = 0-2 ft.</b>	<b>Layer 2: Depth = 2-4 ft.</b>	<b>Layer 3: Depth = 4-7 ft.</b>	<b>Layer 4: Depth = 7-10 ft.</b>
Thermal Properties Setting	Full Thermal	Full Thermal	Full Thermal	Full Thermal
K-Ratio	1	1	1	1
Saturated K <sub>x</sub> (ft/hr)	4.40E-02	2.46E-03	4.57E-03	2.73E-03
Minimum Suction (psf)	0.01	0.01	0.01	0.01
Maximum Suction (psf)	3.50E+06	3.10E+06	3.10E+06	3.10E+06
M <sub>v</sub> (1/psf)	4.79E-06	4.79E-06	4.79E-06	4.79E-06
Mineral Thermal K (BTU/hr/ft/°F)	3.35	3.35	3.35	3.35
Activation Temperature (°F)	73.62	68.35	64.27	64.16
Mass Specific Heat (BTU/g/°F)	3.75E-04	3.75E-04	3.75E-04	3.75E-04

**Table 6. 5. Climate and vegetation boundary conditions.**

<b>Location Latitude</b>	<b>Energy Data Source</b>	<b>Distribution Pattern</b>
35	Estimated Net Radiation	Sinusoid (hrs)
<b>Start Dates (mm/dd/yyyy)</b>	<b>Day No.</b>	<b>Temp (°F)</b>
First Day	1, 2, 3...	Max and Min per day
<b>Relative Humidity</b>	<b>Wind Speed (ft/sec)</b>	<b>Precipitation (in)</b>
Max and Min per day	Average/day	Sum of daily rainfall
<b>Precipitation Period Start and End (hr)</b>	<b>LAI function</b>	<b>LAI Cycle Function</b>
0 - 24	Estimated spline data point function	✓
<b>First Day of Growing Season</b>	<b>Last Day of Growing Season</b>	<b>Grass Quality</b>
60	365	Excellent
<b>PML</b>	<b>Root Depth Distribution</b>	<b>RD Cycle Function</b>
Spline data point function	Triangular	✓

**Table 6. 6. Mesh properties.**

<b>Region</b>	<b>Finite Element Mesh Pattern</b>	Rectangular Grid of Quads
	<b>Element Edge Length</b>	Use Default Size (0.175 ft)
	<b>Quadrilateral Elements</b>	4
<b>Line</b>	<b>Generate mesh along line</b>	-
	<b>Edge length: Number of Divisions</b>	1
<b>Surface Layer</b>	<b>Approximate Global Element Size</b>	0.175 ft
	<b>Number of Elements in Vertical Direction</b>	2
	<b>Number of layers</b>	1

**Table 6. 7. North Base material input parameters.**

<b>Material Property or Program Setting</b>	<b>Layer 1: Depth = 0-0.5 ft.</b>	<b>Layer 2: Depth = 0.5-1 ft.</b>	<b>Layer 3: Depth = 1-2 ft.</b>	<b>Layer 4: Depth = 2-3.5 ft.</b>	<b>Layer 5: Depth = 3.5-6.5 ft.</b>	<b>Layer 6: Depth = 6.5-10 ft.</b>
Thermal Properties Setting	Full Thermal	Full Thermal	Full Thermal	Full Thermal	Full Thermal	Full Thermal
K-Ratio	1	1	1	1	1	1
Saturated $K_x$ (ft/hr)	2.50E-02	2.45E-02	9.99E-04	3.44E-05	1.23E-05	3.93E-04
Minimum Suction (psf)	0.01	0.01	0.01	0.01	0.01	0.01
Maximum Suction (psf)	3.00E+06	2.00E+06	3.00E+06	3.00E+06	3.00E+06	3.00E+06
$M_v$ (1/psf)	4.79E-06	4.79E-06	4.79E-06	4.79E-06	4.79E-06	4.79E-06
Mineral Thermal K (BTU/hr/ft/°F)	3.35	3.35	3.35	3.35	3.35	3.35
Activation Temperature (°F)	74.67	74.67	74.67	74.67	74.67	74.67
Mass Specific Heat (BTU/g/°F)	3.75E-04	3.75E-04	3.75E-04	3.75E-04	3.75E-04	3.75E-04

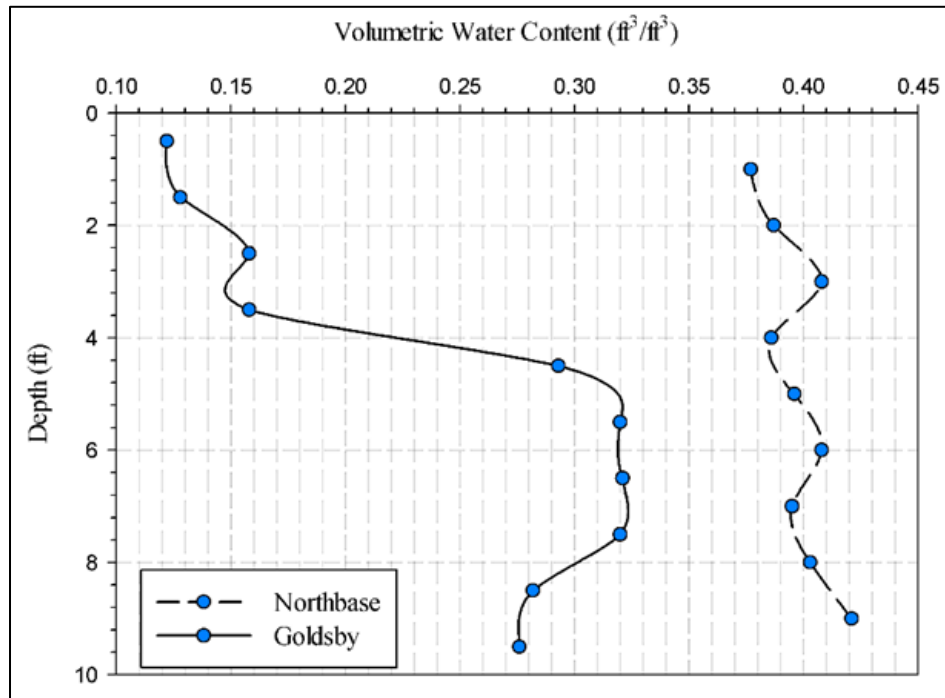


Figure 6. 1. Initial soil profile volumetric water contents.

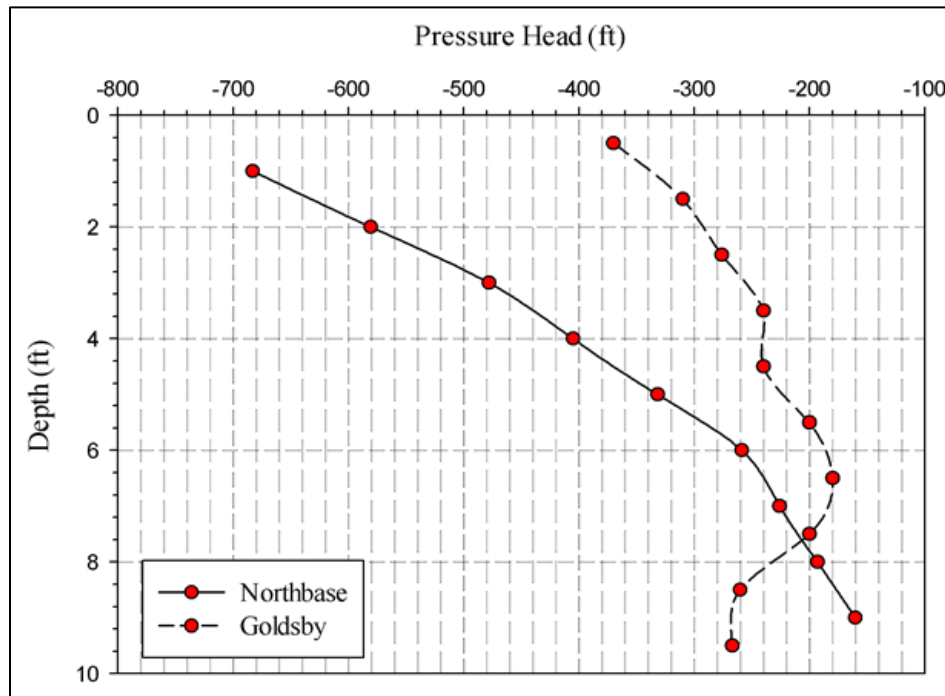


Figure 6. 2. Initial soil profiles pressure head.

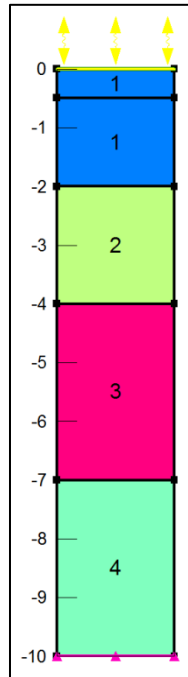


Figure 6. 3. Goldsby: VADOSE/W soil column.

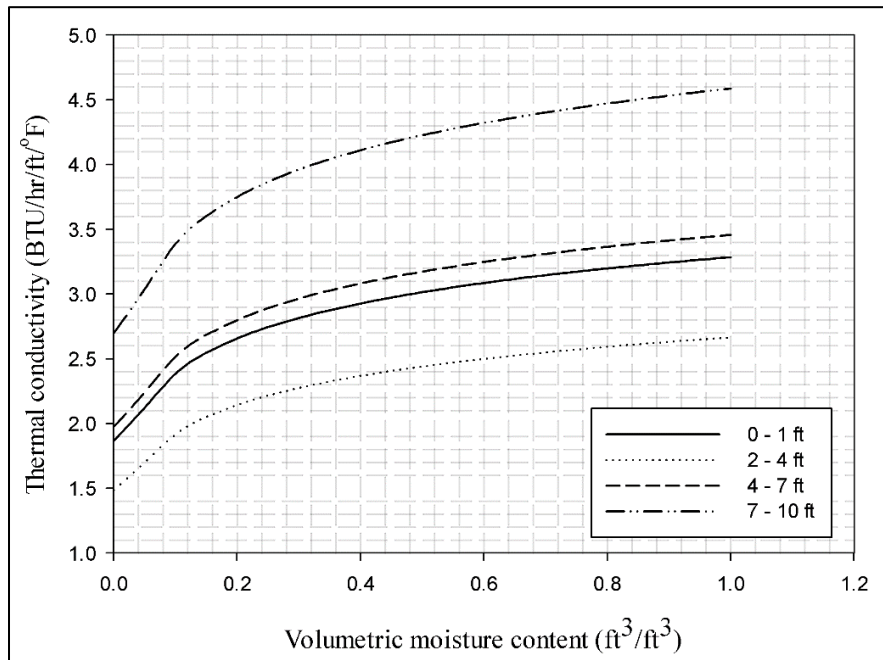


Figure 6. 4 Goldsby: estimated thermal conductivity curves.

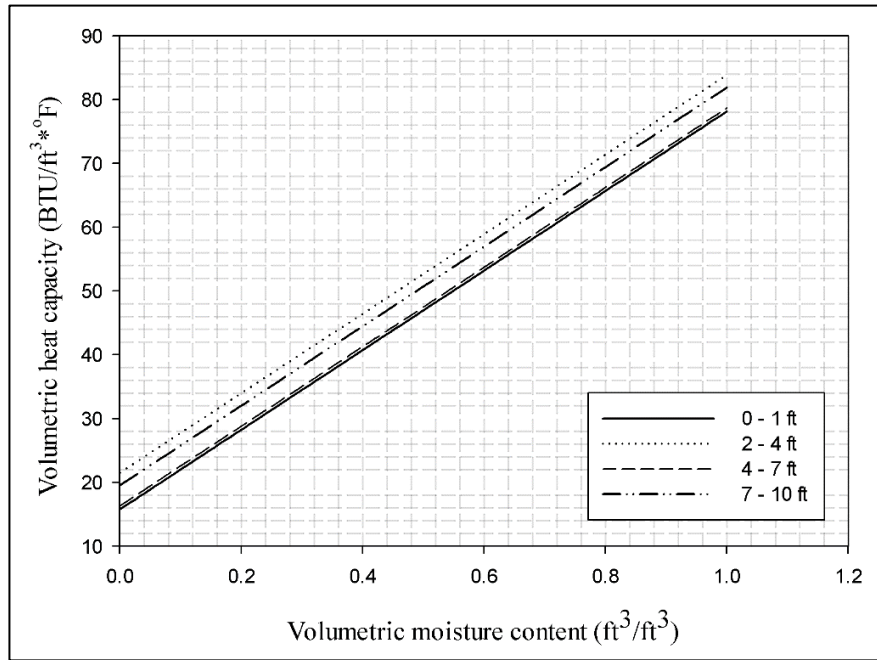


Figure 6. 5. Goldsby: estimated volumetric heat capacity functions.

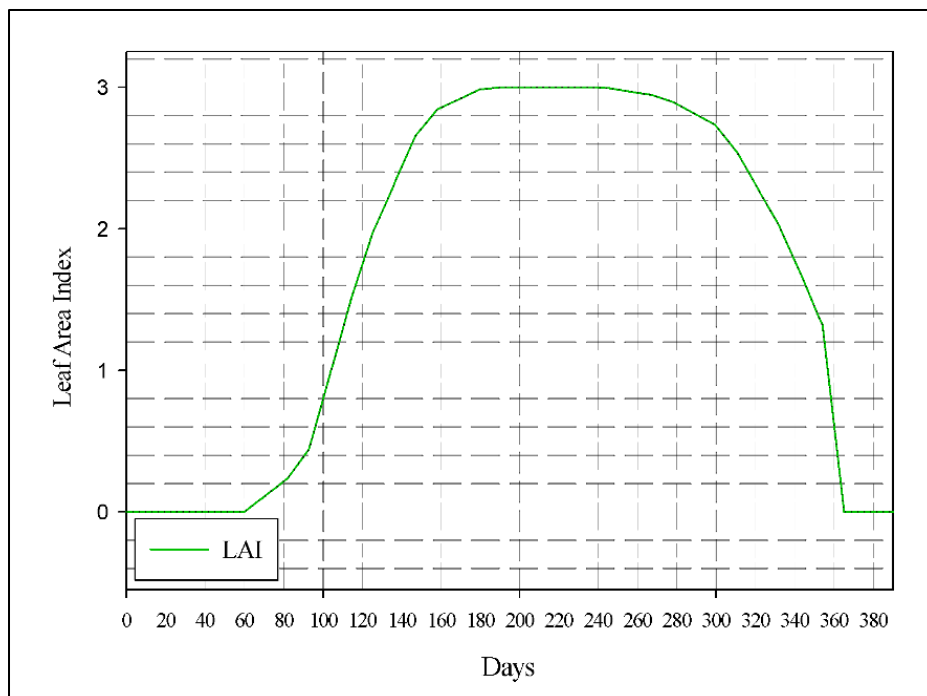


Figure 6. 6. Estimated LAI function for both sites.

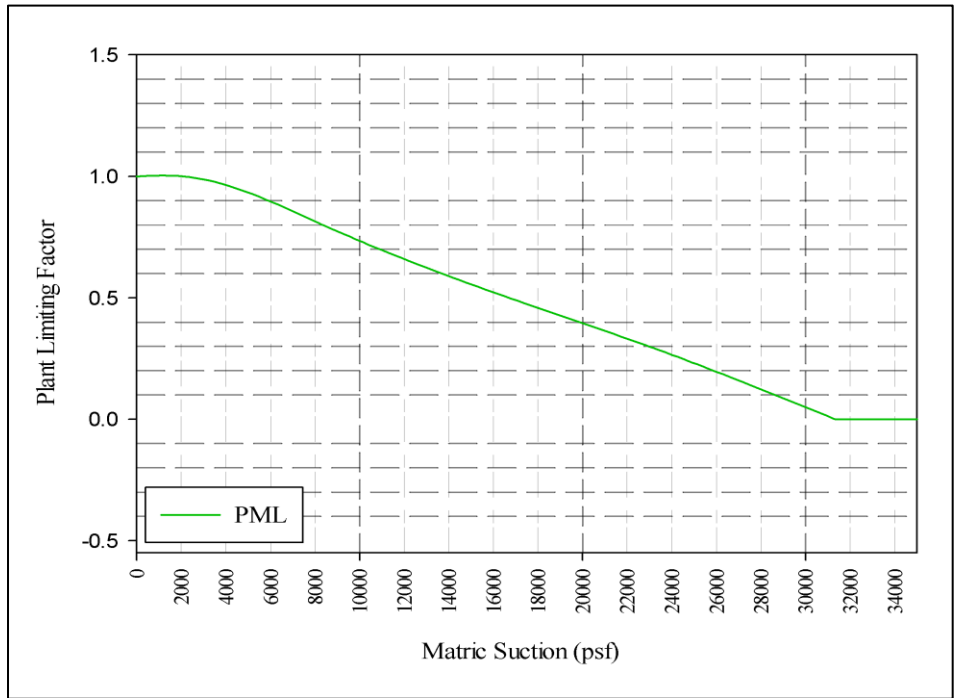


Figure 6. 7. Typical plant moisture limiting function for most types of grasses.

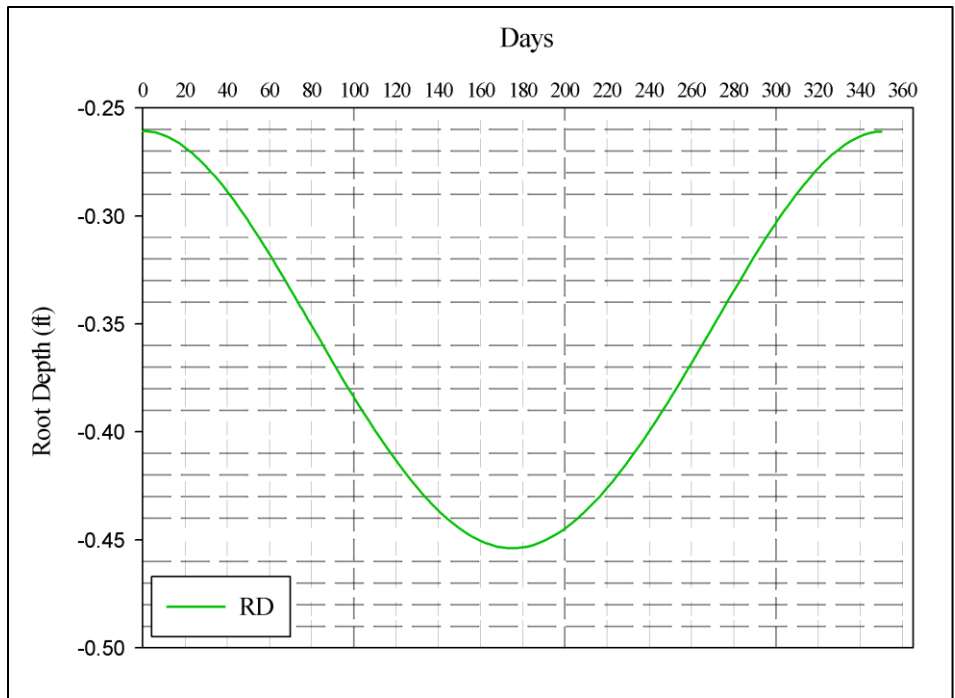


Figure 6. 8. Estimated root depth function.

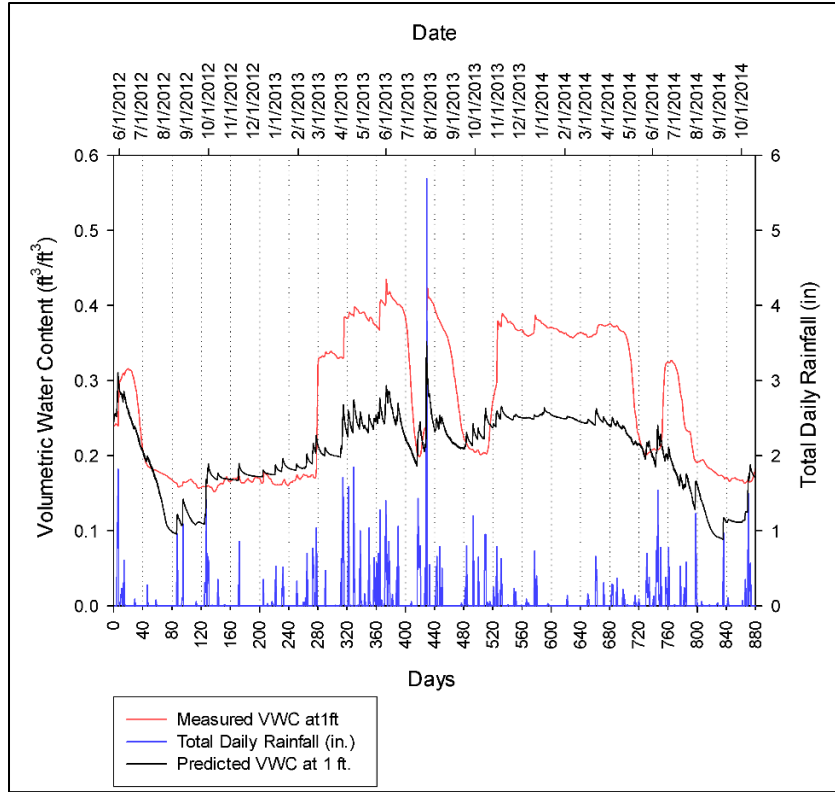


Figure 6. 9. Goldsby: predicted vs. measured VWC values at 1 ft depth.

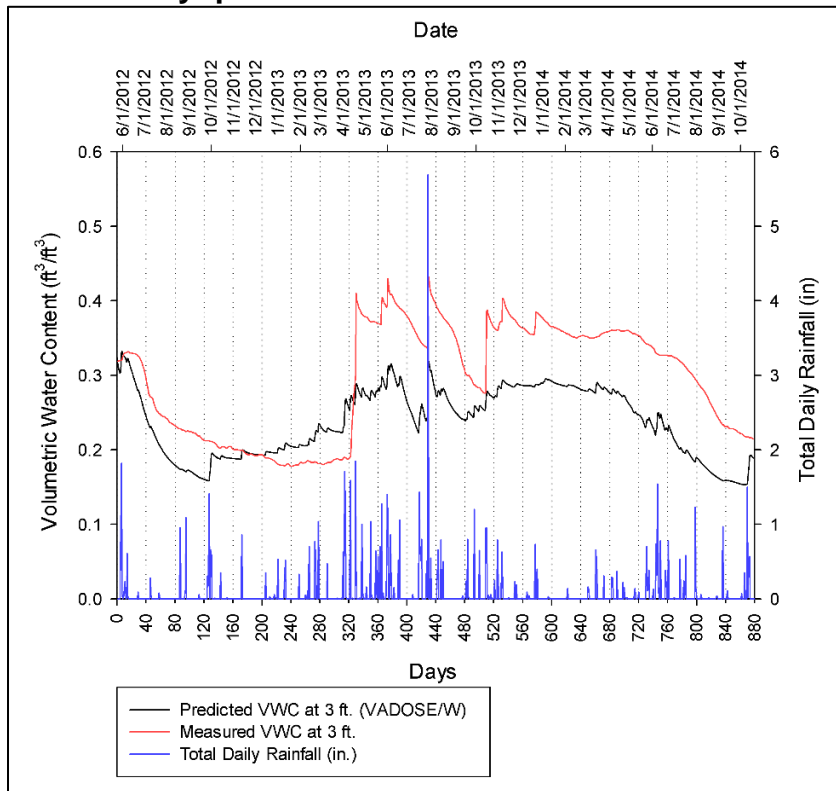


Figure 6. 10. Goldsby: predicted vs. measured VWC values at 3 ft depth.

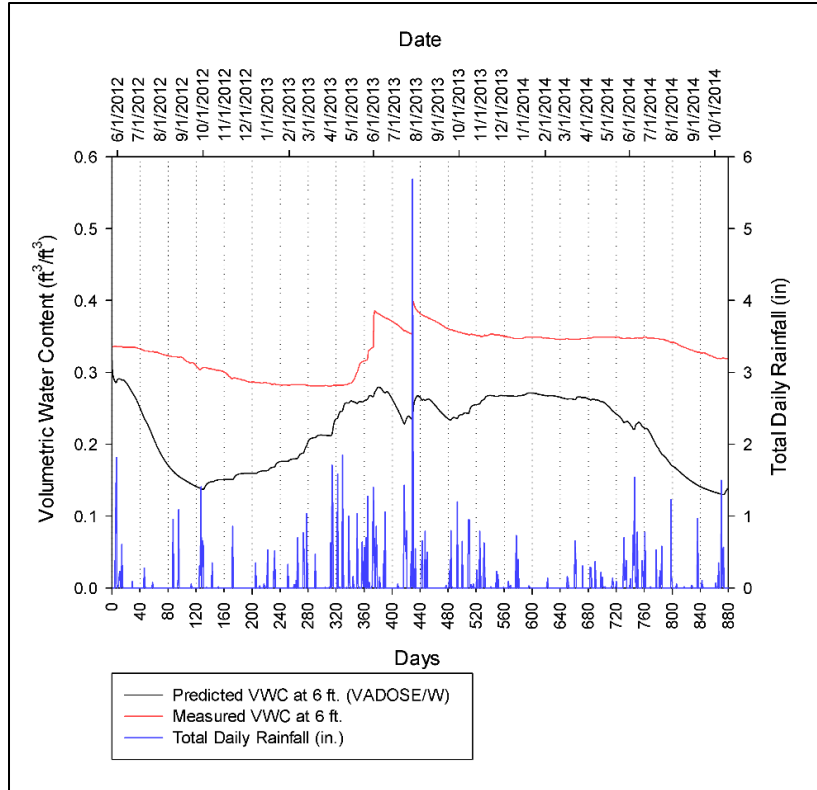


Figure 6. 11. Goldsby: predicted vs. measured VWC values at 6 ft depth.

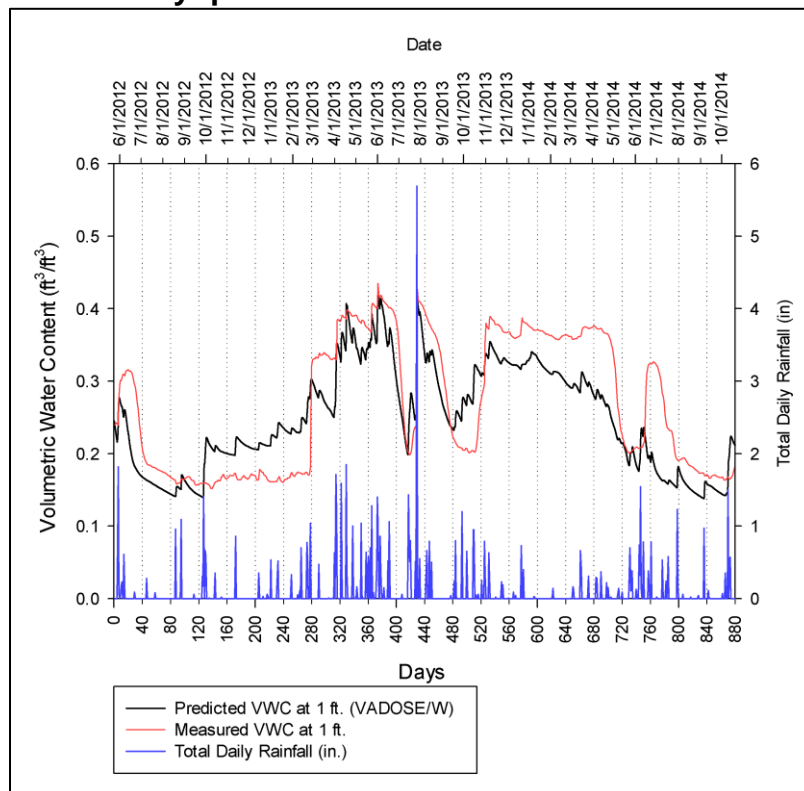


Figure 6. 12. Goldsby: measured vs. predicted VWC values using the modified Ksat value for 1 ft depth.

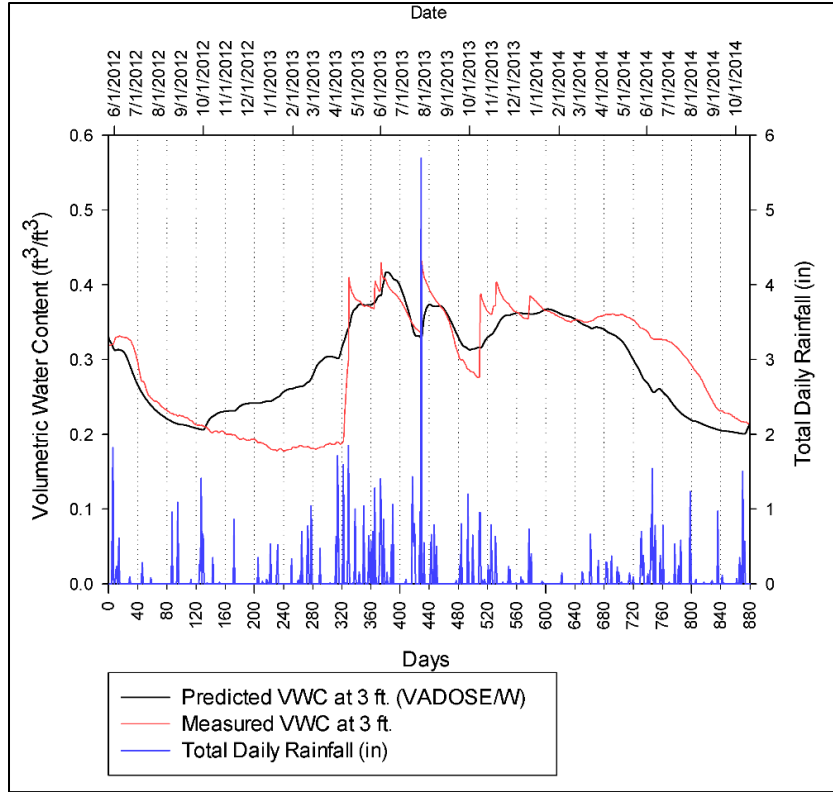


Figure 6. 13. Goldsby: measured vs. predicted VWC values using the modified  $K_{sat}$  value for 3 ft depth.

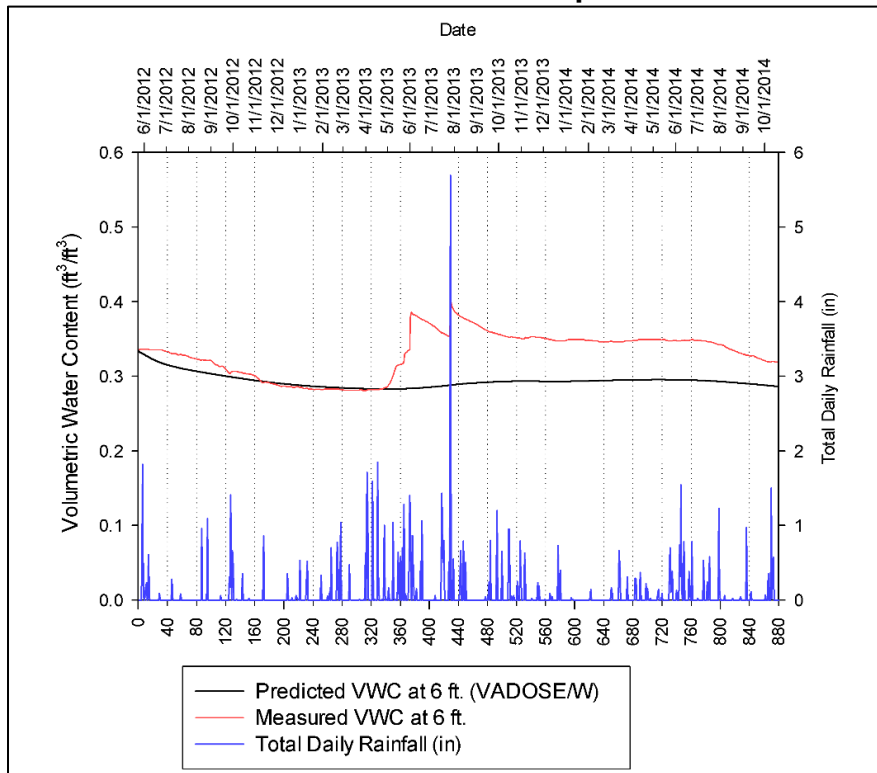


Figure 6. 14. Goldsby: measured vs. predicted VWC values using the modified  $K_{sat}$  value for 6 ft, depth.

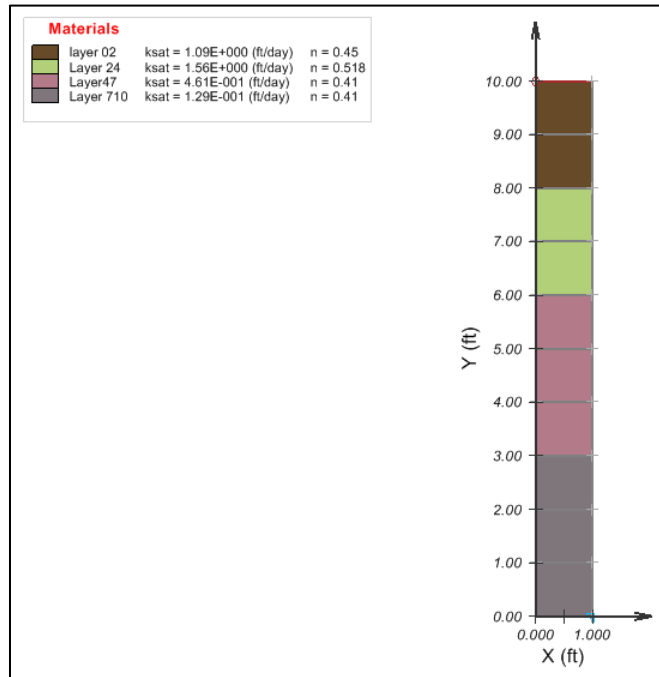


Figure 6. 15. Goldsby: SVFlux soil column.

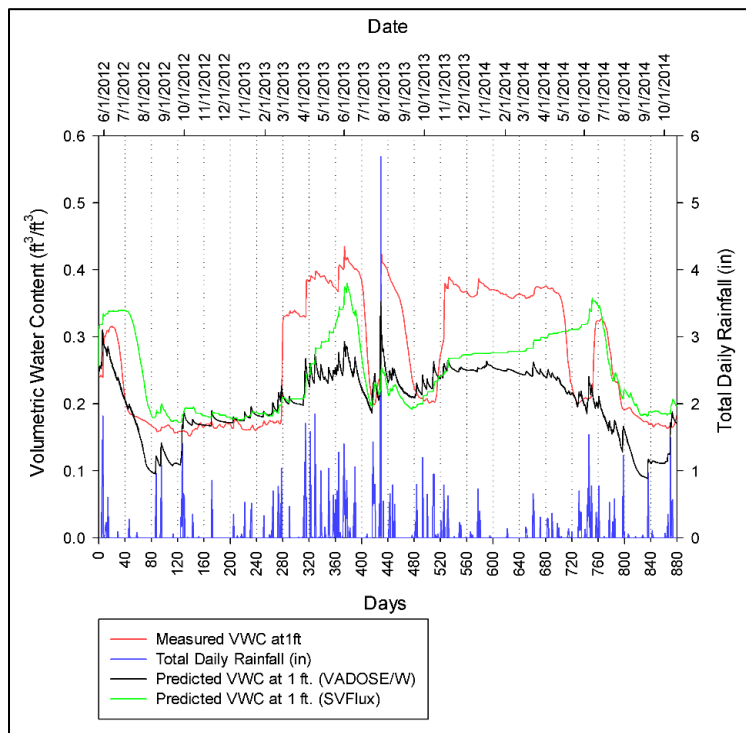
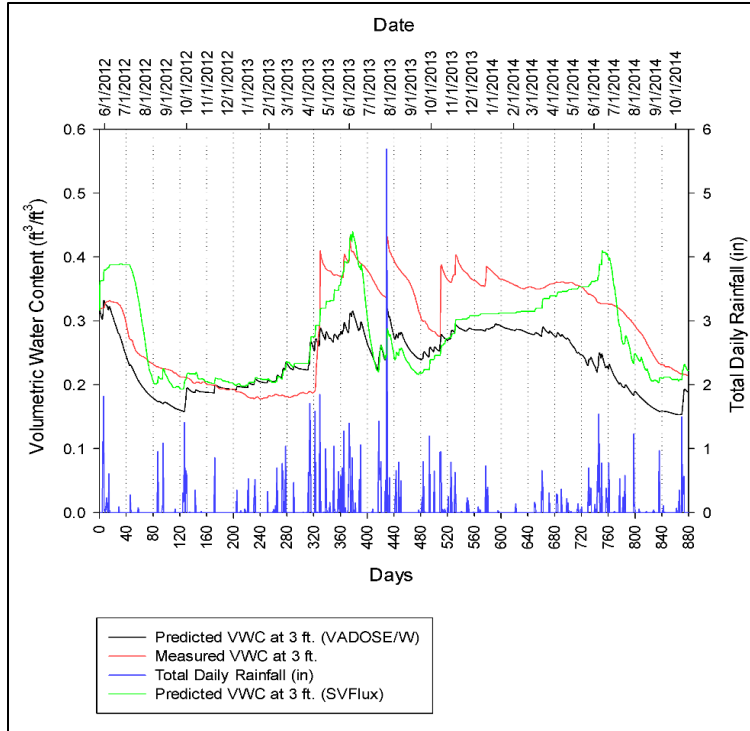
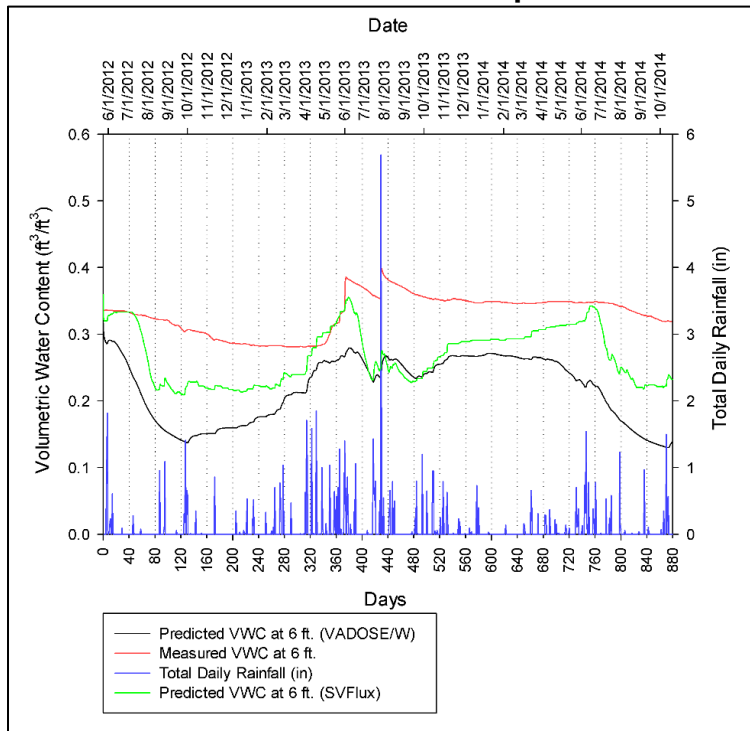


Figure 6. 16. Goldsby: predicted vs. measured VWC values using SVFlux and VADOSE/W for 1ft depth.



**Figure 6. 17. Goldsby: predicted vs. measured VWC values using SVFlux and VADOSE/W for 3ft depth.**



**Figure 6. 18. Goldsby: predicted vs. measured VWC values using SVFlux and VADOSE/W for 6 ft depth.**

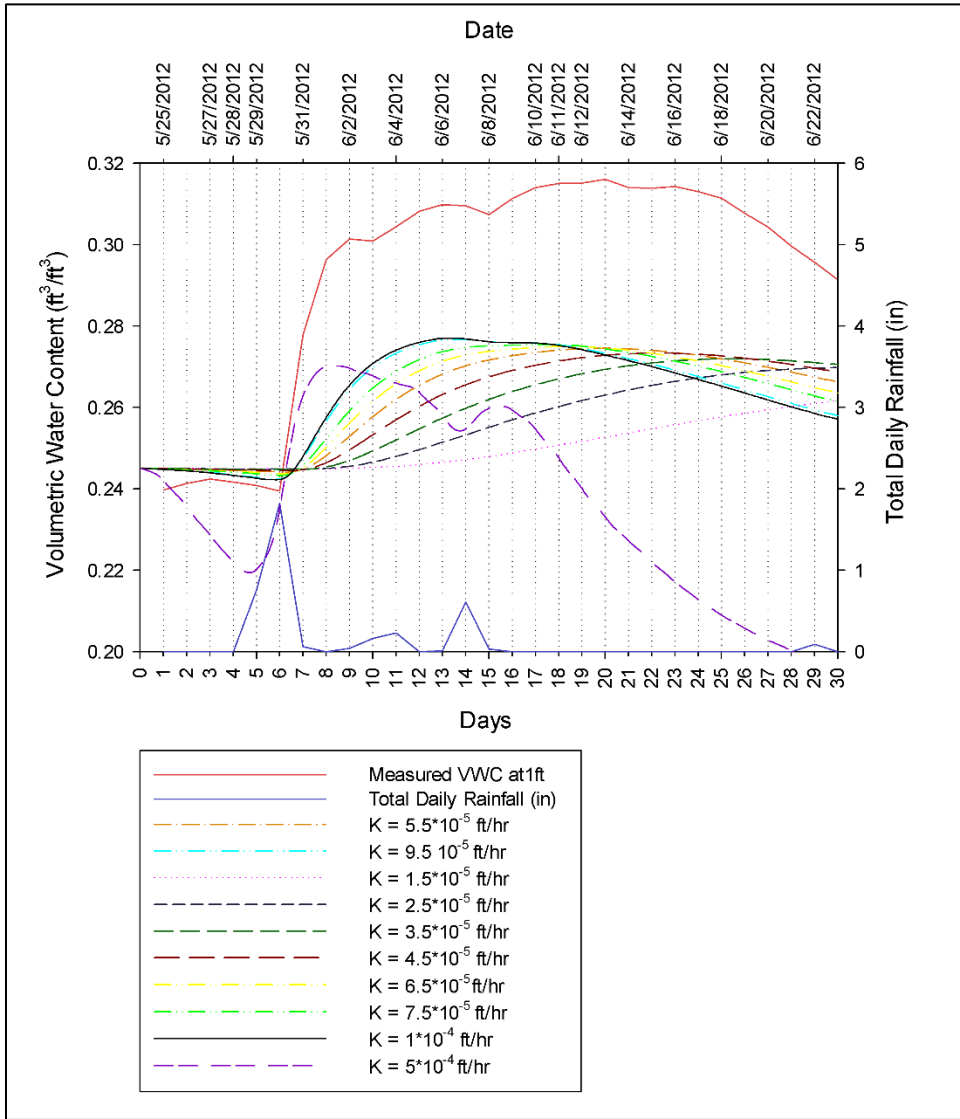


Figure 6. 19. Goldsby: sensitivity analysis.

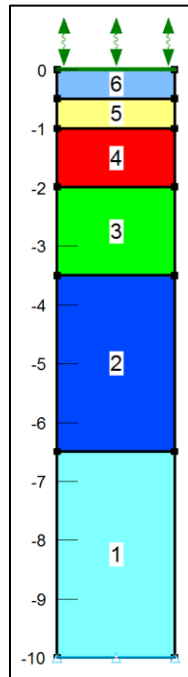


Figure 6. 20. North Base: VADOSE/W soil column.

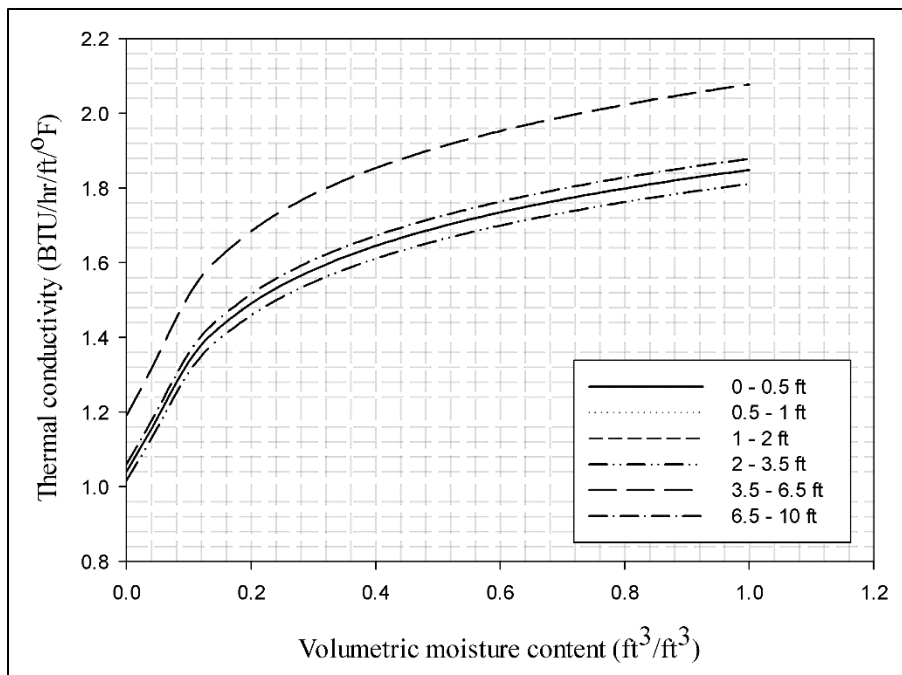
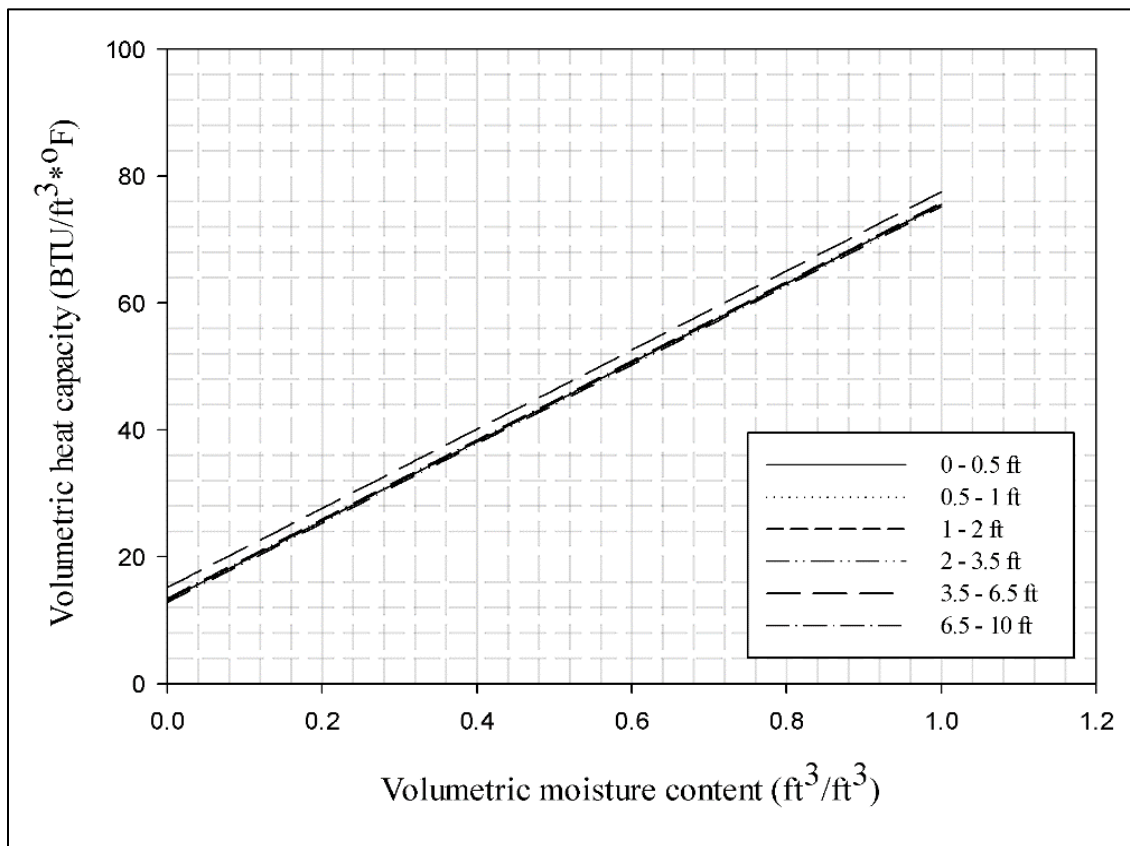


Figure 6. 21. North Base: estimated thermal conductivity function curves.



**Figure 6. 22. North Base: estimated volumetric heat capacity curves.**

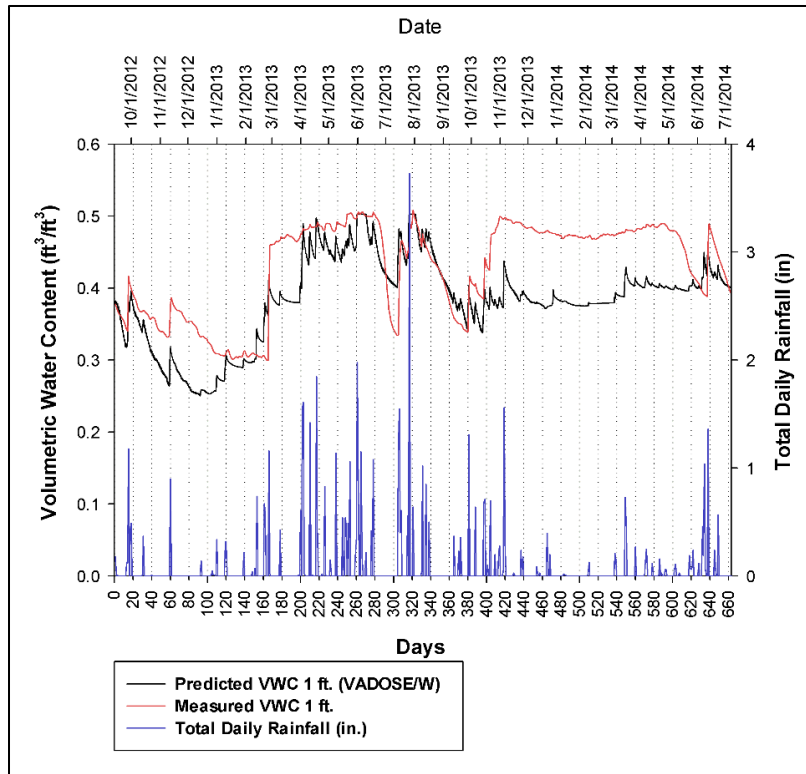


Figure 6. 23. North Base: predicted vs. measured VWC values at 1 ft depth.

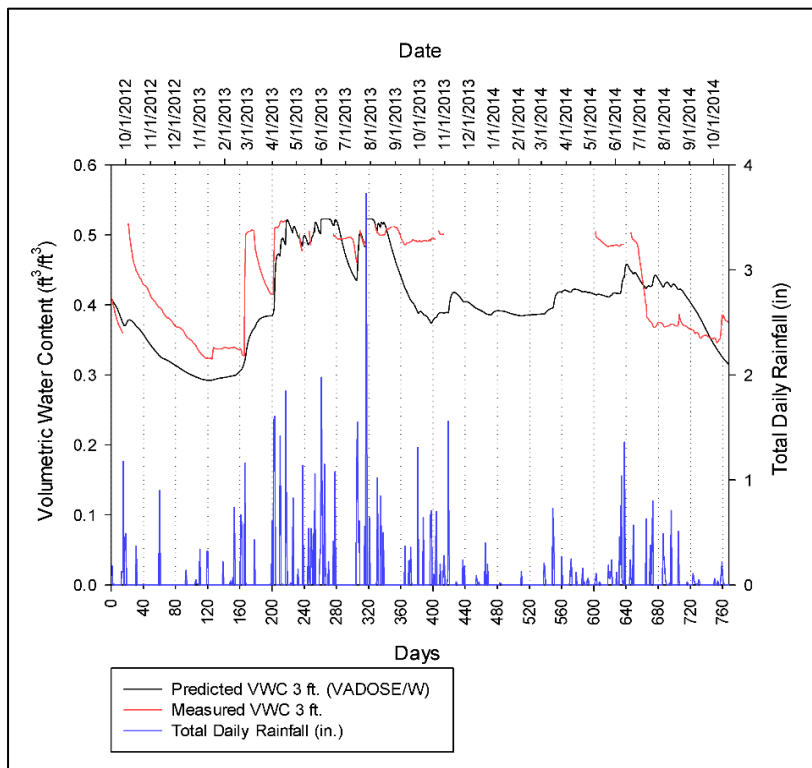


Figure 6. 24. North Base: predicted vs. measured VWC values at 3 ft depth.

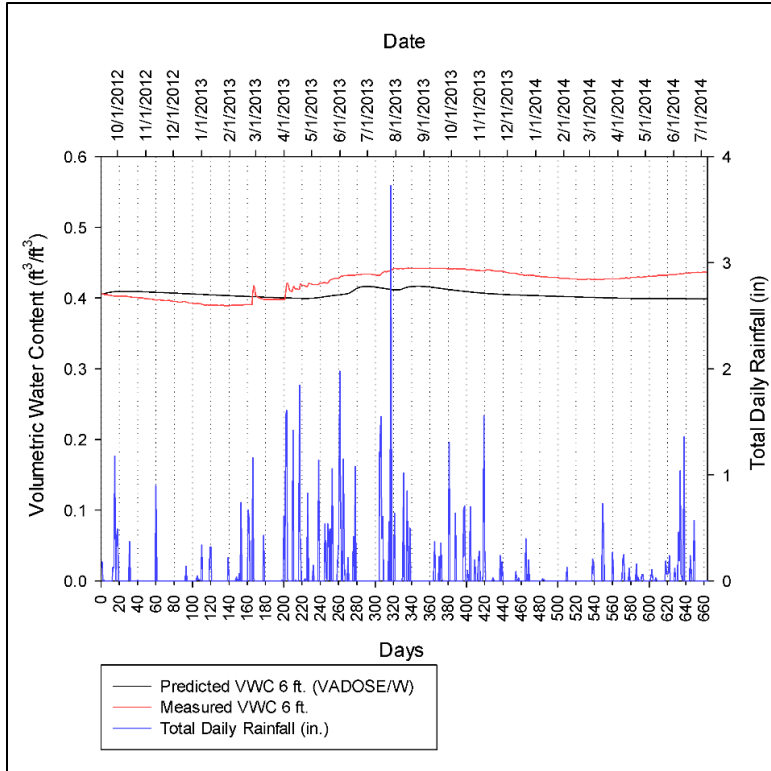


Figure 6. 25. North Base: predicted vs. measured VWC values at 6 ft depth.

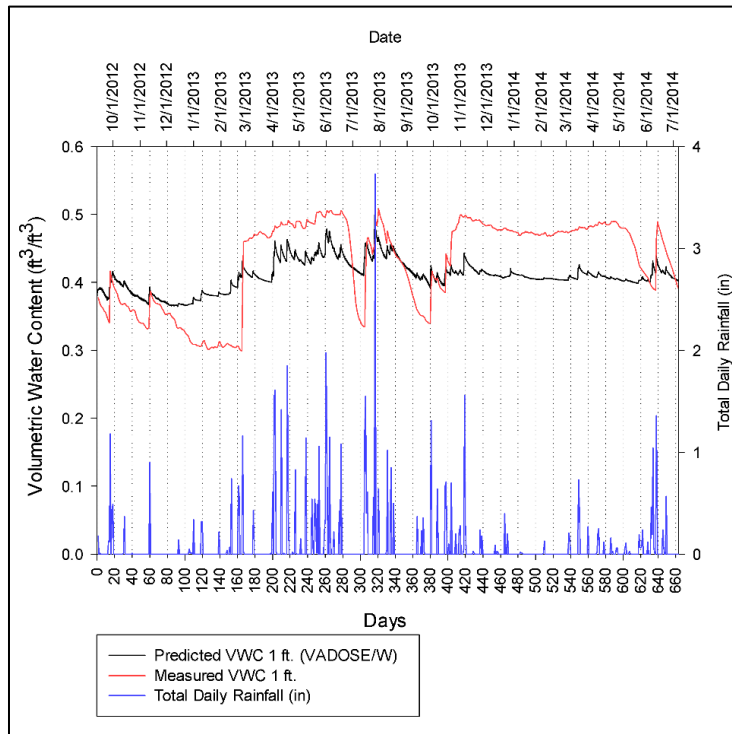


Figure 6. 26. North Base: measured vs. predicted VWC values using a modified  $K_{sat}$  for 1 ft depth.

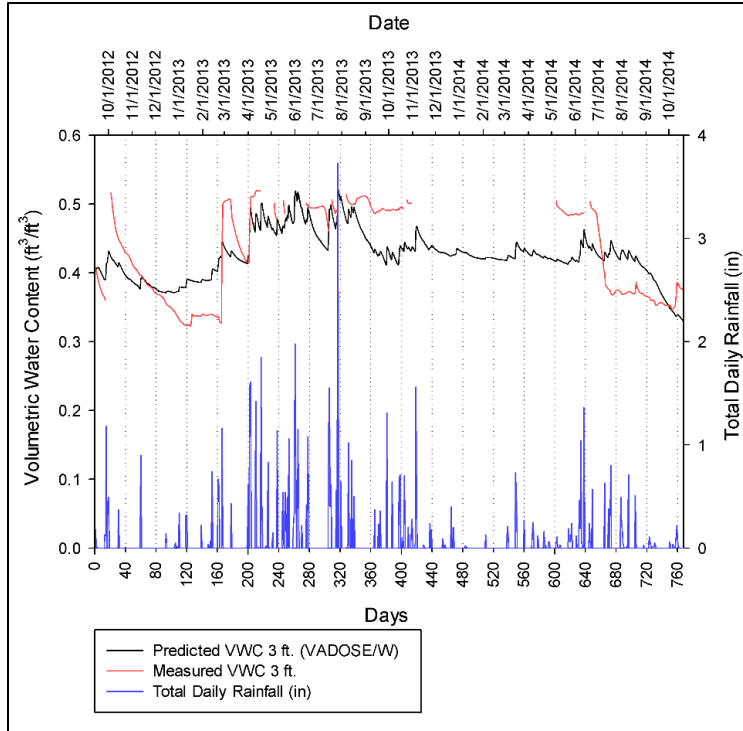


Figure 6. 27. North Base: measured vs. predicted VWC values using a modified  $K_{sat}$  for 3 ft depth.

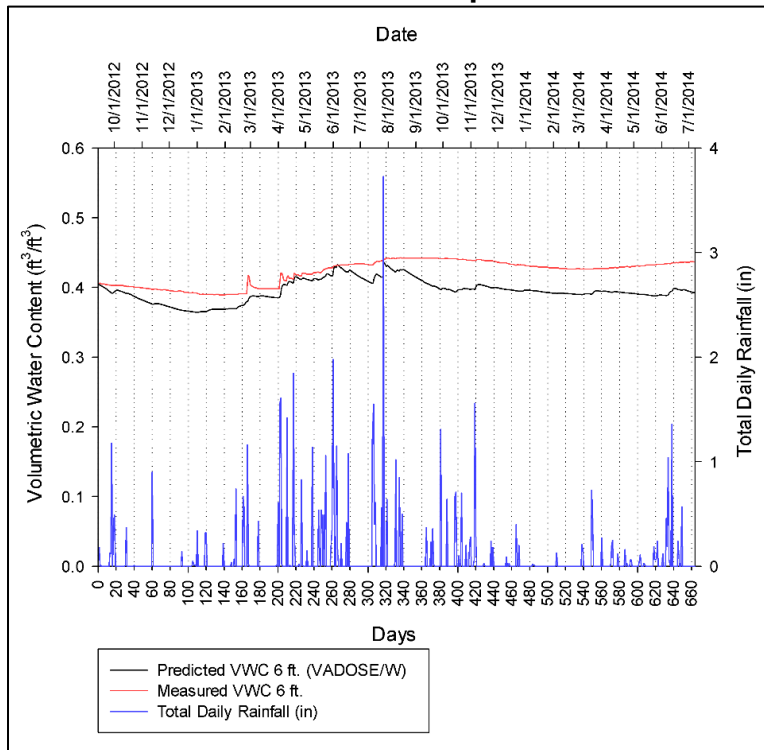


Figure 6. 28. North Base: measured and predicted VWC values using a modified  $K_{sat}$  for 6 ft depth.

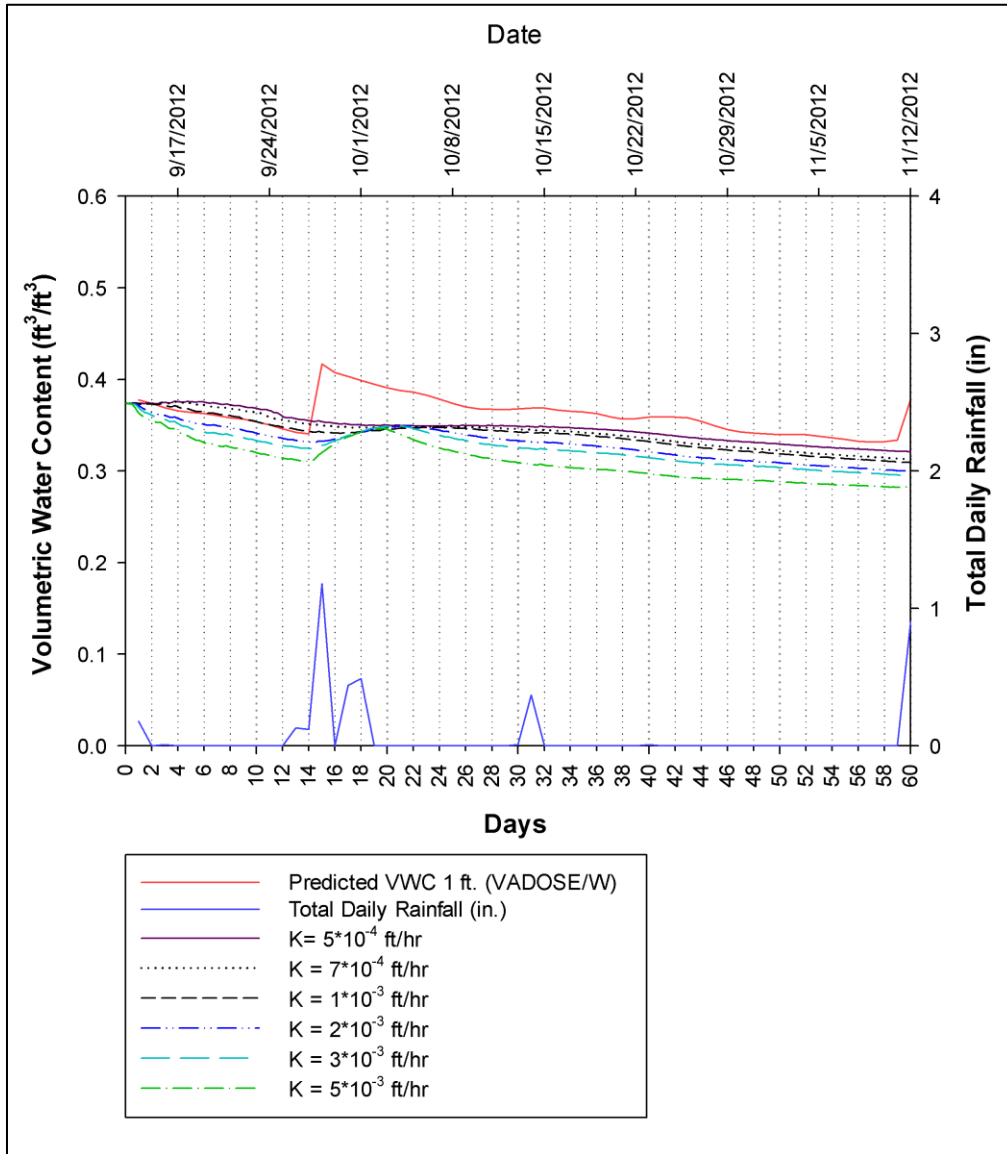


Figure 6. 29. North Base: sensitivity analysis.

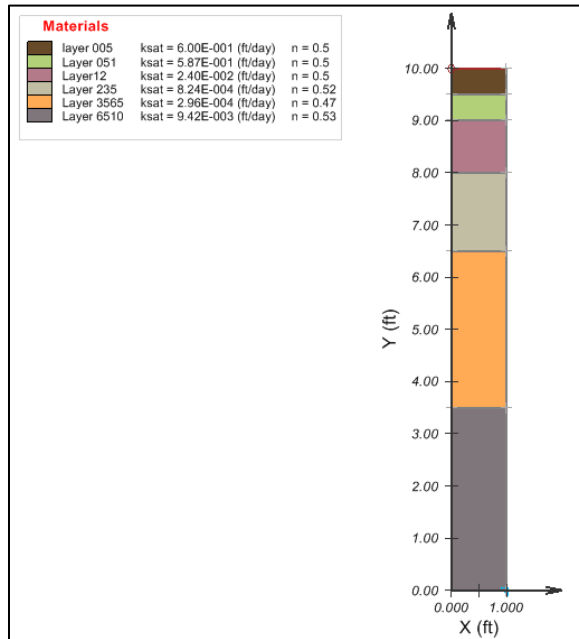


Figure 6. 30. North Base: SVFlux soil column.

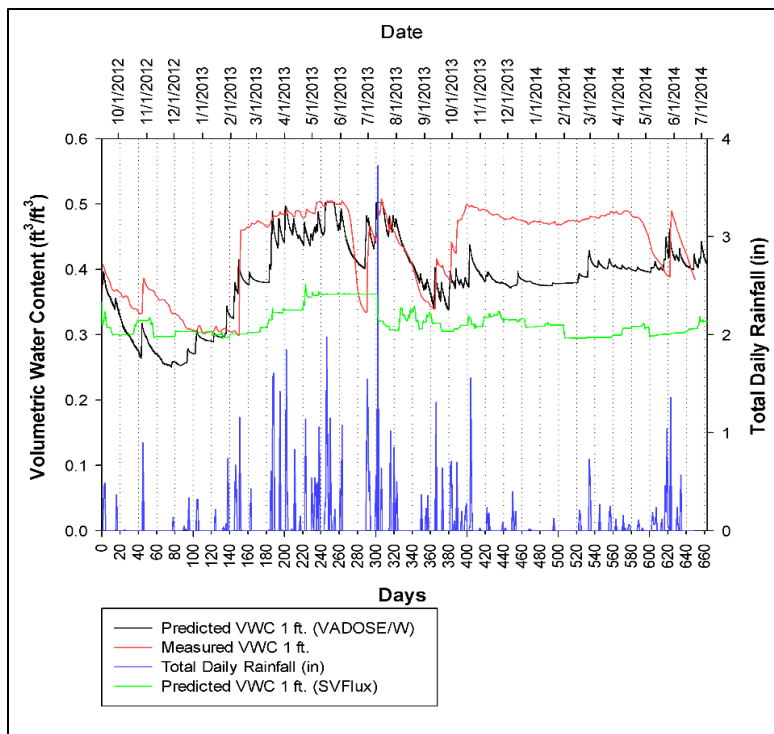


Figure 6. 31. North Base: predicted vs. measured VWC values using SVFlux and VADOSE/W for 1 ft depth.

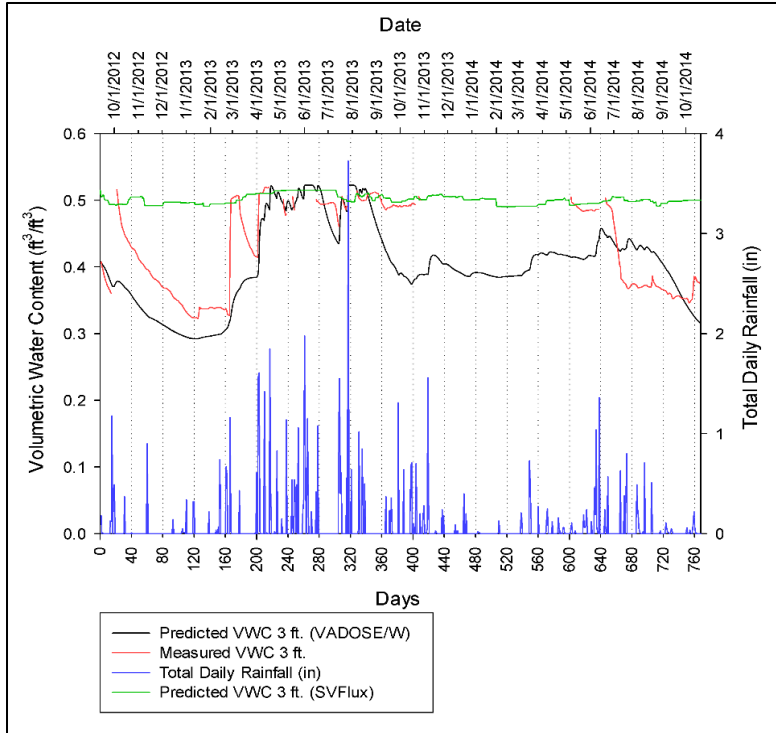


Figure 6. 32. North Base: predicted vs. measured VWC values using SVFlux and VADOSE/W for 3 ft depth.

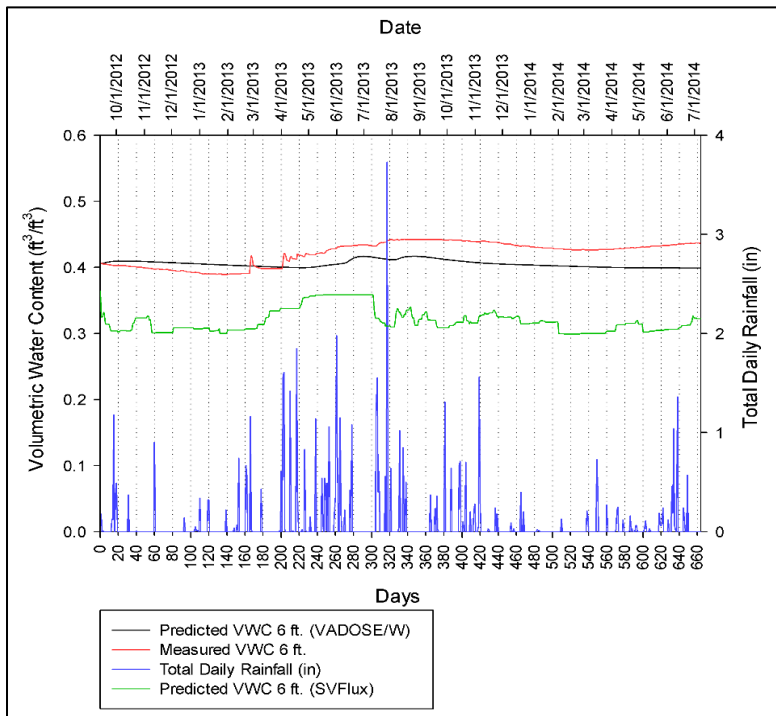


Figure 6. 33. North Base: predicted vs. measured VWC values using SVFlux and VADOSE/W for 6 ft depth.

## **Chapter 7 IN SITU TESTING RESULTS AND INTERPRETATION**

### **7.1 Introduction**

In situ testing was performed at North Base and Goldsby test sites throughout 2013 and 2014. In general, tests were performed in reasonable proximity to each other to help ensure the same strata of soil was tested. While the influence of soil suctions is apparent in many of the test data sets obtained at certain depths during the project period, there is considerable scatter in the relationships developed between soil suction and various test parameters. This is attributed to several factors including site soil variability, variations in contributions of osmotic and matric suction to the measured total suctions at different water contents, accuracy of test measurement procedures for determining moisture content and suction, and accuracy and repeatability of the test methods. In this chapter, the test results are presented and the influence of suction on various aspects of the three in situ tests is discussed.

Relative to the pressuremeter test (PMT), the analysis focused on the influence of suction on the limit pressure, pressuremeter modulus and unload-reload modulus. For the cone penetration test the influence of suction on the tip resistance and skin friction was carefully evaluated. For the standard penetration test the effect of suction on N-value was investigated.

### **7.2 Pressuremeter Test (PMT) Results**

A map of the testing locations at the tests sites was created to ensure that no location was tested more than once during the project period and to the extent possible, keep

the testing locations in reasonable proximity to one another. The test site maps show a small rectangular box which signifies the location of the weather station. Surrounding the weather station are test points indicated by different markers corresponding to the test dates in the legend. For the location maps shown in Figures 7.1 and 7.2, the weather station box is centered at (0, 0) and each side of the box is twelve feet in length. The arrow is pointed in the North direction. Distances are shown in feet.

Locations of PMTs performed at North Base are shown in Figure 7.1. The majority of testing was confined to the northwest corner of the research site. The reason for this was the surface on this portion of the site was the most uniform.

Locations of PMTs performed at Goldsby are shown in Figure 7.2. Testing was performed on all sides of the weather station as the soil surface was relatively uniform and free of any natural slopes or big differences in surface vegetation.

### **7.2.1 Influence of soil suction on PMT Results**

Soil suction was observed to have a profound impact on the results of pressuremeter tests. The PMT stress-strain curves determined from each pressuremeter test are presented for both test sites. Differences in the shape and behavior of some of these stress-strain curves is evident for different test depths at different dates when moisture conditions were different. These differences in the stress-strain behavior result in differences in the interpreted limit pressure ( $P_L$ ), pressuremeter modulus ( $E_p$ ), and unload-reload modulus ( $E_R$ ). These are important parameters used in geotechnical analyses based on pressuremeter testing. A summary of the PMT data collected during the project period is provided in Tables 7.1 to 7.6 for each test depth at both test sites.

Included in the tables are values of limit pressure, pressuremeter modulus, unload-reload modulus, as well as date of testing, soil moisture content, and soil suction determined at each test depth.

#### **7.2.1.1 North Base PMT Results**

The behavior of pressuremeter test results at North Base is examined in detail in this section. The PMT stress-strain curves obtained for North Base at a depth of 3 feet are presented in Figure 7.3. Included in Figure 7.3 are stress-strain curves for all test dates. Many of the curves are clustered in a similar range; however, there is considerable variation in the shape depending on the date of testing, which is partly attributable to variations in soil suction and moisture content on the different test dates.

The limit pressure ( $P_L$ ) obtained from a pressuremeter test provides an indication of a soil's ultimate strength. This value is typically used to calculate shear strength parameters and foundation bearing capacity. Presented in Figure 7.4 is the limit pressure compared to soil suction at the North Base site for the 3-foot depth. The figure shows that as soil suction increases the limit pressure shows a corresponding increase, as expected. There is some slight scatter of the data that can be attributed to factors mentioned previously. Variation in site soil properties at testing locations likely plays an important role in some of the scatter shown. In addition, low measured soil suctions can be significantly affected by the WP4 device measurement accuracy. At the start of the testing regime, Oklahoma had been under drought conditions; however, the weather in spring of 2013 introduced sufficient moisture to bring the region out of these conditions. After this time, during the project period soil conditions never reached the higher soil

suctions encountered prior to spring of 2013. Thus, the timing of the project was fortuitous in this regard.

The pressuremeter modulus is a measure of the soil stiffness. The pressuremeter modulus data for North Base at a depth of 3 feet is presented in Figure 7.5 against soil suction. With the exception of one point corresponding to the highest measured suction, there does not seem to be a strong correlation between soil suction and pressuremeter modulus. It appears, for most of the range of measured suction values, the pressuremeter modulus was less sensitive to suction as compared to the limit pressure. Interestingly, the unload-reload modulus for the same depth does appear to correlate somewhat better with the measured soil suction as shown in Figure 7.6. Unload-reload modulus is calculated in a similar manner to pressuremeter modulus except that unload-reload modulus is determined after an initial loading and unloading of the soil, prior to any significant plastic deformation. The purpose of conducting an unload-reload sequence during the PMT is to eliminate the influence of soil disturbance that may affect the initial loading and determination of  $E_p$ . Possibly the influence of borehole disturbance intrinsic to the determination of  $E_p$  masks to some degree the relationship between modulus and suction. However, the unload-reload sequence may minimize the masking influence of the disturbance resulting in a better defined relationship between  $E_R$  and suction seen in Figure 7.6.

The PMT stress-strain curves for North Base at a depth of 5 feet are presented in Figure 7.7. It is important to note that the first tests completed in February and March of 2013, were completed at a depth of 6 feet. The test depth thereafter was adjusted to 5 feet because the water table at the site was around 9 feet, and so the deepest test

needed to be raised to 7 feet. It was assumed that the small change in depth had minimal effect on test results. Tests conducted early in 2013 have stress-strain curves that indicate stiffer soil compared to tests conducted at later times. The majority of tests conducted after April of 2013 showed a similar grouping of tests results. The softest soil response occurred in August of 2014.

The relationships between interpreted PMT parameters and suction were examined for the 5-foot depth as they were for the 3-foot depth. Generally, the PMT parameters did not correlate strongly with the measured suctions except at the highest measured suction values. The limit pressure, pressuremeter modulus and unload-reload modulus versus suction plots for North Base at a depth of 5 feet are presented in Figures 7.8, 7.9, and 7.10. Considerable scatter is evident in these plots; however, it is noteworthy that in Figure 7.8 and 7.10, the highest limit pressures and unload-reload modulus values, respectively, were obtained during the early dry period and correspond to the high end of the measured suction range.

Due to soft soil conditions, tests were not performed for all dates at 7 feet. It was also difficult to perform unload-reload loops in the soft soil, so in most cases these were not performed at 7 feet. Stress-strain curves for North Base for a depth of 7 feet are shown in Figure 7.11. All but one test fell in a similar range; the softest test response was obtained at the end of April 2013 and appears to have been performed in a particularly soft, wet area because tests conducted after this were similar to other tests.

As shown in Figures 7.12, 7.13 and 7.14, there is very little correlation between measured suction and the pressuremeter parameters. This is attributed to the low range

of suctions encountered at a depth of 7 feet and the limited accuracy of the WP4 at low suctions, among other factors discussed below.

The lack of strong correlations between PMT parameters and measured suction for depths of 5 and 7 feet, as compared to 3 feet, may be attributed to a number of factors. 1) First, at higher water contents there appears to be significant variation in the measured total suction, between about 7 and 113 psi, for example, for the data from 7 feet deep. In other words, the measured total suction varies over a relatively larger range when water contents approach the saturated water contents. Furthermore, there is no correlation between the water contents and measured suctions for the 7-foot data as shown in Table 7.3. The explanation may be that the measured suctions at high water contents reflect mainly the osmotic suction in the soil since the matric suction is likely to be low. Since the WP4 measures total suction, it reflects the sum of the matric and osmotic potential. It would appear the variations in measured suction are likely due to variations in osmotic suction. Further, osmotic suction is expected to have relatively little impact on the soil behavior in comparison to the matric suction. This would explain why the measured total suction varies significantly and shows no consistent trend relative to the pressuremeter response for a depth of 7 feet.

Extending this reasoning further, looking at data from a depth of 3 feet, for example the limit pressure data in Figure 7.4, it is observed that total suction measurements are in a range of mostly 200 to 500 psi and the correlation between suction and limit pressure is quite strong. It is likely that the matric suction represents a significant component of the measured total suction above approximately 150 to 200 psi, for this soil. Since matric suction would have the dominant influence on the soil

mechanical response, this explains the improved correlation for suctions above 200 psi in Figure 7.4, as compared to the lack of correlation in Figure 7.12 for suctions less than 120 psi. Interestingly, the degree of correlation seen for the limit pressure-suction relationship for a depth of 5 feet in Figure 7.8, while poor, is marginally better than for a depth of 7 feet and not nearly as good as 3 feet. The range of measured total suctions for the 5-foot depth is 46-168 psi, compared to 7-113 psi for 7 feet and 91-463 psi for 3 feet.

2) Another factor that may contribute to the scatter in PMT data plotted against low measured total suctions is the accuracy of the WP4 at low suction. The reported accuracy of the WP4 is plus or minus 14.5 psi for measurements in the range of 0 to 1450 psi. This is significant for measured suctions below 100 psi.

3) Natural variability in the soil profiles is another factor that will contribute to the observed scatter noted above. This includes variations in soil constituents, density and stress history, among others.

4) Finally, test method accuracy and experimental errors may contribute to scatter.

#### **7.2.1.2 Goldsby PMT Results**

Goldsby pressuremeter data is examined in a similar manner to the North Base data in this section. Figure 7.15 shows the PMT stress-strain curves for Goldsby tests for a depth of 3 ft. It is noticeable from this figure that there is a wider range of test results for the Goldsby site compared to North Base results. There is greater variation between the stiffest and softest test result. Tests with lower suctions during wet periods of the year

have softer shaped stress-strain curves than for tests conducted in dry periods of the year.

The limit pressure versus soil suction for Goldsby for 3 feet is shown in Figure 7.16. There is a noticeable relationship between increasing soil suctions and limit pressure, as was observed for the North Base soil at the same depth. The soil suction at North Base for 3 feet ranges from 46 psi to 339 psi.

The pressuremeter modulus data for Goldsby for 3 feet are shown in Figure 7.17. The trend observed for limit pressure versus suction is also seen with modulus. This differs from the North Base results at the same depth. Relative to North Base, it seems the determination of pressuremeter modulus for the Goldsby site soil was less affected by the initial borehole disturbance. Finally, Figure 7.18 presents the unload-reload modulus versus suction. The trend of increasing suction corresponding to increasing modulus is also noticeable here. The correlation is not as strong as was observed for pressuremeter modulus or limit pressure; however it is still showing the expected positive correlation.

The stress-strain curves and pressuremeter parameters plotted against measured total suction for depths of 6 and 9 feet for the Goldsby site are shown in Figures 7.19 to 7.26. Similar to North Base, there is a lack of correlation observed in the pressuremeter response parameters plotted against matric suction. It is believed the same factors discussed relative to the North Base results are responsible for the lack of correlation. Namely, the importance of matric suction at higher water contents is masked by the dominant and variable osmotic suction reflected in the WP4 total suction measurements. Consider that the total suction ranges at the Goldsby PMT test locations

during the project were 46-339 psi at 3 feet, 35-131 psi at 6 feet, and 9-110 psi at 9 feet. Similar to North Base, correlations were weak or lacking for measured suction ranges below about 150 psi.

### **7.3 Cone Penetration Test (CPT) Results**

The map of cone penetration test locations at North Base is presented in Figure 7.27.

The weather station is centered on the figure with the arrow directed towards North. The CPTs conducted at North Base were limited to the south of the weather station due to a water pipe running east to west on the north end of the test site. Three tests were performed per test date. Distances are shown in feet. The map of cone penetration tests conducted at Goldsby are presented in Figure 7.28. The weather station is found at the center of the map.

#### **7.3.1 Influence of soil suction on CPT Results**

##### **7.3.1.1 North Base CPT Results**

The influence of soil suction at North Base was investigated by comparing the average of three cone penetration tests conducted on a particular day. The tip resistance and sleeve friction were compared to total soil suction measured using the WP4 in samples obtained at the field site on the day of testing. In general there does seem to be evidence that would suggest larger suctions increase the tip resistance measured on a given day. Skin friction ratio at North Base seemed to be variably affected by changes in soil suction.

Tip resistance and soil suction versus depth for North Base are shown in Figure 7.29. The results show that tests conducted on 2/4/2013, 9/3/2013, and 9/10/2014 were performed in relatively dry conditions. This is reflected in the high values of tip resistance above 5 feet and reflected in soil suction measurements that are higher for these times than other times. The CPT results also show that the active layer of fluctuating moisture conditions appears to exist above a depth of 5 feet because at this point the CPT results seem to converge.

Sleeve friction is shown versus soil suction and depth in Figure 7.30. Sleeve friction appears less sensitive to soil suction variations; however, the data suggest the suction has some influence. Looking at the soil suction at a depth of 3 feet the highest suctions were obtained on 2/4/2013, while some of the lowest suctions measured occurred on 11/21/2013. At the same 3-foot depth the highest sleeve friction was also obtained on 2/4/2013, while the lowest sleeve friction was seen on 11/21/2013. The remainder of the friction data are scattered between these points; however, generally higher sleeve frictions are observed to occur when measured suctions are higher.

Shallow depths reflect the effect of changes in soil suction on cone penetration parameters the most noticeably. Therefore, in Figure 7.31 the tip resistance, sleeve friction, and soil suction are shown for 1- and 3-foot depths during the entire test period. The one foot data shows an interesting trend. During the winter, which is typically a wetter time in Oklahoma, the soil suction and tip resistance show relatively low results. As the season changes to late summer the tip resistance and soil suction peak and shows cyclical results the following year.

The seasonal cyclical behavior observed for the 1-foot CPT results is also noticeable for the 3-foot results in Figure 7.31. The variations are not as dramatic as at 3 feet because the variations in soil suction are generally lower after the first test date in comparison to the 1-foot results. The general trend for 3-foot data indicates tip resistance increases with increasing soil suction.

The CPT parameters obtained for depths of 1 and 3 feet were also compared directly to soil suction as shown in Figure 7.32. The tip resistance seems to correlate well with soil suction for both depths with tip resistance increasing with increasing soil suction. Sleeve friction shows agreement for both depths. The correlation between sleeve friction and soil suction is strong and shows that increasing suction increases sleeve friction.

#### **7.3.1.2 Goldsby CPT Results**

The Goldsby CPT data are presented in similar fashion to the North Base data. Tip resistance and sleeve friction are presented versus depth next to soil suction in Figure 7.33 for the Goldsby site. Similar to North Base, the results show significant variation in the CPT results in the upper 6 feet. Tests conducted in February 2013 and September 2014 show tip resistances that are nearly 20 psi higher than all other results above a depth of 5 feet. These higher tip resistances correspond to higher measured suctions. There is one anomaly, which is the February 2015 test that shows a very high suction profile, but low tip resistance until 4 feet. This may be the result of a local “soft spot” due to natural site variability or possibly errors in the measurement/interpretation procedures for the CPT or suction measurements.

The sleeve friction versus depth and soil suction are presented in Figure 7.34. While friction ratios are quite variable with depth and suction, these results tend to indicate tests conducted in soil with low suction generally resulted in increased sleeve friction.

Figure 7.35 presents the tip resistance, sleeve friction, and soil suction at 1 and 3 feet test depths for Goldsby during the entire test period. The tip resistance is shown to start initially high then decrease and stabilize until September of 2014. The 1 foot tip resistance is higher than the tip resistance at 3 feet with the exception of the initial point. The soil suction for the initial test date is significantly higher than the soil suction at later dates. There is an increase in soil suction through 2014, which is reflected by an increase in tip resistance and decrease in friction ratio.

Figure 7.36 presents the tip resistance and sleeve friction as a function of soil suction for the 1- and 3- foot depths. At 1-foot depth there seems to be a positive correlation between increased soil suction and tip resistance. The trend is similar for 3 feet; however, there does seem to be more scatter at higher suctions. The friction ratio at 1 foot shows very small changes. With a slight increasing trend in the data. At 3 feet the data seem to indicate friction ratio changes little with increasing soil suction. Similar to North Base, friction ratios at Goldsby don't indicate strong trends one way or the other.

## **7.4 Standard Penetration Test (SPT) Results**

The map of SPT locations at North Base is presented in Figure 7.37. The map of Goldsby SPT locations is presented in Figure 7.38. The arrow on each map is directed in the North direction. Distances are shown in feet.

### **7.4.1 Influence of soil suction on SPT Results**

The SPT conducted at North Base indicates that soil suction has a direct impact on the measured N-value. North Base SPT versus depth and soil suction is presented in Figure 7.39. The N-value seems to increase for soils with increased soil suction and decrease with a decrease in suction. The tests conducted in February, and May 2013, show the largest N-Values especially below 2 feet depth. The suction values also are shown to be highest for these for these dates.

Goldsby SPT results are presented in Figure 7.40. This figure shows a similar trend to what is observed for the SPT at North Base, as well as, the CPT results from both sites. SPT N-value is shown to increase with an increase in soil suction. The test results from Goldsby show the phenomena better than the results obtained from North Base. The tests conducted in February 2013 and September 2014 both show larger N-values and larger soil suction. Other tests presented show lower N-values and lower soil suction measurements.

## **7.5 A Methodology to Interpret In Situ Test Results in Unsaturated Soil**

### **7.5.1 Introduction**

In situ testing in Norman, Oklahoma over the past two years has resulted in a database of results in two different unsaturated soil profiles. The goal of collecting these data was to aid in the formulation of a method for interpreting PMT, CPT and SPT results in light of potential changes in soil water content and matric suction. Currently there are no agreed upon methods for interpreting in situ tests in unsaturated soils. Historical attempts at developing methods of interpretation are demonstrated in the literature (Miller and Muraleetharan 2000, Tan 2005, Miller 2012, Russell et al. 2010, Lehane et al. 2004, Russell and Khalili 2006, Pereira et al. 2003, Cudmani and Osinov 2001); however, there are no standard recommendations for practice. While many of these methods are promising, some are rather specialized to particular soil types, while others are overly cumbersome in terms of their application to practice. Since many of the theoretical approaches are complex and lack the necessary validation to be used in practice, a relatively simple empirical approach was taken in this study. The goal was to develop some empirically based recommendations for estimating the influence of matric suction on in situ test parameters using data collected as part of this study as well as data gathered from other studies. Like all empirical correlations, users must be wary of the possible variations in resulting predictions in light of the limitations of the original data sets. However, the methods proposed will at least give engineers a sense of how important a role suction may play in the conduct and interpretation of their in situ test

results in certain soil types. In this way they can entertain the possibility of additional testing or increased factors of safety in their geotechnical designs.

Two primary goals for the development of the empirical method of interpretation were established as follows:

- 1) First, the method should allow an engineer to predict how much change will occur in a given in situ test parameter in a given soil type if the suction changes a specified amount from some initial value corresponding to the date of testing. In other words, the question: “what will be the limit pressure if the suction decreases by 100 psi from the date of testing?” for example, can be answered. For this project, the PMT parameters addressed included the limit pressure, pressuremeter modulus, and unload-reload modulus. The CPT parameters included the tip resistance and for the SPT parameter, the N-value.
- 2) The second goal in developing this method was to include as many soil types as possible by utilizing to the extent possible, results from other published studies. Data from in situ testing in unsaturated soil, along with suction measurements, is scarce in the literature. A few additional data sets were obtained in the case of CPT results, while one additional data set was included in the PMT results.

### **7.5.2 Estimating the Influence of Suction on PMT Limit Pressure and Moduli**

Figures 7.41 and 7.42 show the normalized PMT parameters plotted against the measured total suctions for North Base and Goldsby test sites, respectively. While the coefficients of determination ( $r^2$ ) indicate weak correlations, in general the trends are fairly obvious and follow expectations. These two figures can be used to get an idea of

expected changes in PMT parameters due to variations in suction, for relatively lean (CL-ML to CL) to moderately plastic (CL to CH) clayey soils found at the Goldsby and North Base test sites, respectively. These soils cover a range of PI from about 7 to 40.

To make use of these relations, consider in Figure 7.41 the slope of the normalized limit pressure versus suction best fit line is  $0.120 \text{ (psi}^{-1}\text{)}$ . Similarly, for Goldsby soil shown in Figure 7.42, the slope of the same curve is  $0.184 \text{ (psi}^{-1}\text{)}$ . This suggests that for lean to fat clays similar to those tested, the normalized limit pressure will change about 0.12 per 1 psi change in suction for the higher PI clayey soils and about 0.18 per 1 psi change in suction for the lower PI clayey soils.

To apply this knowledge to practice, consider the following example. An engineer has results from a pressuremeter test at a depth of 6 feet in a moderately plastic lean clay. Limit pressure and PMT modulus interpreted from the test are,  $P_L=250 \text{ psi}$  and  $E_p=3500 \text{ psi}$ . Samples taken from the test location on the day of testing reveal a total suction of 300 psi, and soil total unit weight is estimated at 125 pcf. The computed overburden stress ( $\sigma_{vo}$ ) is 5.21 psi at the test depth and the normalized limit pressure ( $P_L/\sigma_{vo}$ ) and normalized PMT modulus ( $E_p/\sigma_{vo}$ ) are then 48 psi and 672 psi. The engineer is concerned the soil was relatively dry at the time of testing and wants to know the impact of a suction decrease of 100 psi on the limit pressure and PMT modulus. Looking at Figures 7.41 and 7.42, a roughly average rate of change in  $P_L/\sigma_{vo}$  and  $E_p/\sigma_{vo}$  is estimated from the slopes of the corresponding trend lines in these figures; the values are 0.15 and 1.1, respectively. Thus, the normalized limit pressure after a 100 psi decrease in suction will be 33 ( $48-100*0.15$ ). Assuming the overburden pressure remains the same, which is reasonable, the limit pressure after the 100 psi

suction decrease will reduce from 250 to 172 psi ( $33 \times 5.21$ ). Similarly, the normalized PMT modulus will decrease to 562 ( $672 - 100 \times 1.1$ ) and the corresponding PMT modulus will be 2928 psi, down from 3500 psi. This example shows how observations from the current study can be used to guide an engineer's interpretation of in situ tests in unsaturated soil. However, the correlations should not be used for determining design values due to the limited number of test sites and soil types represented and due to the inherent scatter in the data.

Figures 7.43, 7.44 and 7.45 compare normalized parameters from both test sites as well as data obtained from a previous study of pressuremeter tests in unsaturated soil in a calibration chamber. The latter data came from a project conducted by a former Ph.D. student at the University of Oklahoma (Tan 2005). The results in Figures 7.43, 7.44 and 7.45 are plotted in a log-log space showing normalized parameters versus suction. The use of these figures is intended to be more qualitative than quantitative. The comparisons suggest limit pressure (Figure 7.43) is much more sensitive to soil type and changes in suction in comparison to normalized moduli (Figures 7.44, 7.45).

### **7.5.3 Estimating the Influence of Suction on CPT Tip Resistance**

Normalized tip resistance versus suction for North Base and Goldsby soils are presented in Figure 7.46. While the correlations are weak, there is a relatively consistent trend of increasing normalized tip resistance with increasing suction (as expected) for suctions above 100 psi. Because there are other factors besides suction that influence the tip resistance, such as variations in soil type, density, degree of weathering, and stress history to mention a few, it is not surprising there is considerable

scatter in these plots since they represent data in the variable stratigraphy from zero to 10 feet of depth. Nevertheless, they provide some insight into potential variations in tip resistance that may occur due to suction changes. These plots can be used, in the manner described previously for normalized PMT parameters, to provide a crude assessment of changes in tip resistance that may occur due to a change in suction.

In Figure 7.47 the normalized tip resistance is plotted against suction in a log-log space for North Base and Goldsby soils and different soils for which data were available. Shown in this figure with the North Base and Goldsby data are data from calibration chamber studies on low PI lean clay (Tan 2005) and silty sand (Yang and Russell 2015), as well as poorly graded sand from a field study (Lehane et al. 2004). The figure provides some indication of the influence of suction on various soil types, which appears most significant for the higher PI clayey soils.

#### **7.5.4 Estimating the Influence of Suction on SPT N-Values**

Standard penetration test interpretation in unsaturated soils can be extremely useful due to the widespread use of the test for geotechnical investigations. In Figure 7.48 the N-values, corrected for overburden pressure, obtained at the North Base and Goldsby site are plotted against the measured total suction obtained at specific test depths on corresponding test dates. The overburden correction of Liao and Whitman (1985) was used, whereby the N-value is multiplied by the square root of atmospheric pressure divided by the overburden pressure. The lower graph in Figure 7.48 shows the uncorrected N-value plotted against suction for comparison.

It can be seen from Figure 7.48 that by accounting for overburden pressure, an obvious trend results in the corrected N-Value versus suction results. While the degree of correlation is not terribly strong, as indicated by  $r^2$ , there is a noticeable increase in corrected N-value as suction increases, as expected. The scatter observed is likely due to natural variations in soil type, density, stress history, etc. that was also observed to affect the normalized CPT tip resistance. Figure 7.48 can be used in a similar manner to provide a rough quantitative indication of expected changes in corrected N-values due to suction changes. As with other correlations, care must be used in this application due to the limited number of sites investigated.

**Table 7. 1. North Base: summary of PMT Data for 3 ft depth.**

<b>Date</b>	<b>Suction (psi)</b>	<b>Moisture Content (%)</b>	<b>P<sub>L</sub> (psi)</b>	<b>E<sub>P</sub> (psi)</b>	<b>E<sub>R</sub> (psi)</b>
2/1/2013	463	14.8	211	1336	8028
3/11/2013	302	14.5	103	483	1770
4/12/2013	360	14.7	211	1348	3229
4/30/2013	378	15.8	97	915	4925
10/11/2013	428	16.2	155	809	-
1/7/2014	225	23.5	38	529	1110
3/31/2014	223	21.6	46	497	1481
7/25/2014	91	20.6	62	1037	1770
8/22/2014	245	20.0	64	1062	2523
10/31/2014 – A	226	18.0	88	1032	2240
10/31/2014 – B	270	19.0	74	946	2240

**Table 7. 2. North Base: summary of PMT data for 5 ft depth.**

<b>Date</b>	<b>Suction (psi)</b>	<b>Moisture Content (%)</b>	<b>P<sub>L</sub> (psi)</b>	<b>E<sub>P</sub> (psi)</b>	<b>E<sub>R</sub> (psi)</b>
2/1/2013 (6')	96	17.2	122	2743	-
3/11/2013 (6')	73	16.2	125	4221	-
4/12/2013	117	13.8	287	2069	8931
4/30/2013	168	16.1	213	1980	4728
10/11/2013	103	21.0	60	1081	-
1/7/2014	122	19.5	63	944	2039
3/31/2014	71	22.9	73	948	2879
7/25/2014	46	20.8	94	1611	4041
8/22/2014	100	20.4	79	858	2343
10/31/2014 - A	110	18.5	99	1398	3268
10/31/2014 - B	77	17.8	101	1587	3268

**Table 7. 3. North Base: summary of PMT data for 7 ft depth.**

Date	Suction (psi)	Moisture Content (%)	P <sub>L</sub> (psi)	E <sub>P</sub> (psi)	E <sub>R</sub> (psi)
4/12/2013	45	19.5	113	2282	4128
4/30/2013	59	18.2	23	452	-
10/11/2013	84	21.0	57	1299	-
1/7/2014	113	26.1	89	1462	4700
7/25/2014	7	20.3	84	1232	-
8/22/2014	54	22.6	81	1044	2425
10/31/2014 - A	77	19.2	86	935	4090
10/31/2014 - B	16	19.9	103	1310	4090

**Table 7. 4. Goldsby: summary of PMT Data for 3 ft depth.**

Date	Suction (psi)	Moisture Content (%)	P <sub>L</sub> (psi)	E <sub>P</sub> (psi)	E <sub>R</sub> (psi)
2/1/2013	307	13.5	181	1251	997
3/13/2013	310	10.6	112	775	931
4/15/2013	62	20.4	30	204	472
5/2/2013	81	20.3	32	222	320
6/10/2013	87	21.4	26	181	486
10/16/2013	125	13.5	41	282	519
1/8/2014	81	19.2	47	327	532
3/31/2014	46	18.8	28	194	622
7/23/2014	103	15.1	85	585	828
8/22/2014	174	13.7	71	487	551
10/17/2014-A	196	10.5	83	574	649
10/17/2014-B	339	9.8	139	960	855

**Table 7. 5. Goldsby: summary of PMT Data for 6 ft depth.**

Date	Suction (psi)	Moisture Content (%)	P <sub>L</sub> (psi)	E <sub>P</sub> (psi)	E <sub>R</sub> (psi)
2/1/2013	73	15.6	182	2953	-
3/13/2013	104	12.2	156	3139	4034
4/15/2013	54	14.3	127	2625	9823
5/2/2013	90	13.8	159	3463	9209
6/10/2013	131	12.7	65	914	5671
10/16/2013	64	18.5	82	2183	-
1/8/2014	86	17.6	61	810	5132
3/31/2014	35	21.2	96	2222	7741
7/23/2014	86	16.2	55	1075	7382
8/22/2014	93	14.8	135	2864	8301
10/17/2014-A	84	15.1	66	982	2866
10/17/2014-B	90	13.8	100	1269	6079

**Table 7. 6. Goldsby: summary of PMT Data for 9 ft depth.**

Date	Suction (psi)	Moisture Content (%)	P <sub>L</sub> (psi)	E <sub>P</sub> (psi)	E <sub>R</sub> (psi)
2/1/2013	90	17.8	270	1919	10835
3/13/2013	46	16.9	160	2211	3362
4/15/2013	46	18.1	116	1719	5782
5/2/2013	75	17.2	122	2242	10346
6/10/2013	87	17.1	101	2107	7303
10/16/2013	73	20.3	117	2204	8370
1/8/2014	110	21.8	107	2148	5348
3/31/2014	9	20.5	110	2188	13207
7/23/2014	67	18.1	133	1929	10926
8/22/2014	81	17.2	138	2796	15776
10/17/2014-A	78	18.0	117	3229	-
10/17/2014-B	68	17.6	117	1751	2426

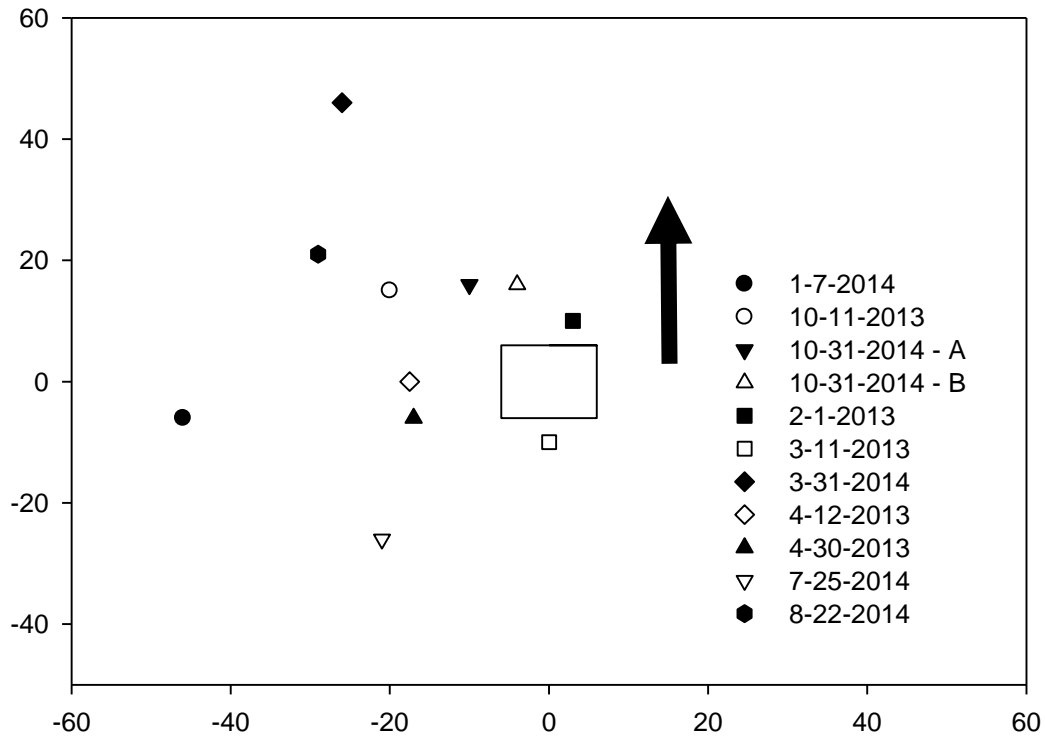


**Figure 7.1. North Base: PMT location map.**

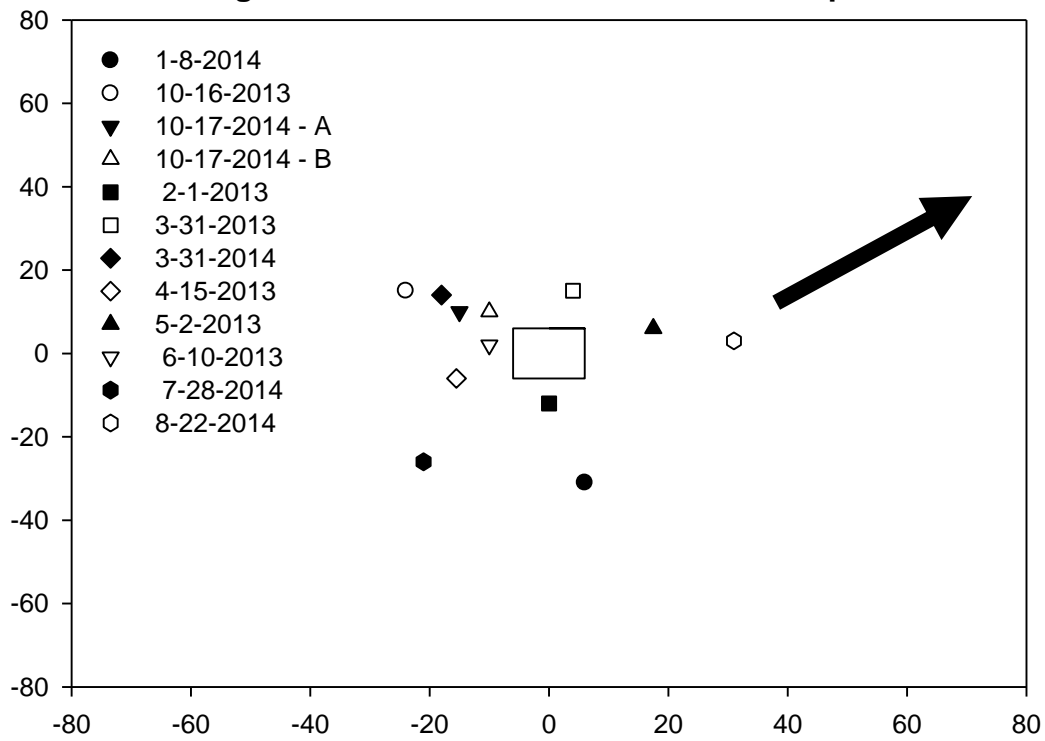


**Figure 7.2. Goldsby: PMT location map.**

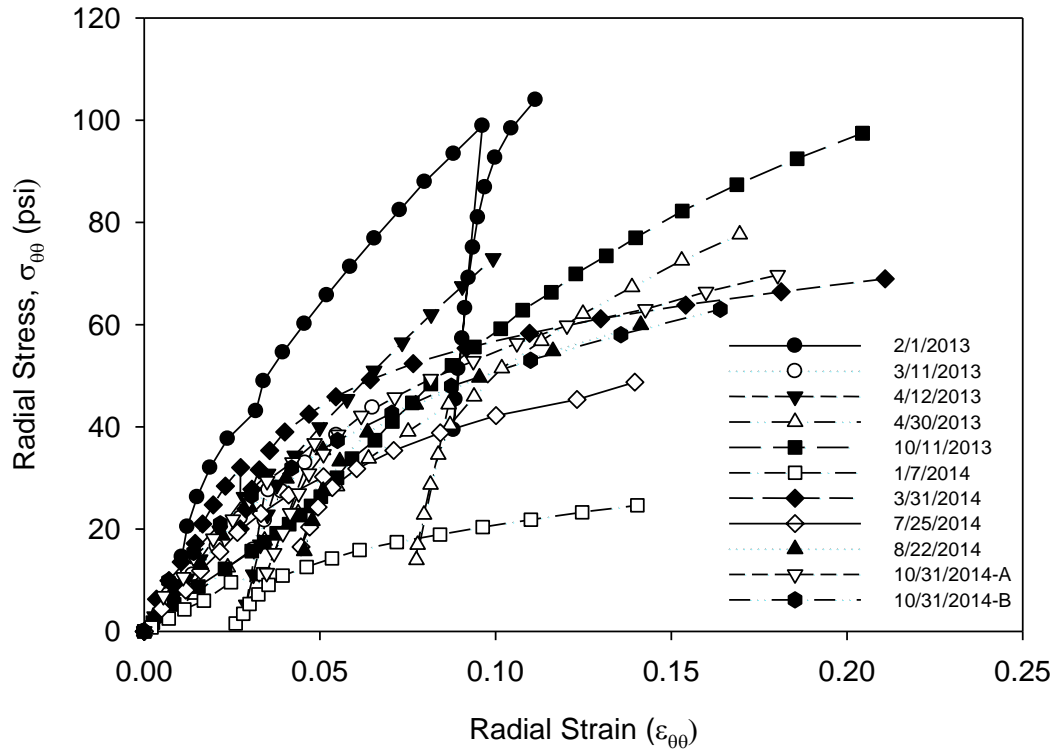


Figure 7. 3. North Base: PMT stress-strain curves for 3 ft depth.

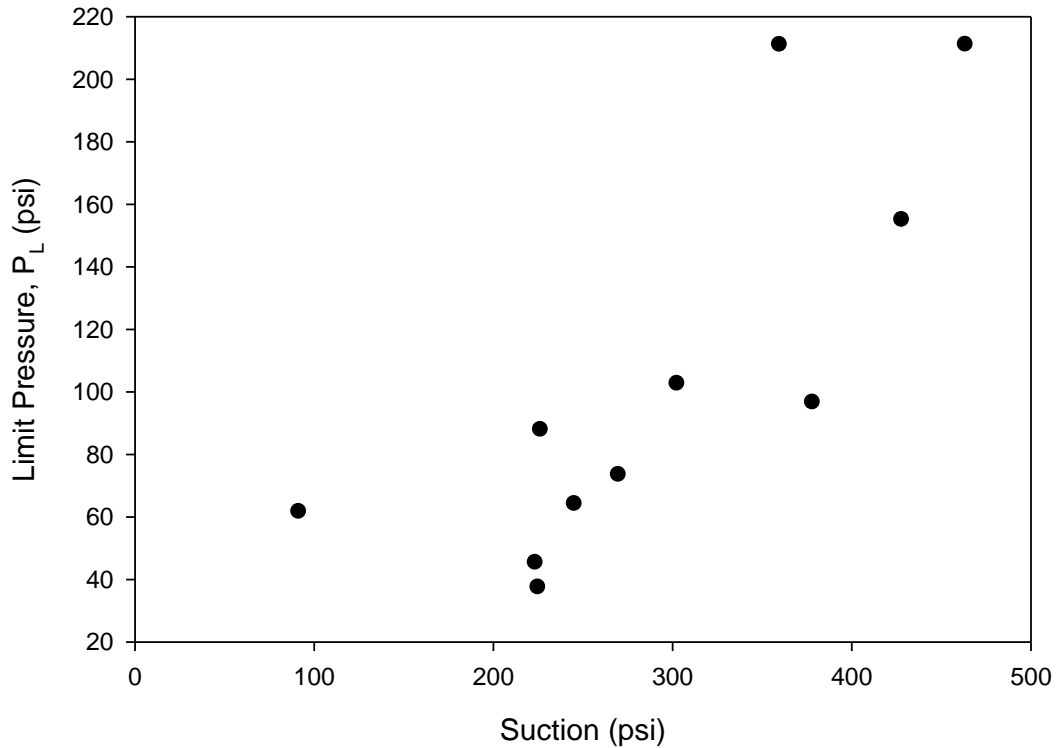
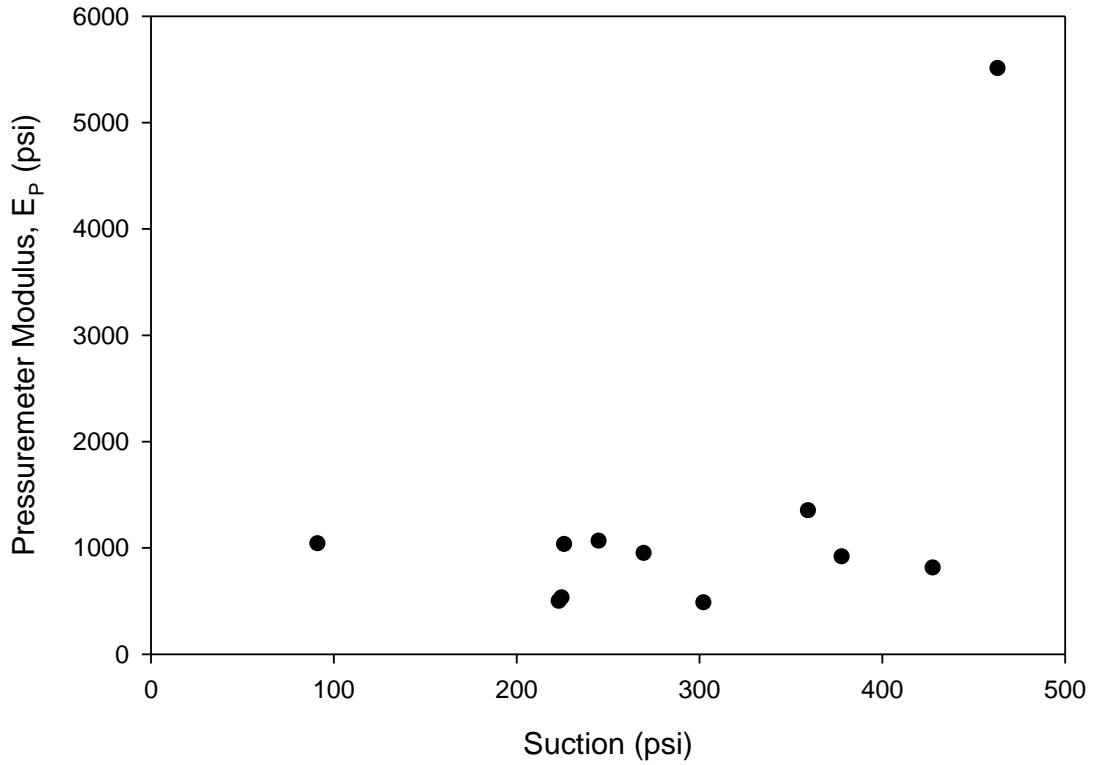
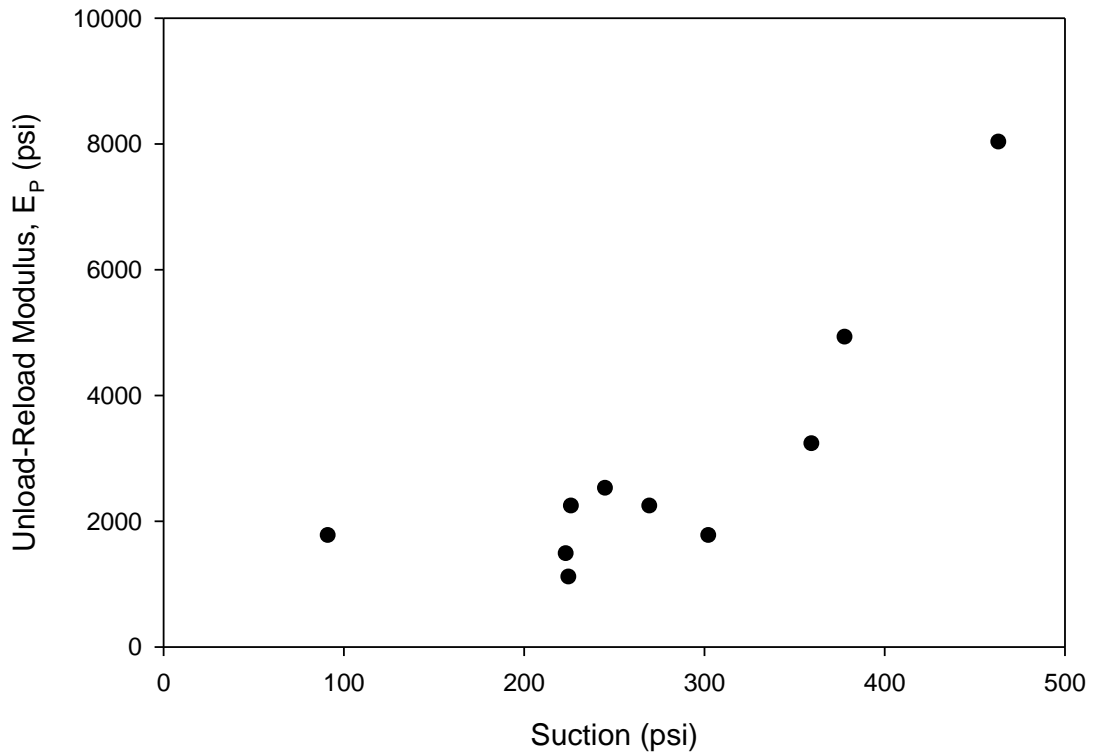


Figure 7. 4. North Base: limit pressure versus suction for 3 ft depth.



**Figure 7. 5. North Base: PMT modulus versus suction for 3 ft depth.**



**Figure 7. 6. North Base: unload-reload modulus versus suction for 3 ft depth.**

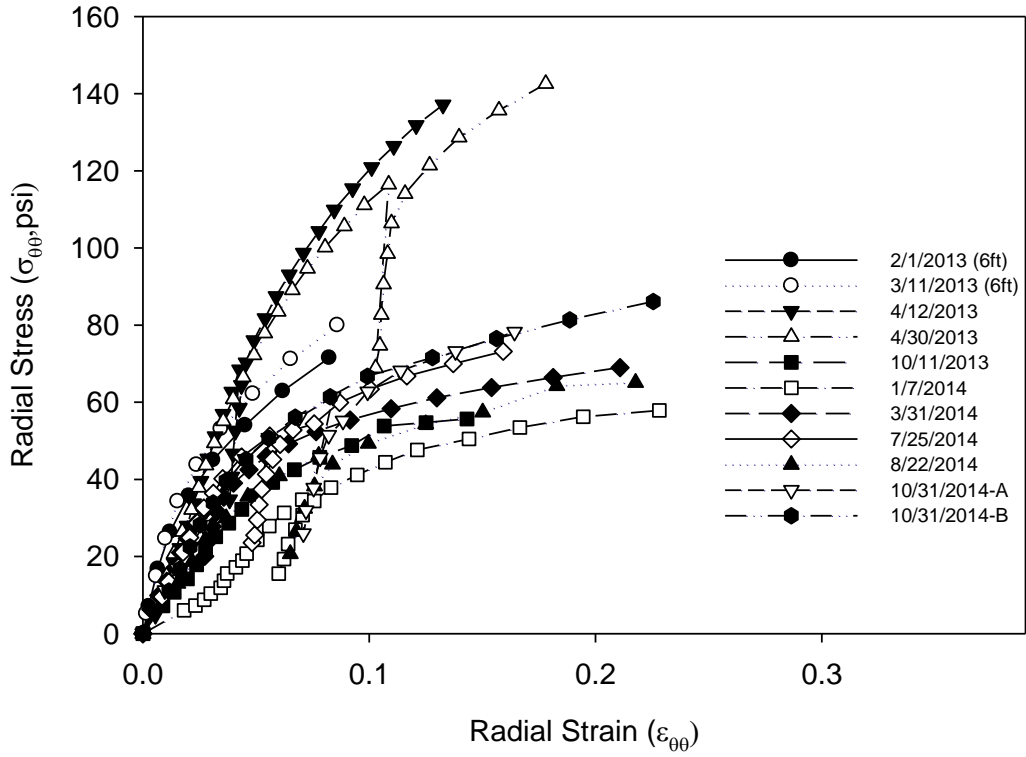


Figure 7. 7. North Base: PMT stress-strain curves for 5 ft depth.

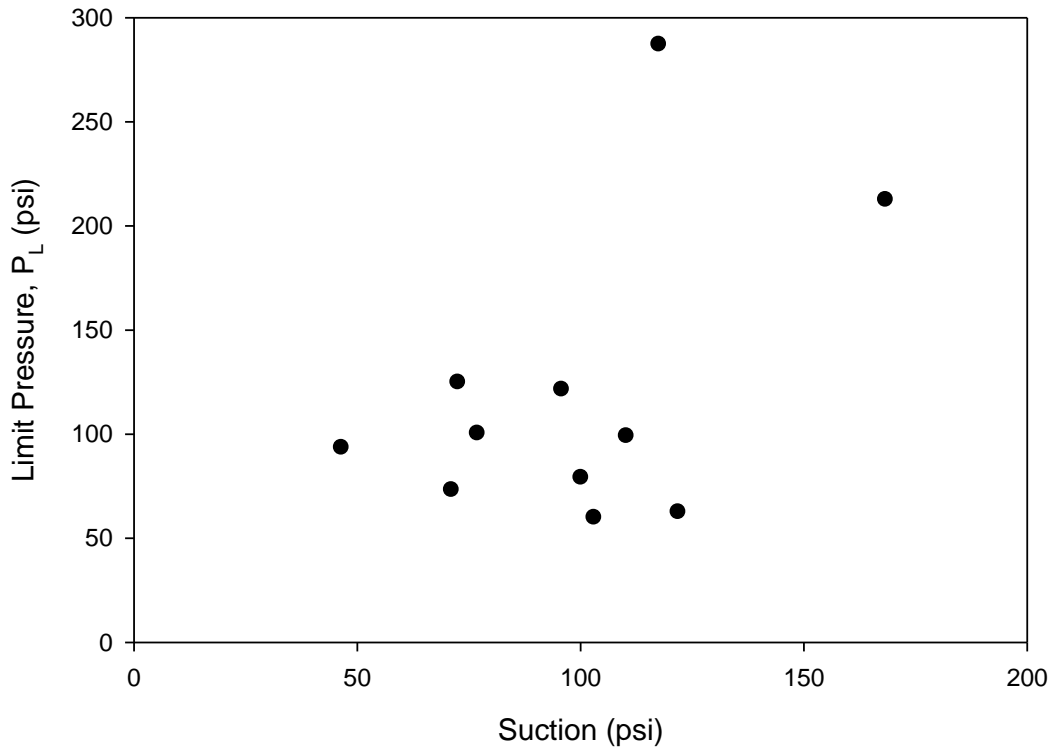
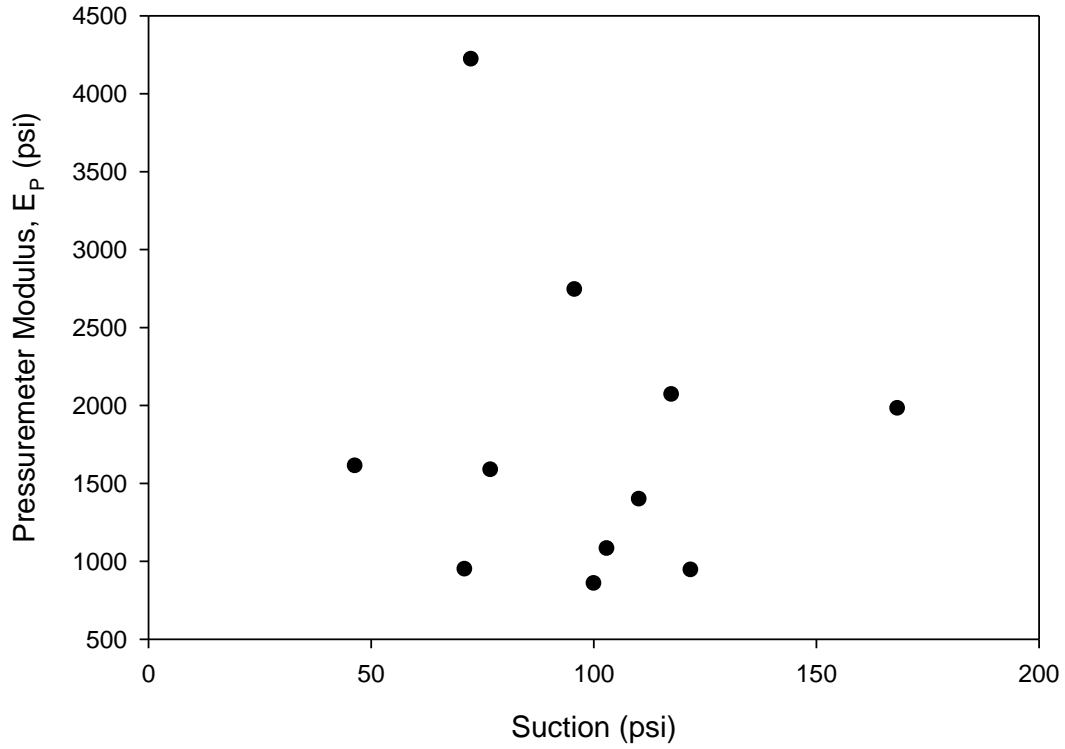
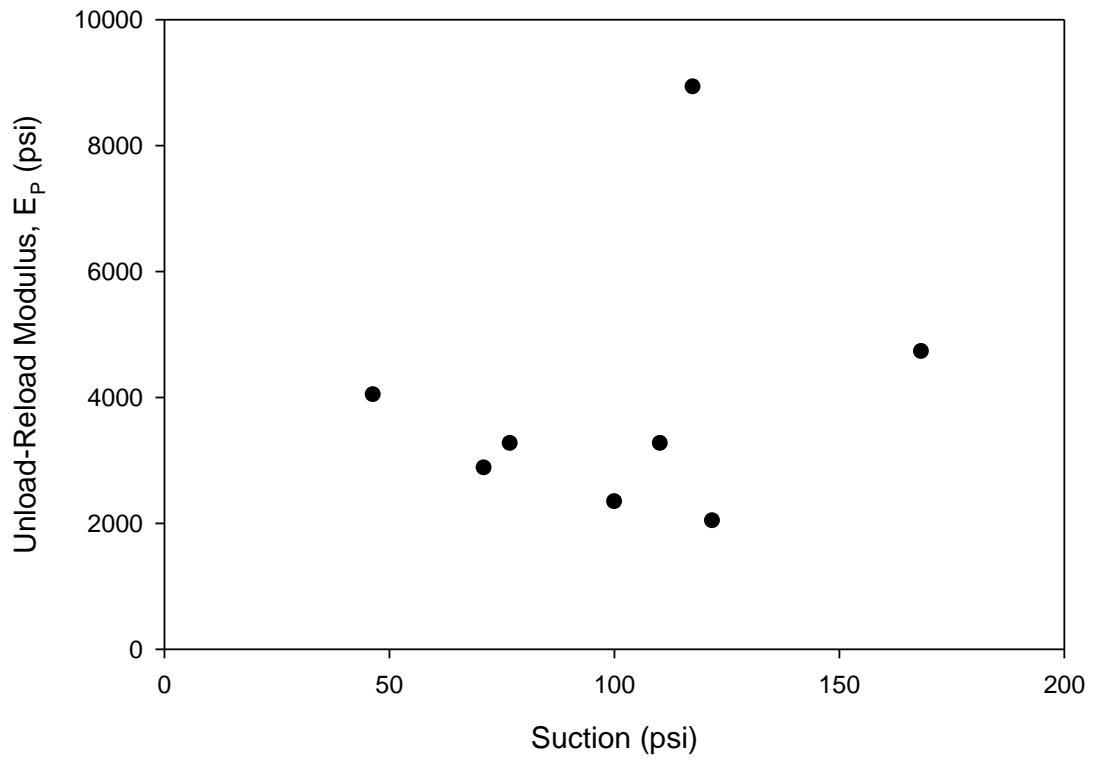


Figure 7. 8. North Base: limit pressure versus suction for 5 ft depth.



**Figure 7. 9. North Base PMT modulus versus suction for 5 ft depth.**



**Figure 7. 10. North Base: unload-reload modulus versus suction for 5 ft depth.**

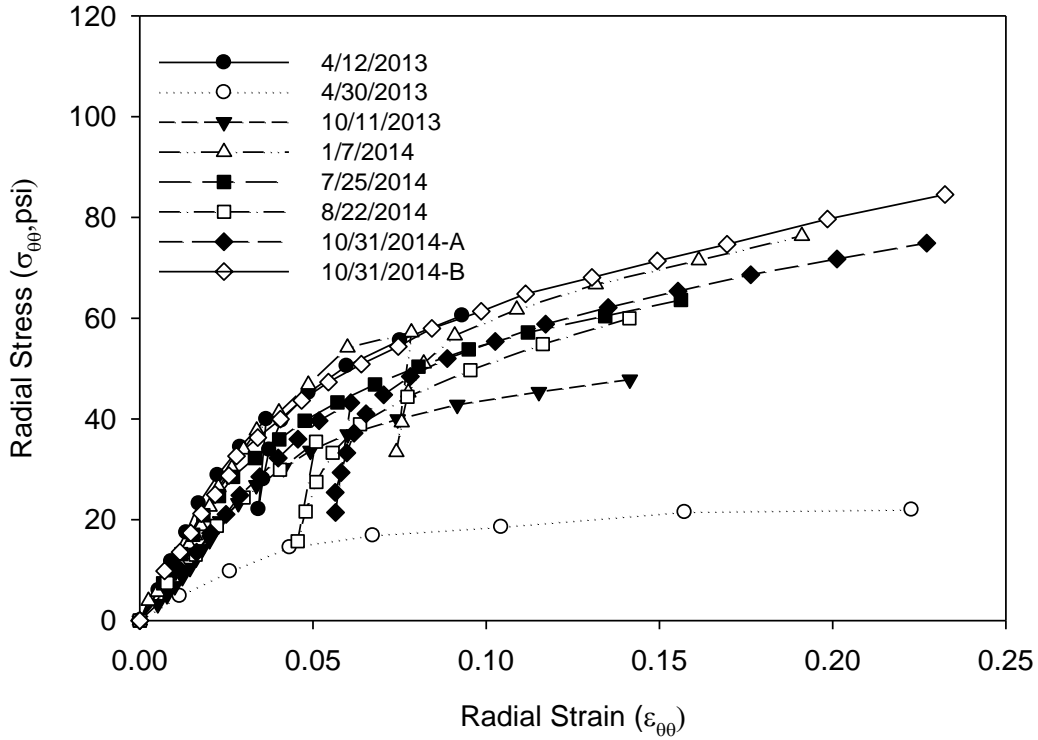


Figure 7.11. North Base: PMT stress-strain curves for 7 ft depth.

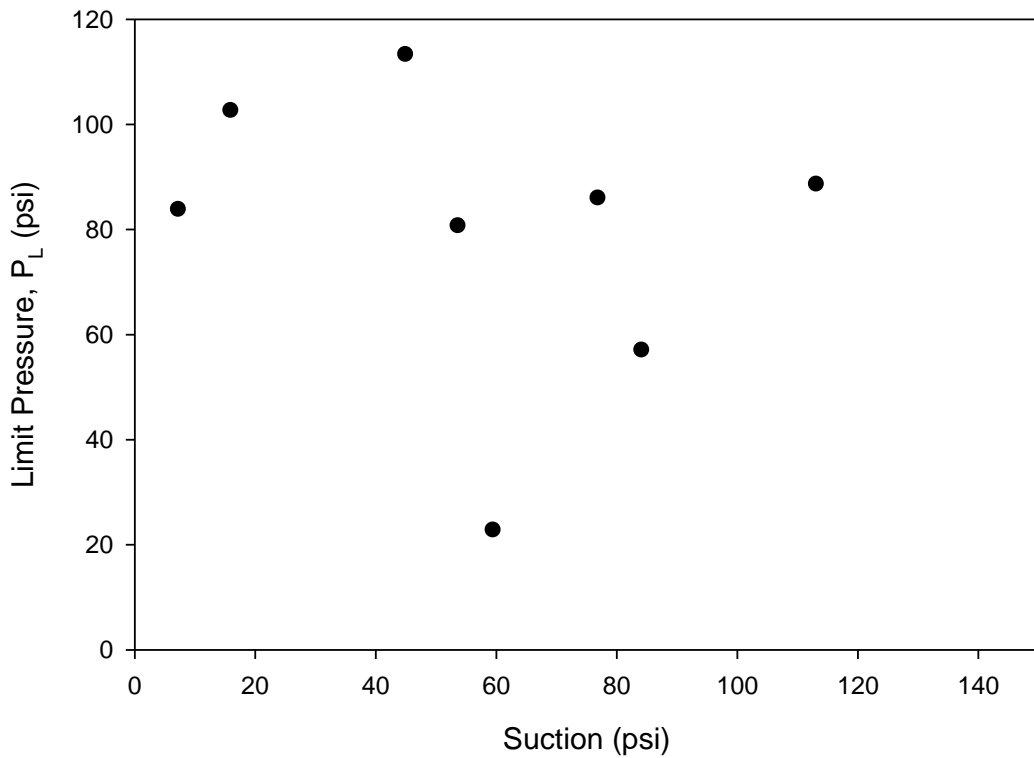
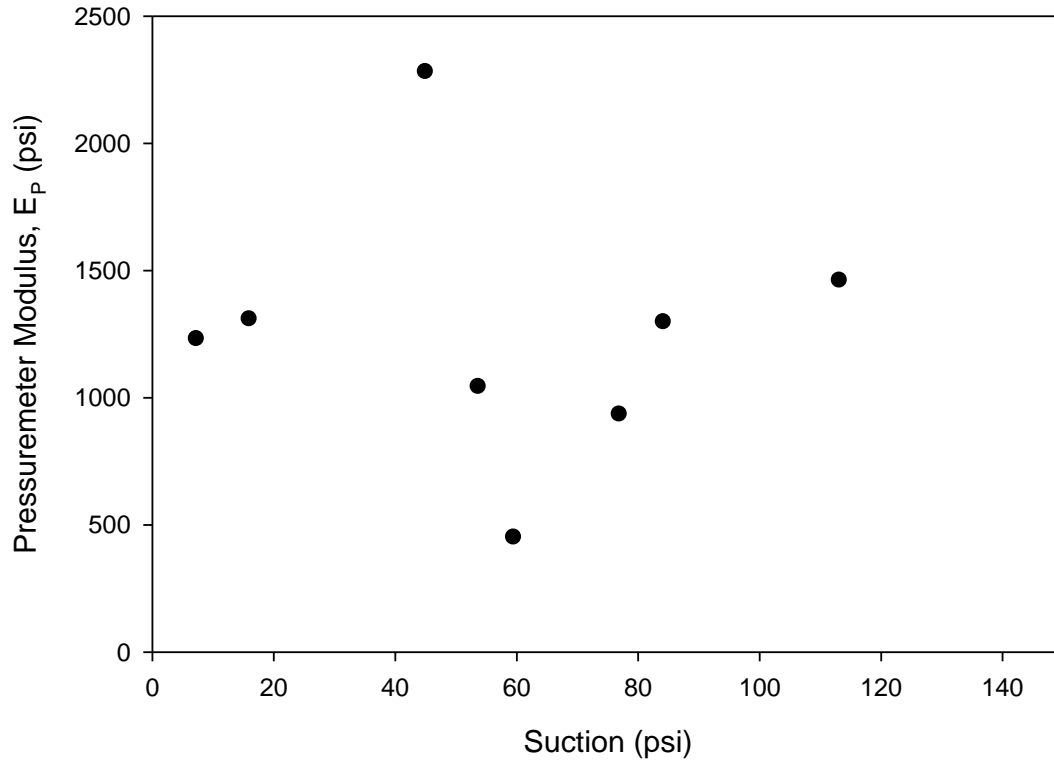
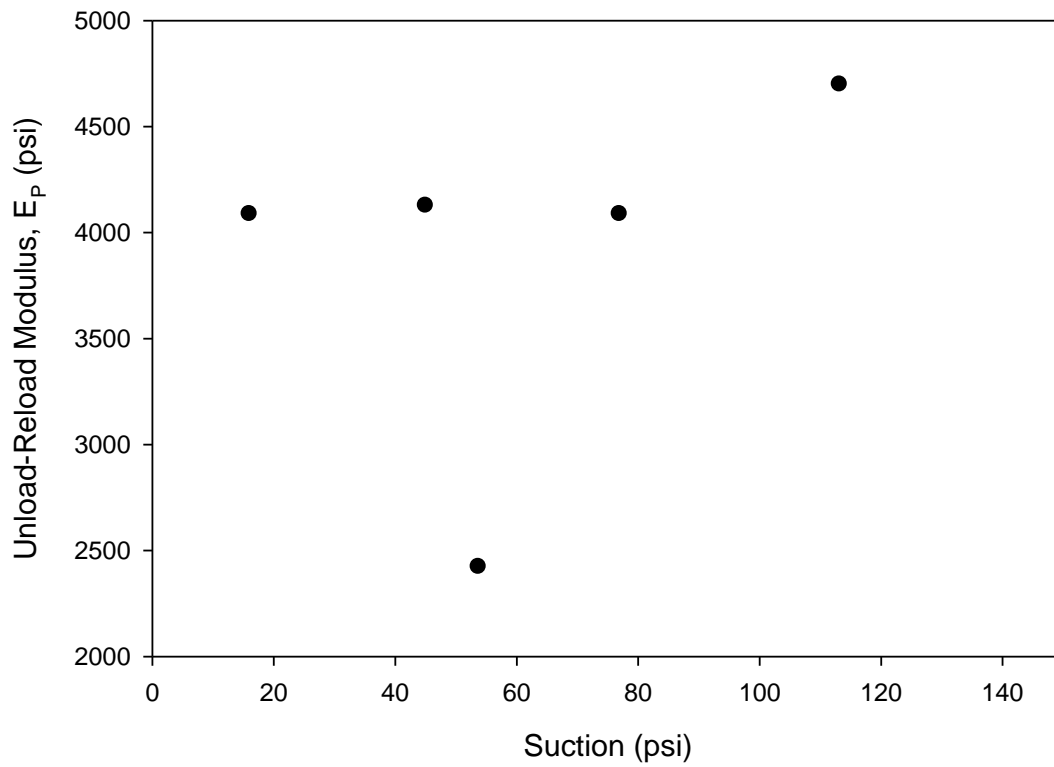


Figure 7.12. North Base: limit pressure versus suction for 7 ft depth.



**Figure 7. 13. North Base: PMT modulus versus suction for 7 ft depth.**



**Figure 7. 14. North Base: unload-reload modulus versus suction for 7 ft depth.**

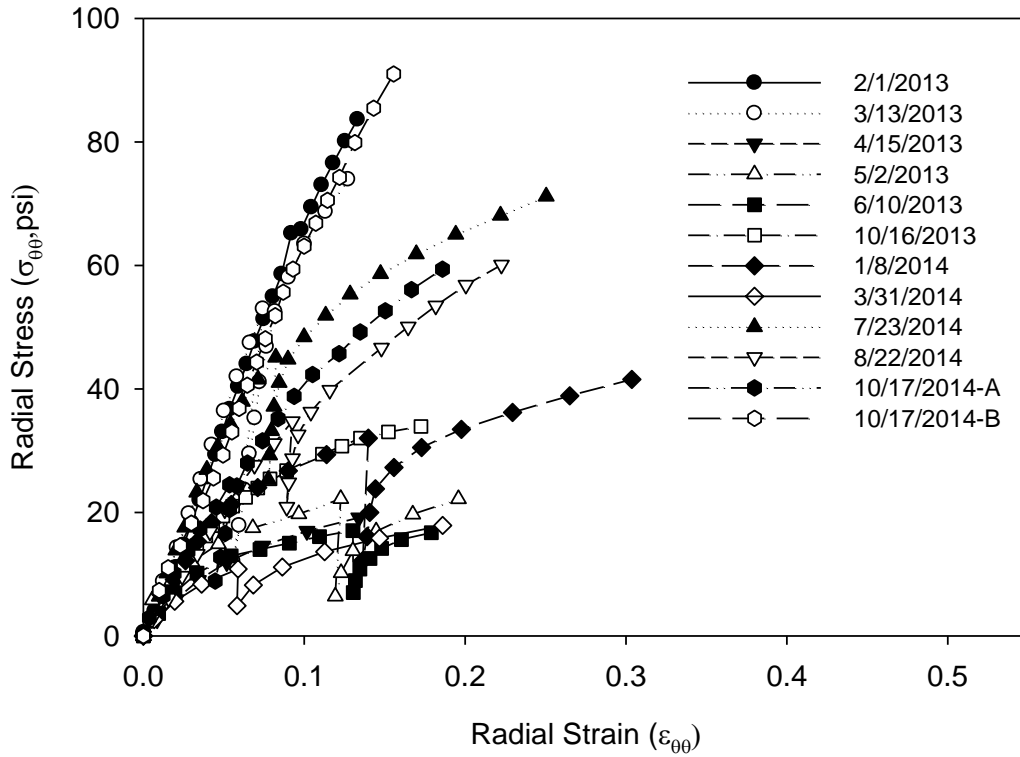


Figure 7. 15. Goldsby: PMT stress-strain curves for 3 ft depth.

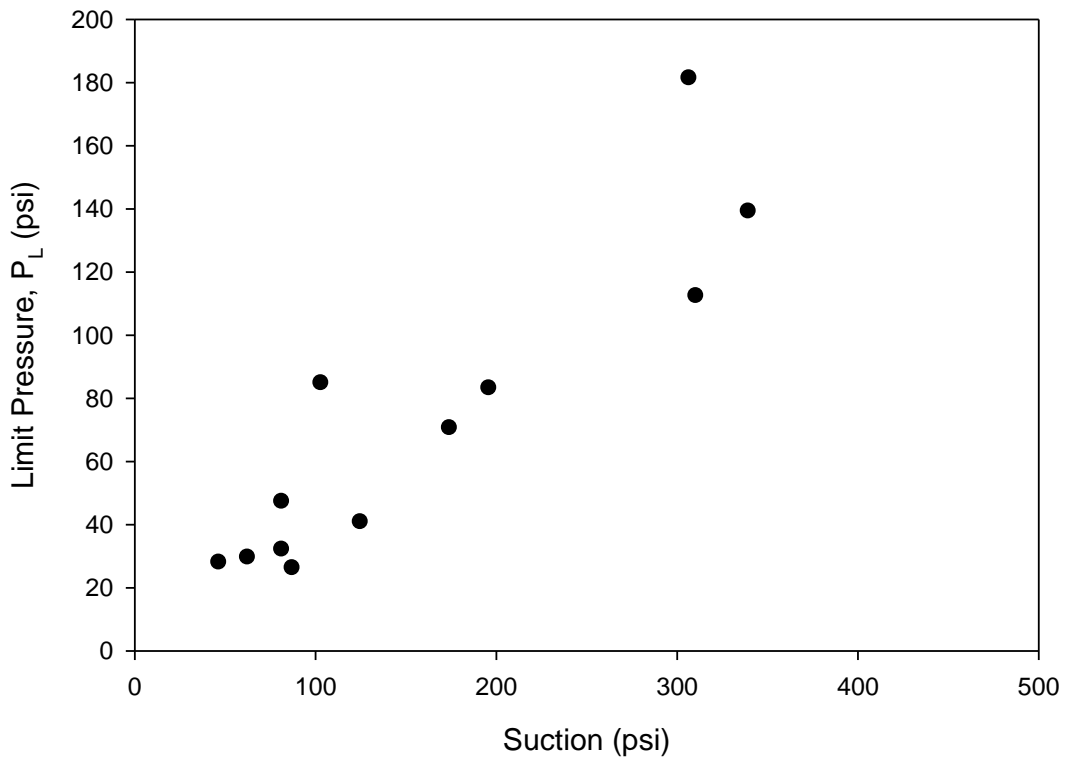
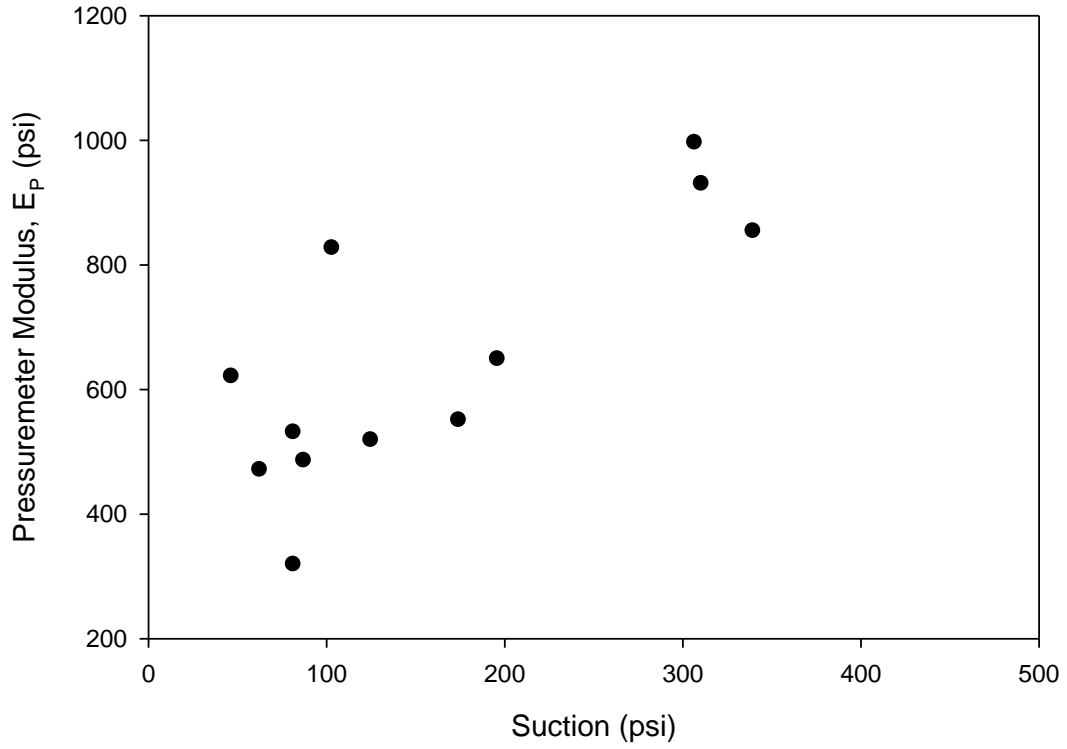
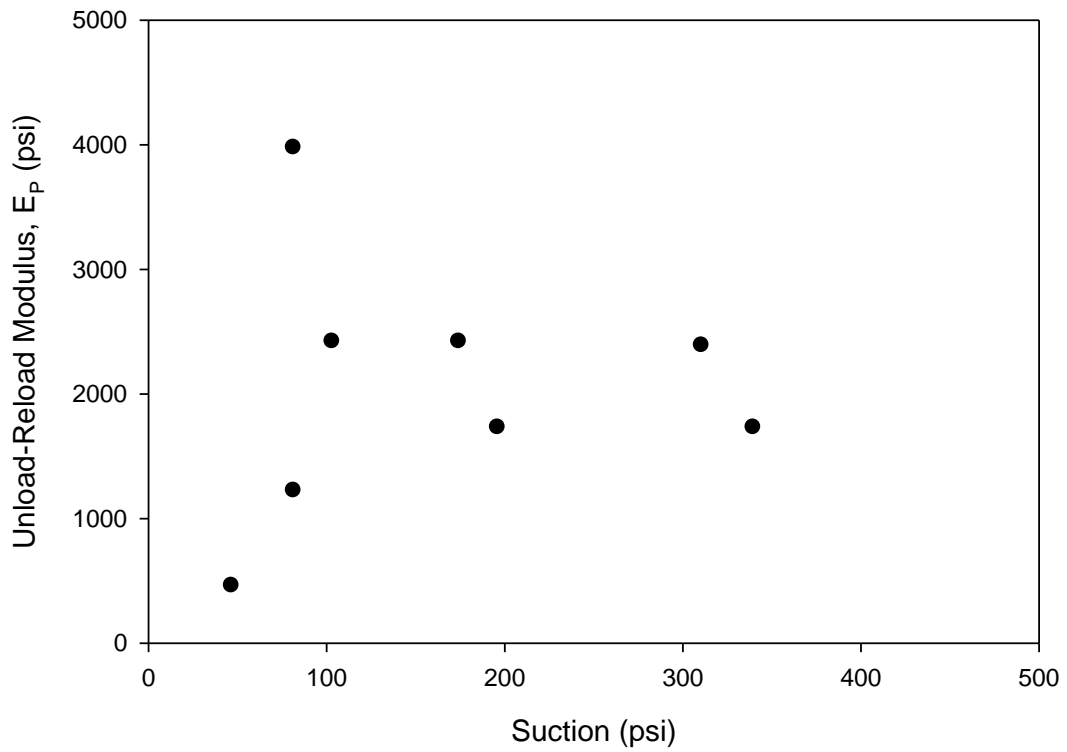


Figure 7. 16. Goldsby: limit pressure versus suction for 3 ft depth.



**Figure 7. 17. Goldsby: PMT modulus versus suction for 3 ft depth.**



**Figure 7. 18. Goldsby: unload-reload modulus versus suction for 3 ft depth.**

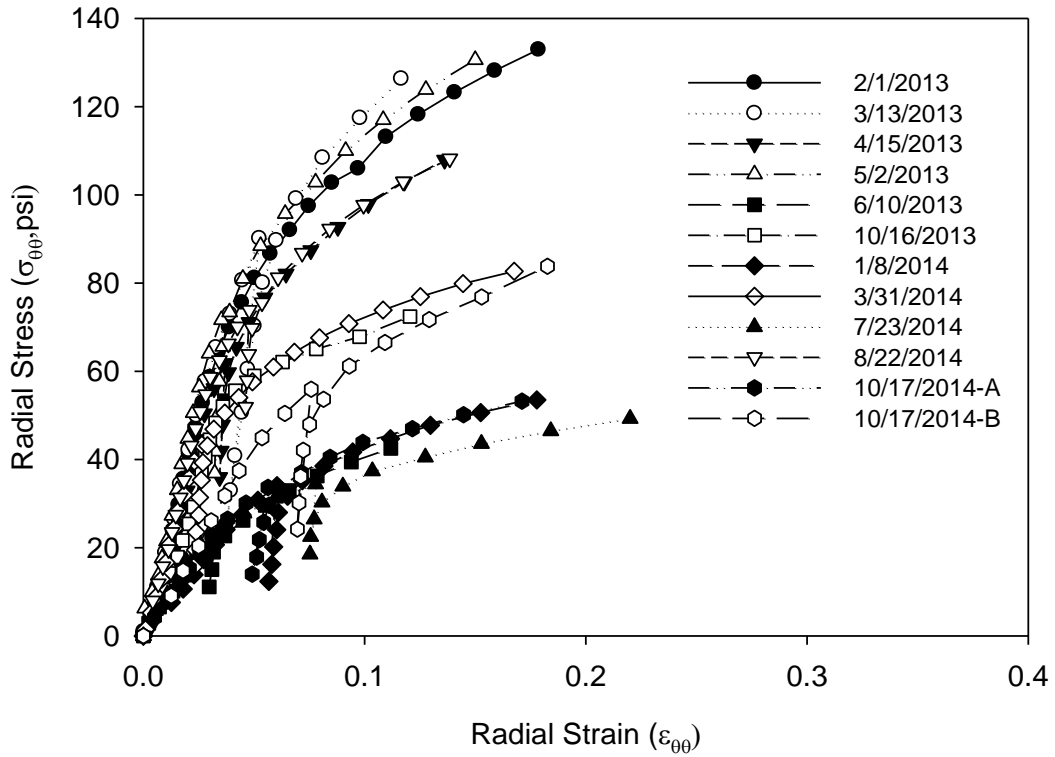


**Figure 7. 19. Goldsby: PMT stress-strain curves for 6 ft depth.**

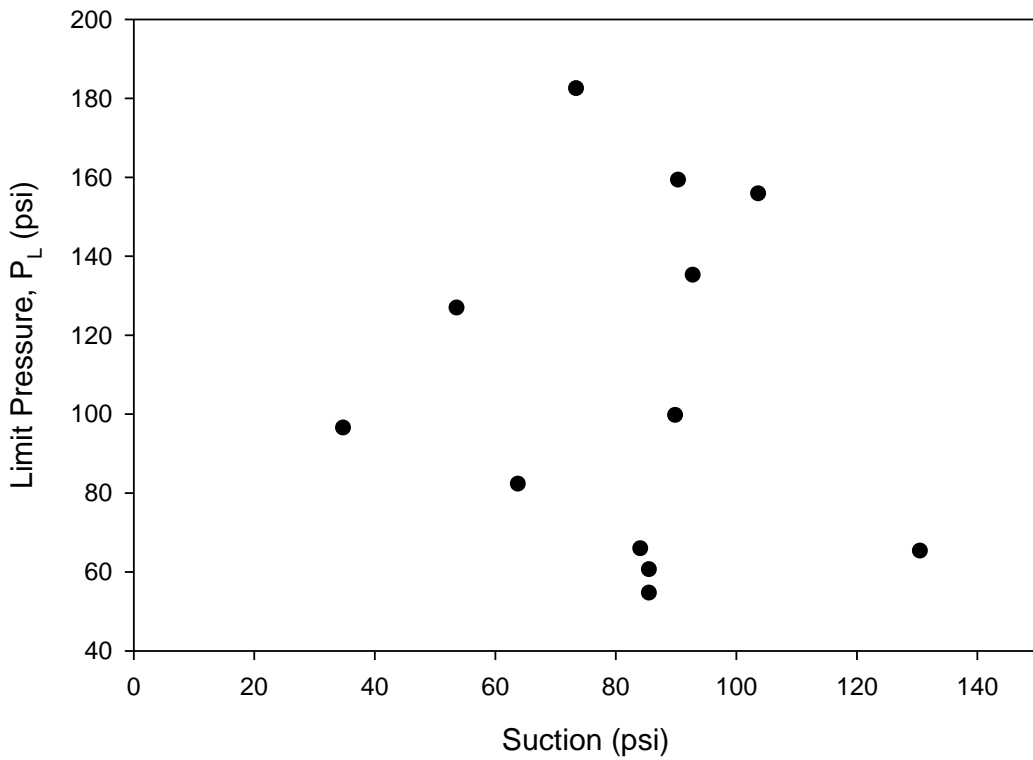


**Figure 7. 20. Goldsby: limit pressure versus suction for 6 ft depth.**

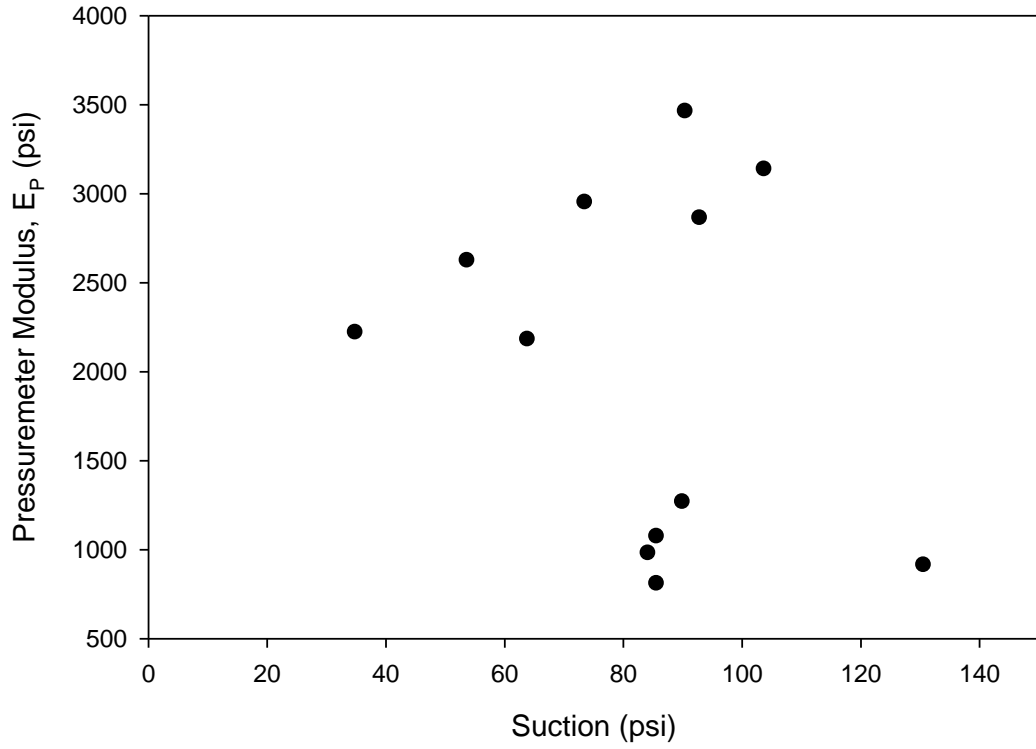


**Figure 7. 21. Goldsby: PMT modulus versus suction for 6 ft depth.**

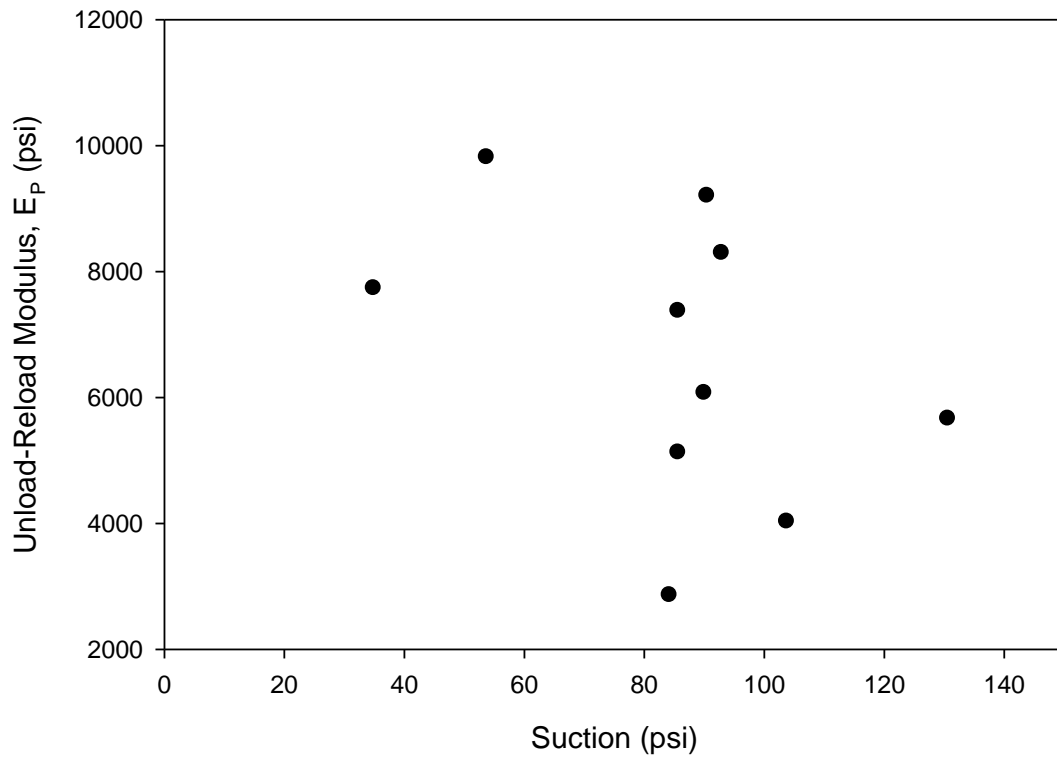


**Figure 7. 22. Goldsby: unload-reload modulus versus suction for 6 ft depth.**

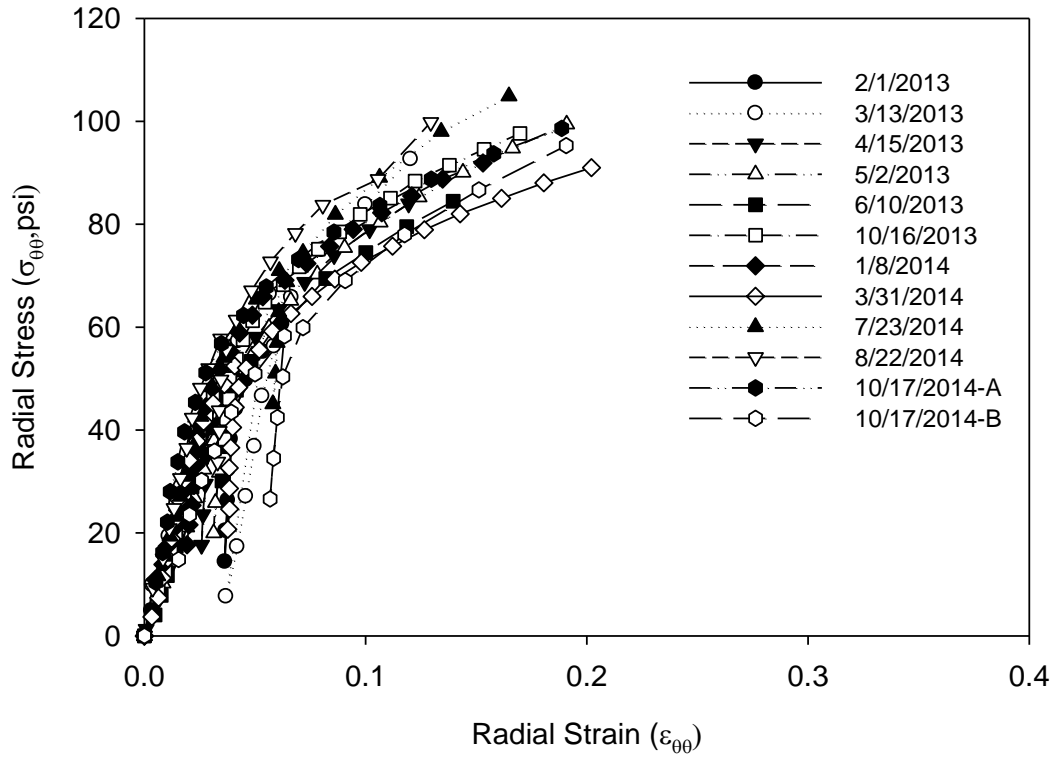


**Figure 7. 23. Goldsby: PMT stress-strain curves for 9 ft depth.**

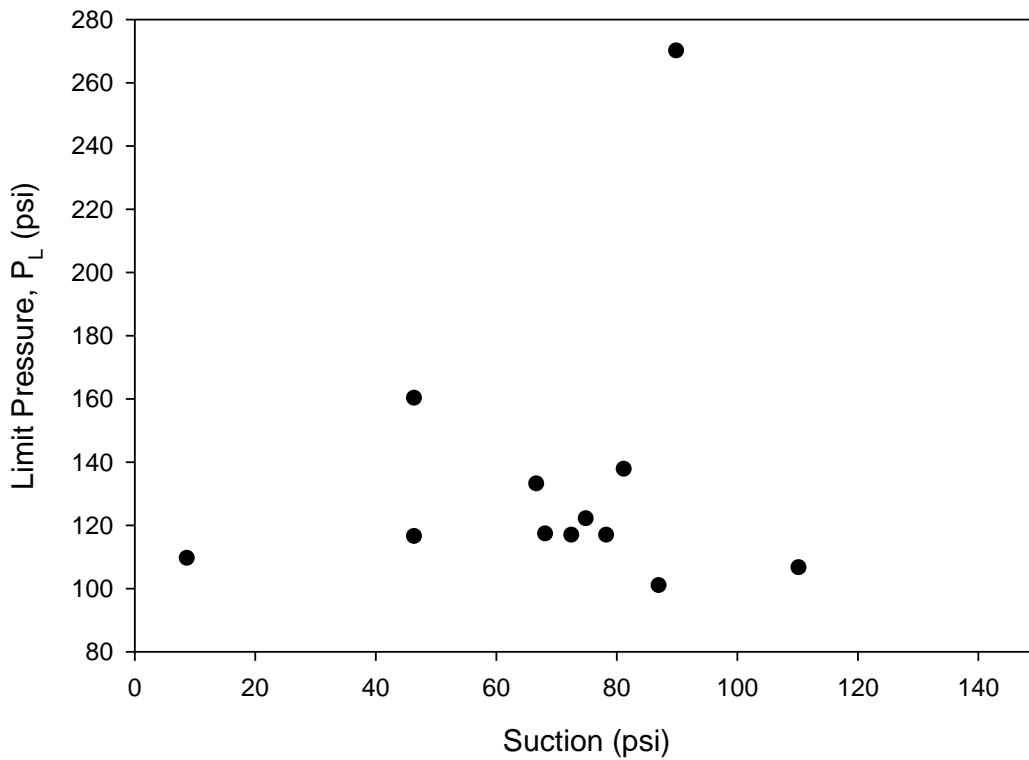


**Figure 7. 24. Goldsby: limit pressure versus suction for 9 ft depth.**

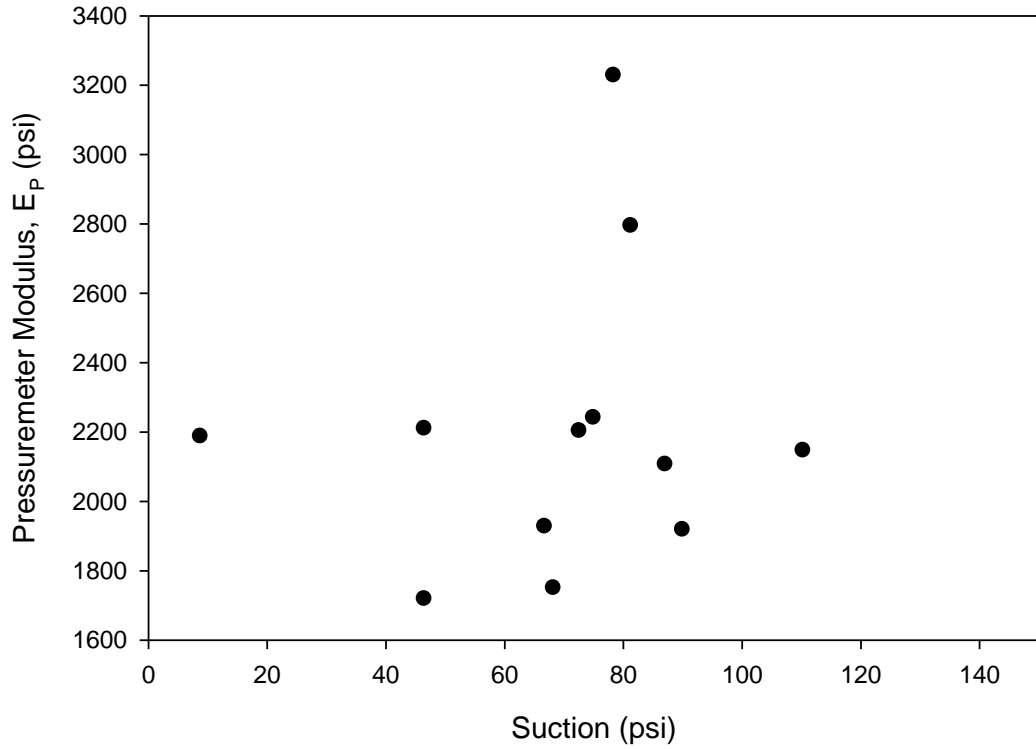


**Figure 7. 25. Goldsby: PMT modulus versus suction for 9 ft depth.**

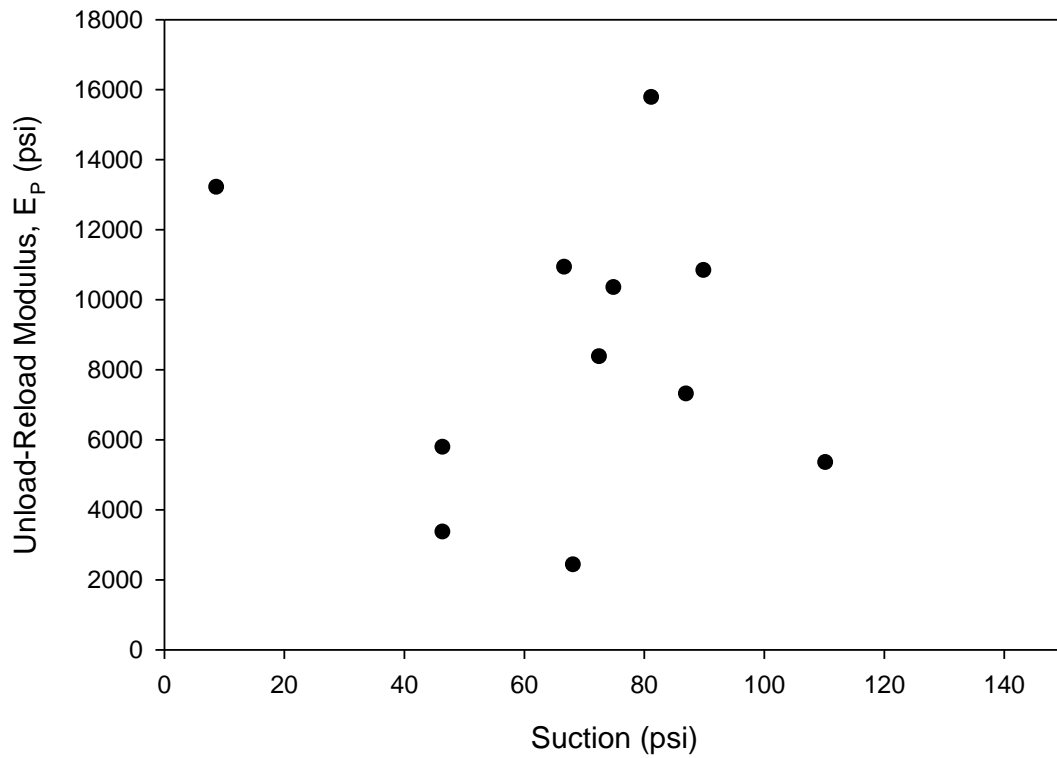


**Figure 7. 26. Goldsby: unload-reload modulus versus suction for 9 ft depth.**

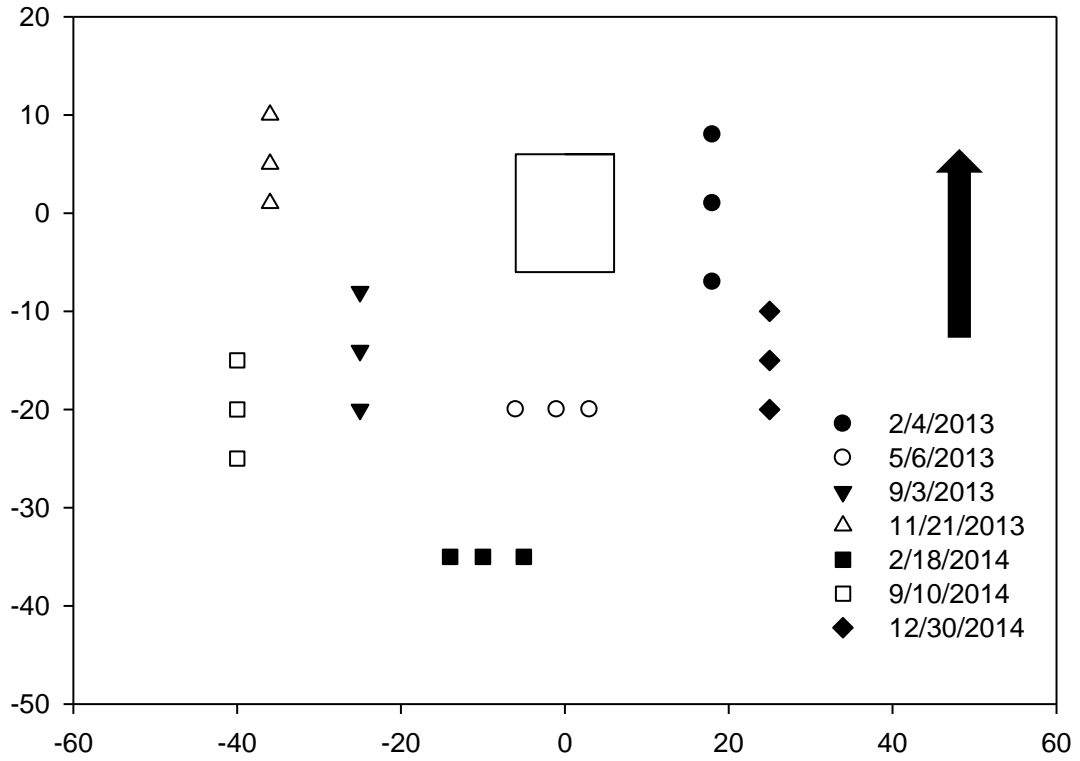


Figure 7. 27. North Base: CPT location map.

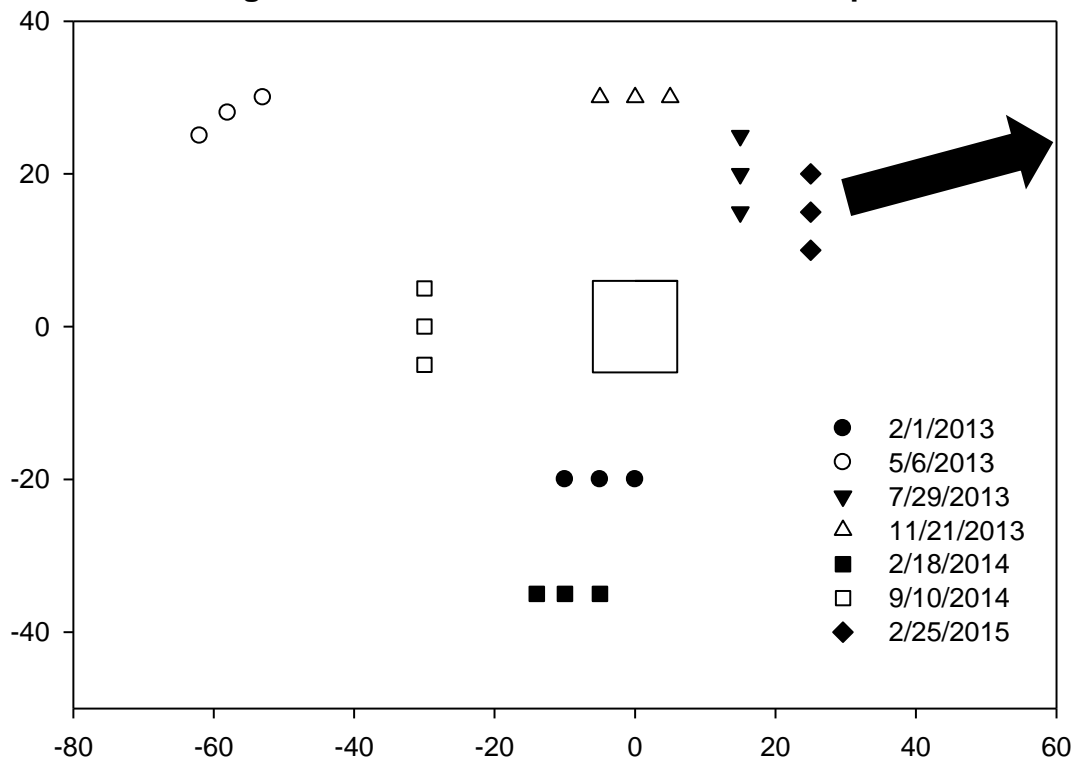


Figure 7. 28. Goldsby: CPT location map.

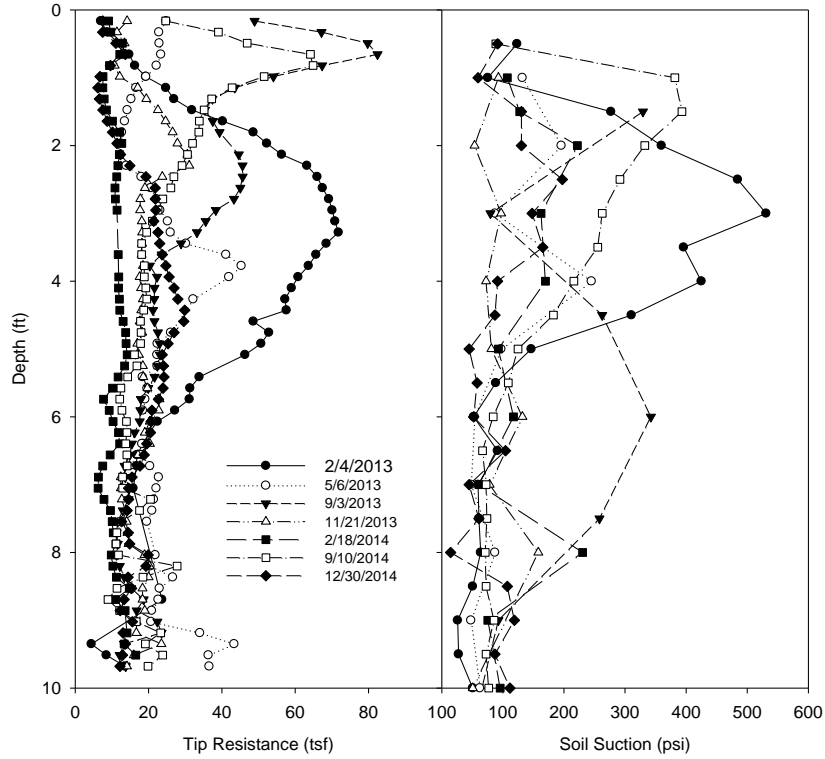


Figure 7. 29. North Base: tip resistance and suction versus depth.

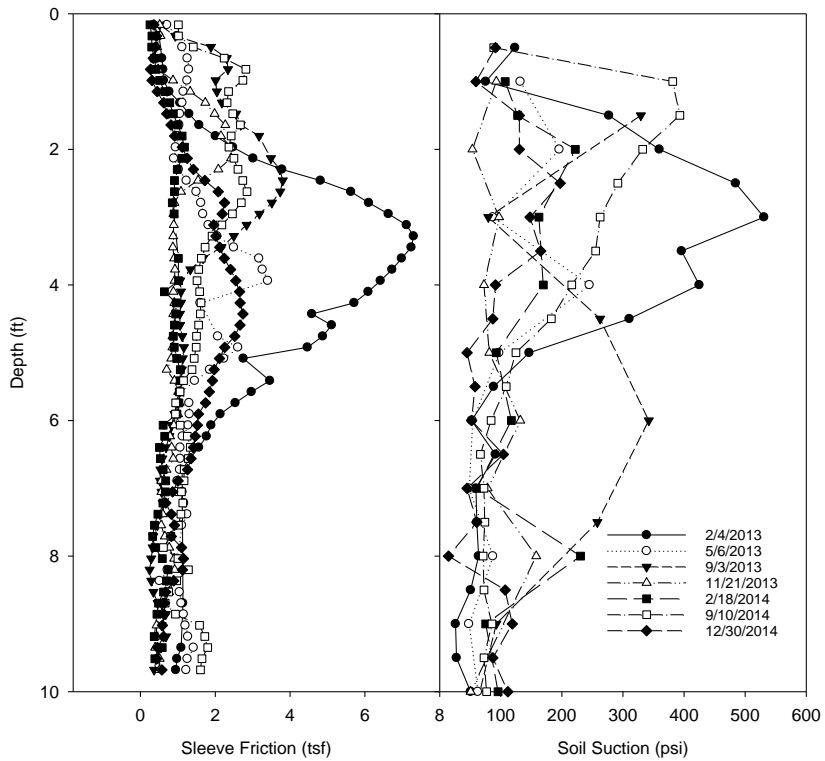


Figure 7. 30. North Base: sleeve friction and suction versus depth.

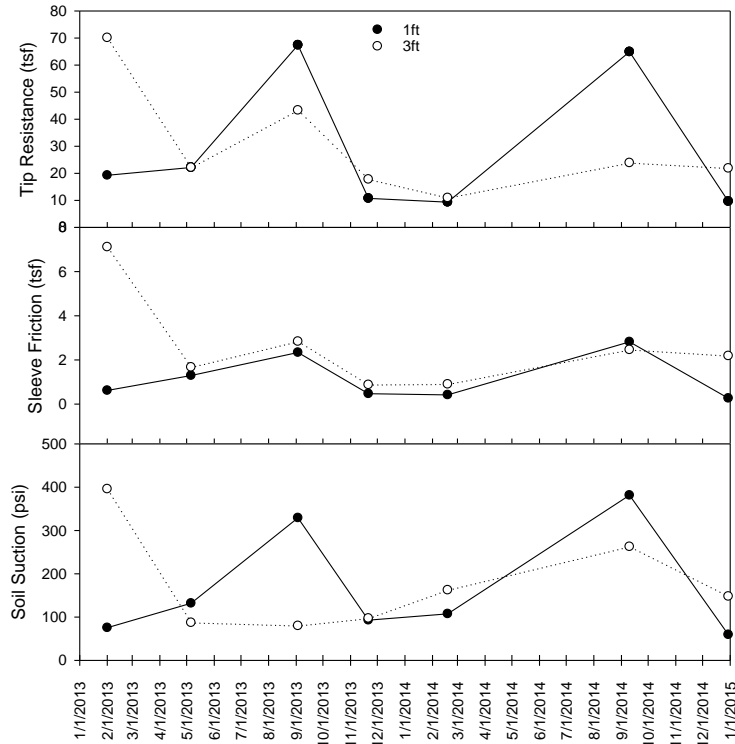


Figure 7. 31. North Base: CPT parameters during test period at 1 ft and 3 ft depths.

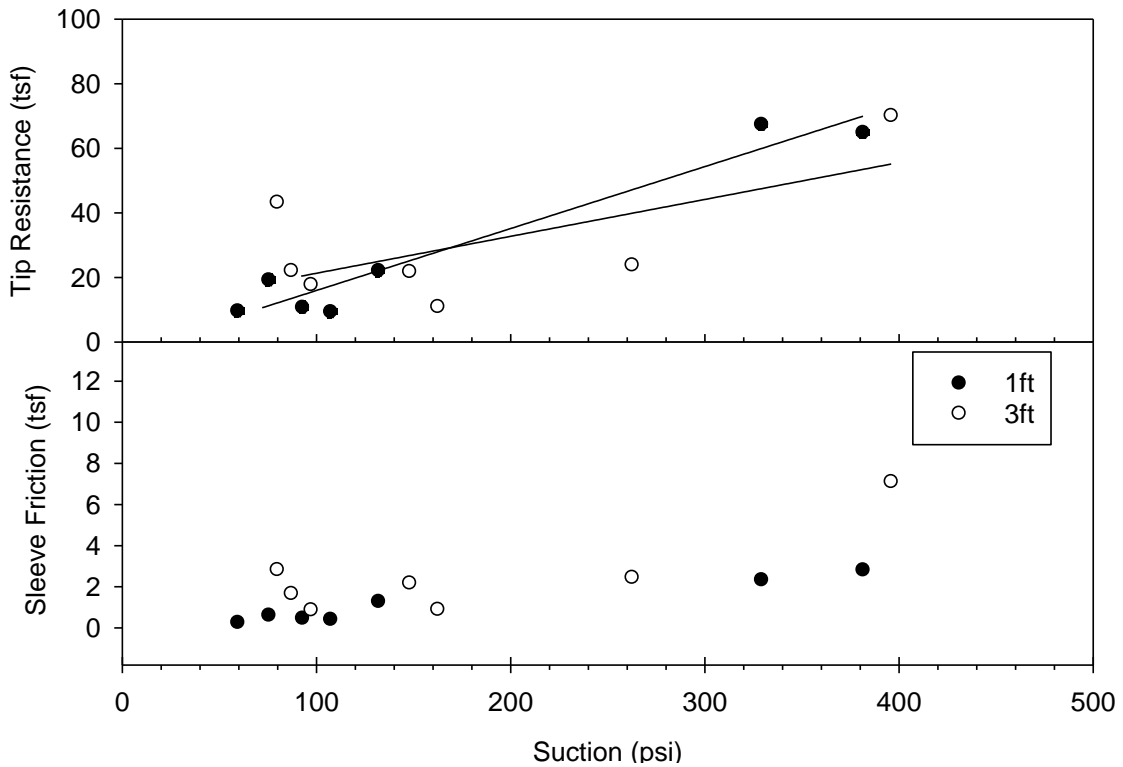


Figure 7. 32. North Base: CPT parameters versus suction at 1 ft and 3 ft depths.

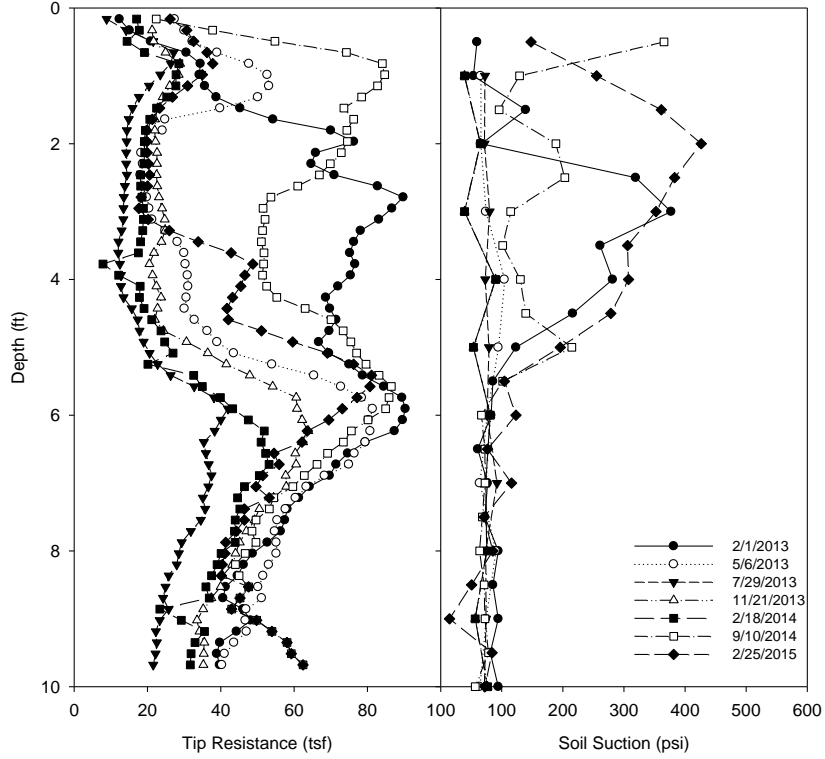


Figure 7. 33. Goldsby: tip resistance and suction versus depth.

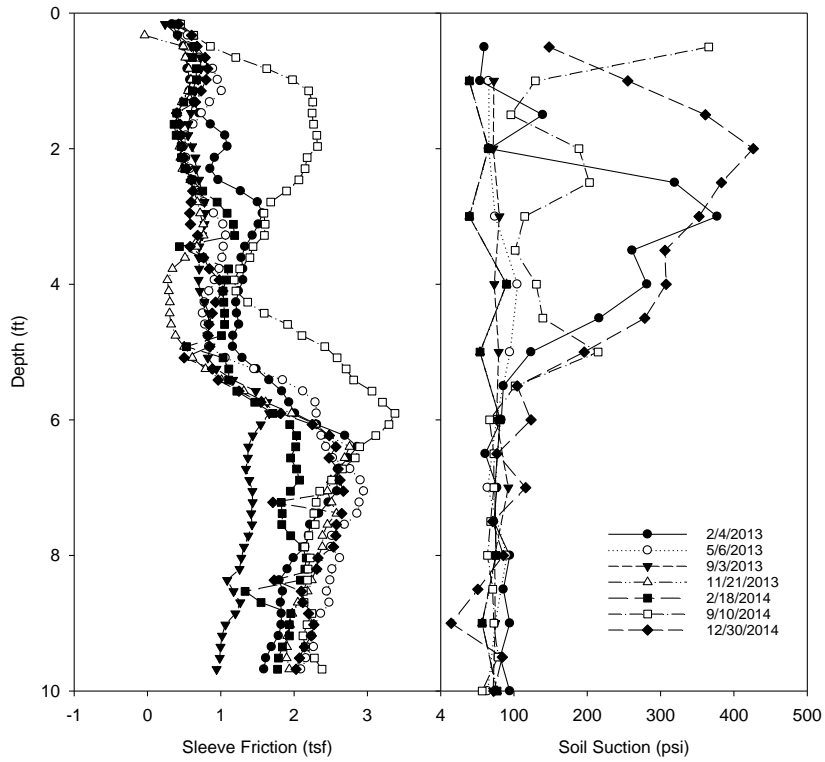


Figure 7. 34. Goldsby: skin friction and suction versus depth.

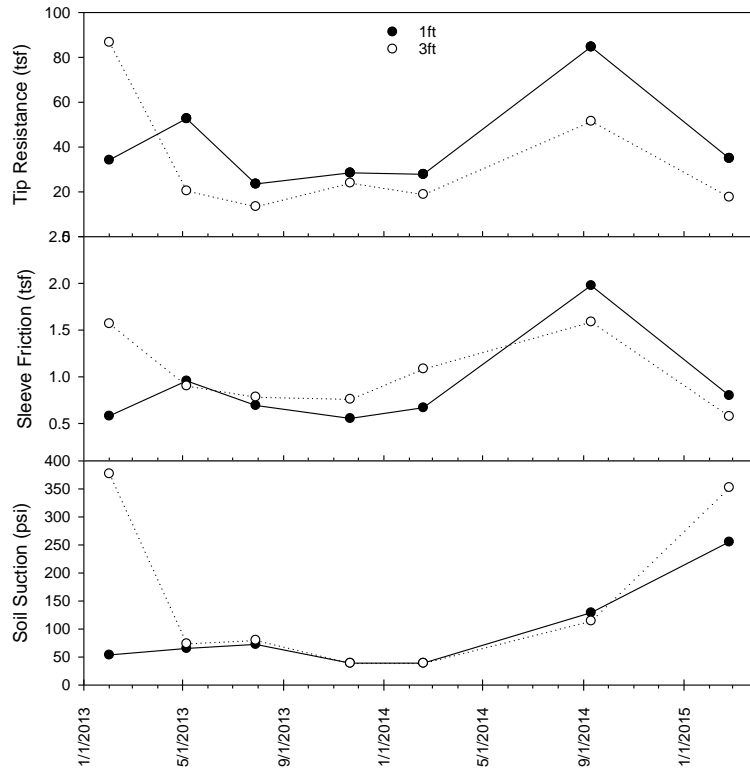


Figure 7. 35. Goldsby: CPT parameters during test period for 1 ft and 3 ft depths.

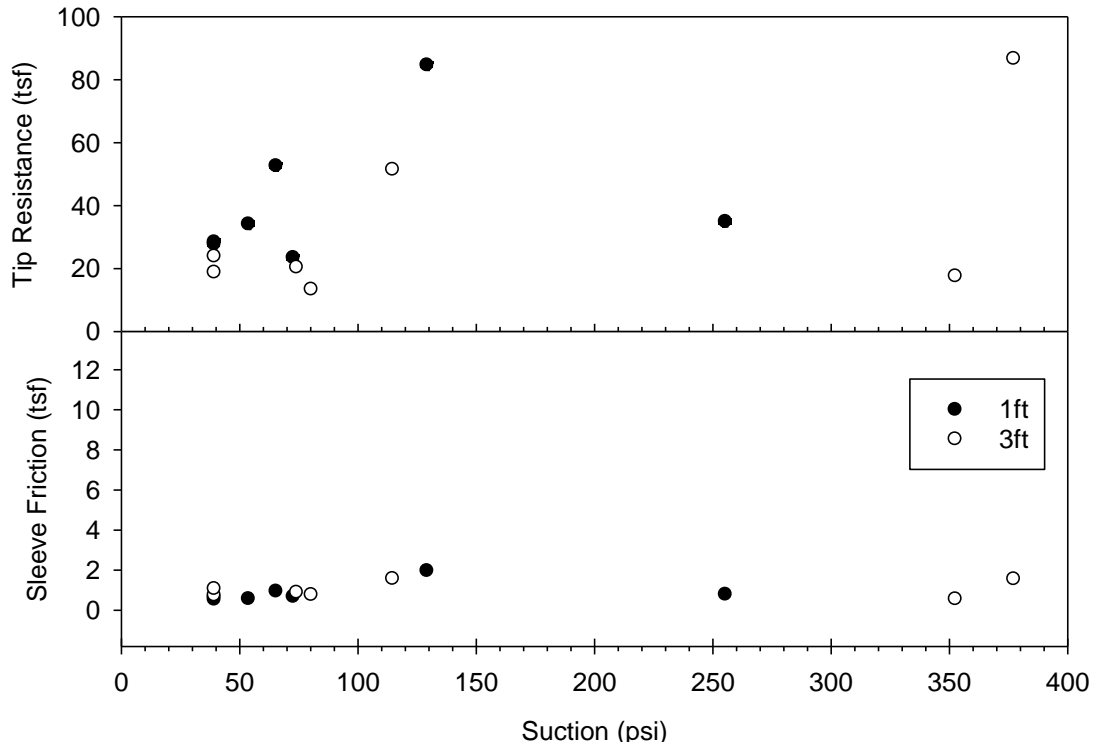


Figure 7. 36. Goldsby: CPT parameters versus suction for 1 ft and 3 ft depths.

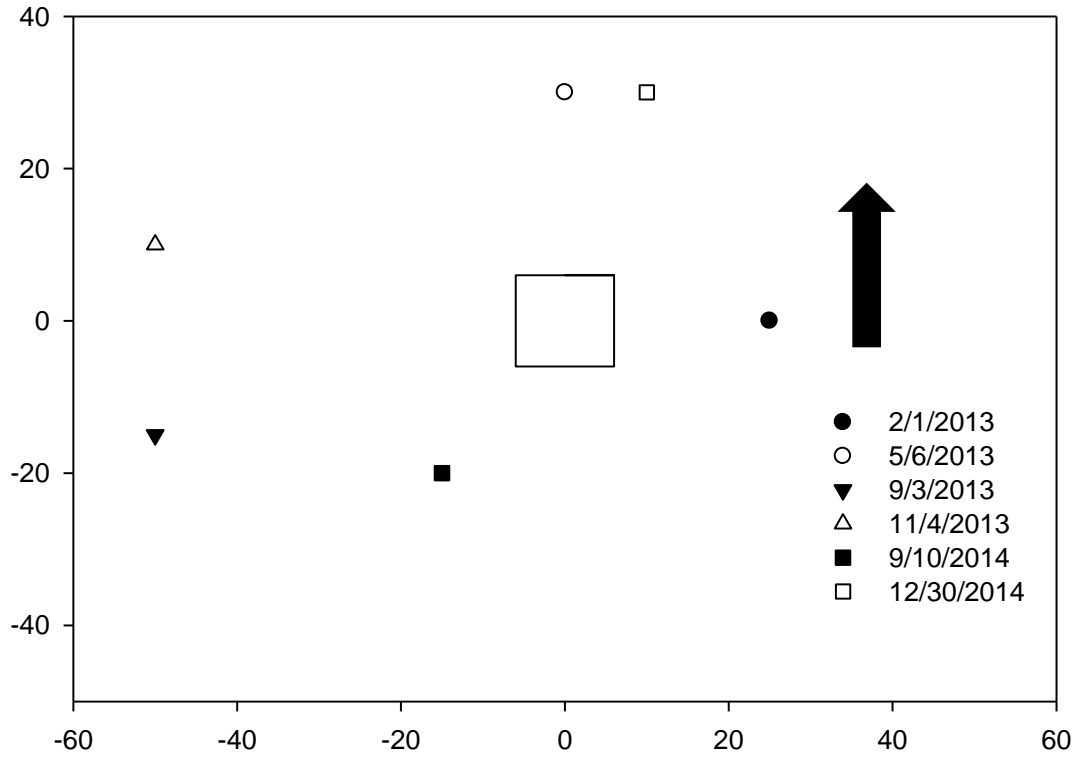


Figure 7. 37. North Base: SPT location map.

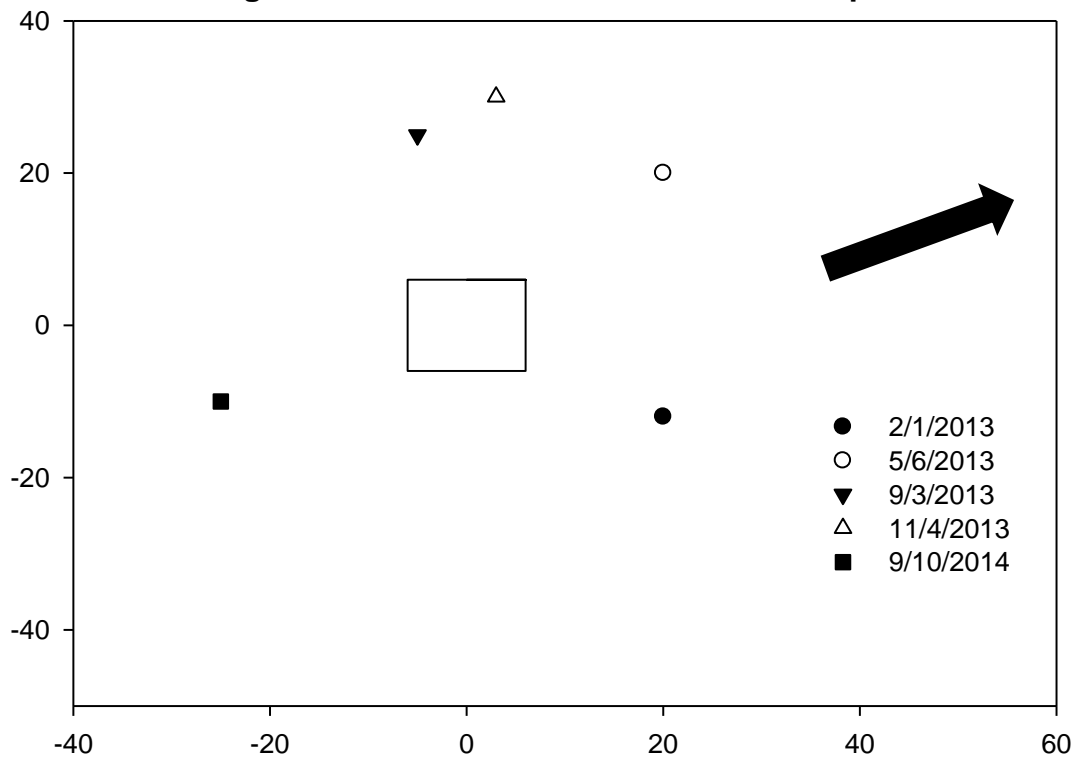


Figure 7. 38. Goldsby: SPT location map.

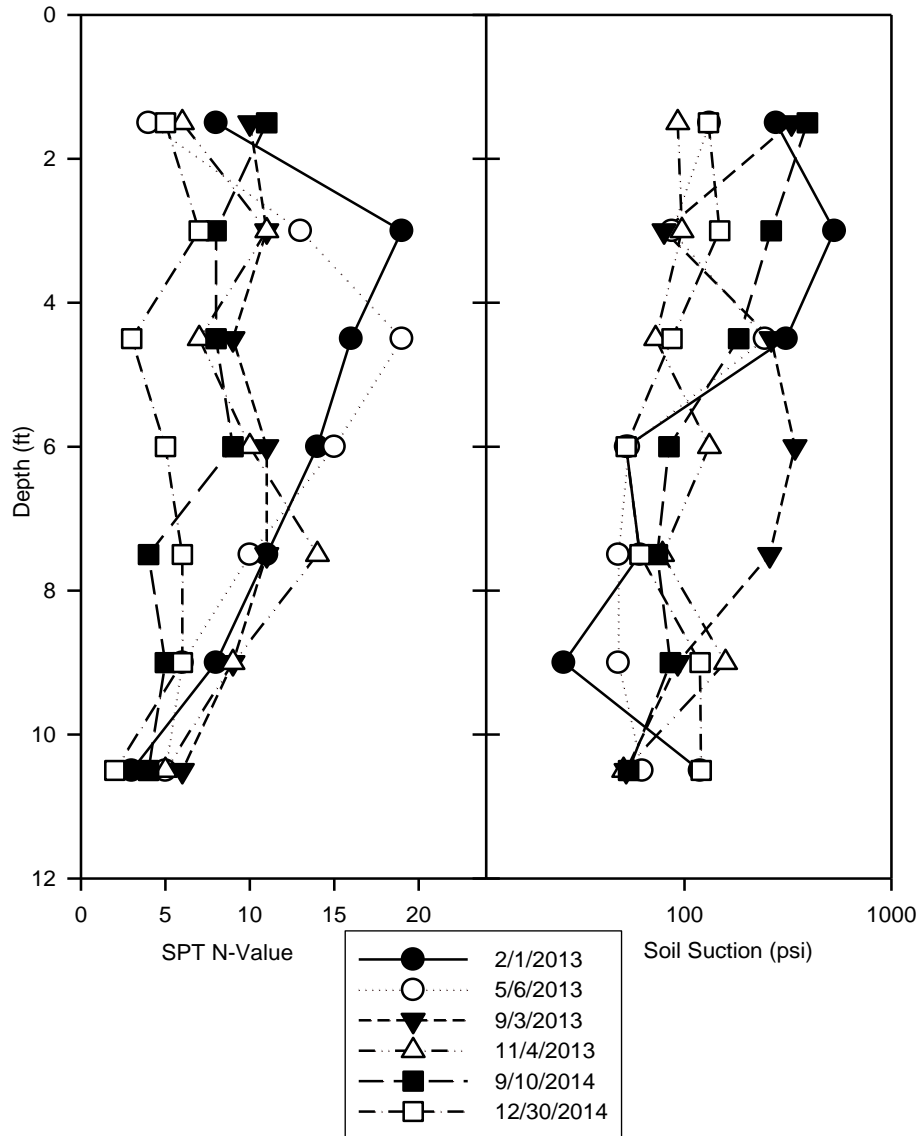


Figure 7. 39. North Base: SPT N-value and suction versus depth.

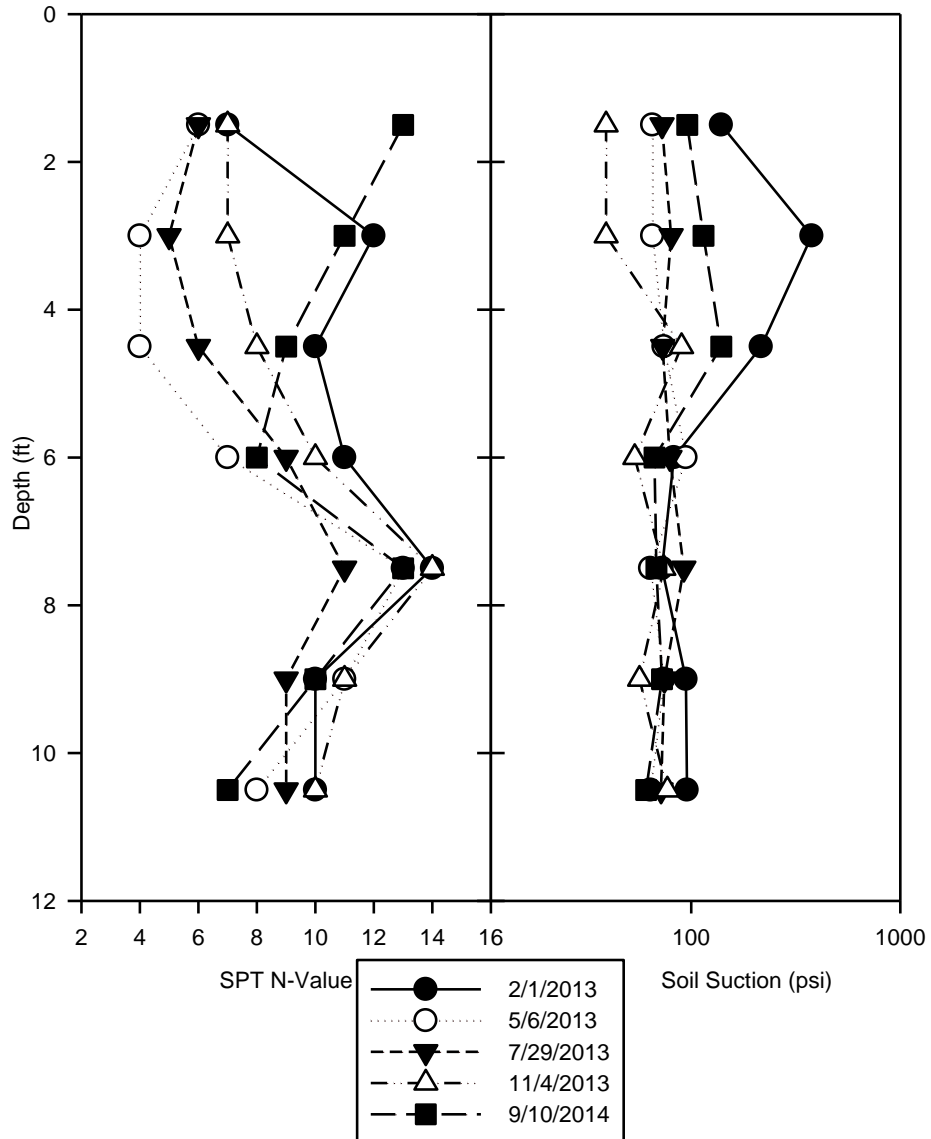


Figure 7. 40. Goldsby: SPT N-value and suction versus depth.

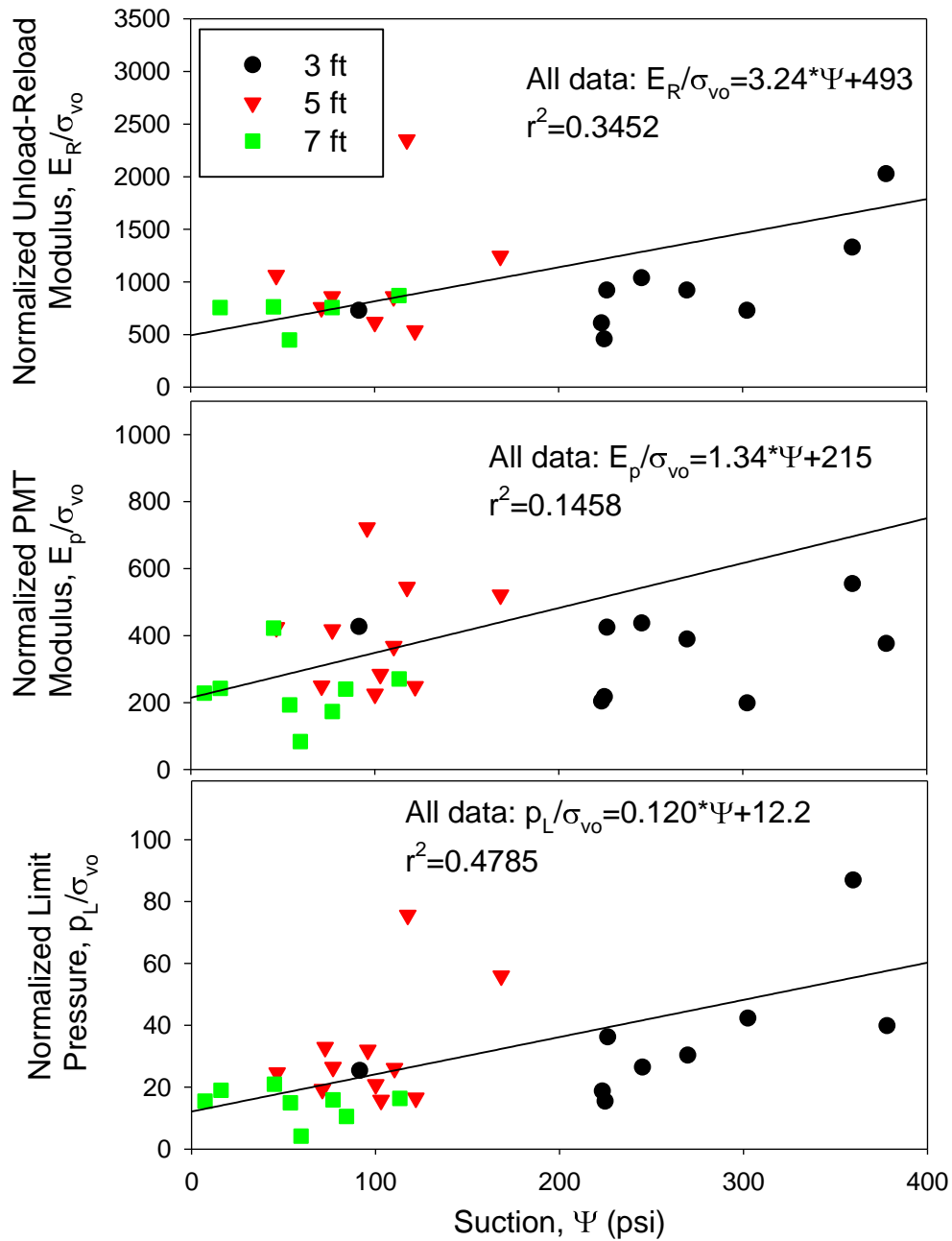


Figure 7. 41. North Base: Normalized PMT limit pressure and moduli versus suction.

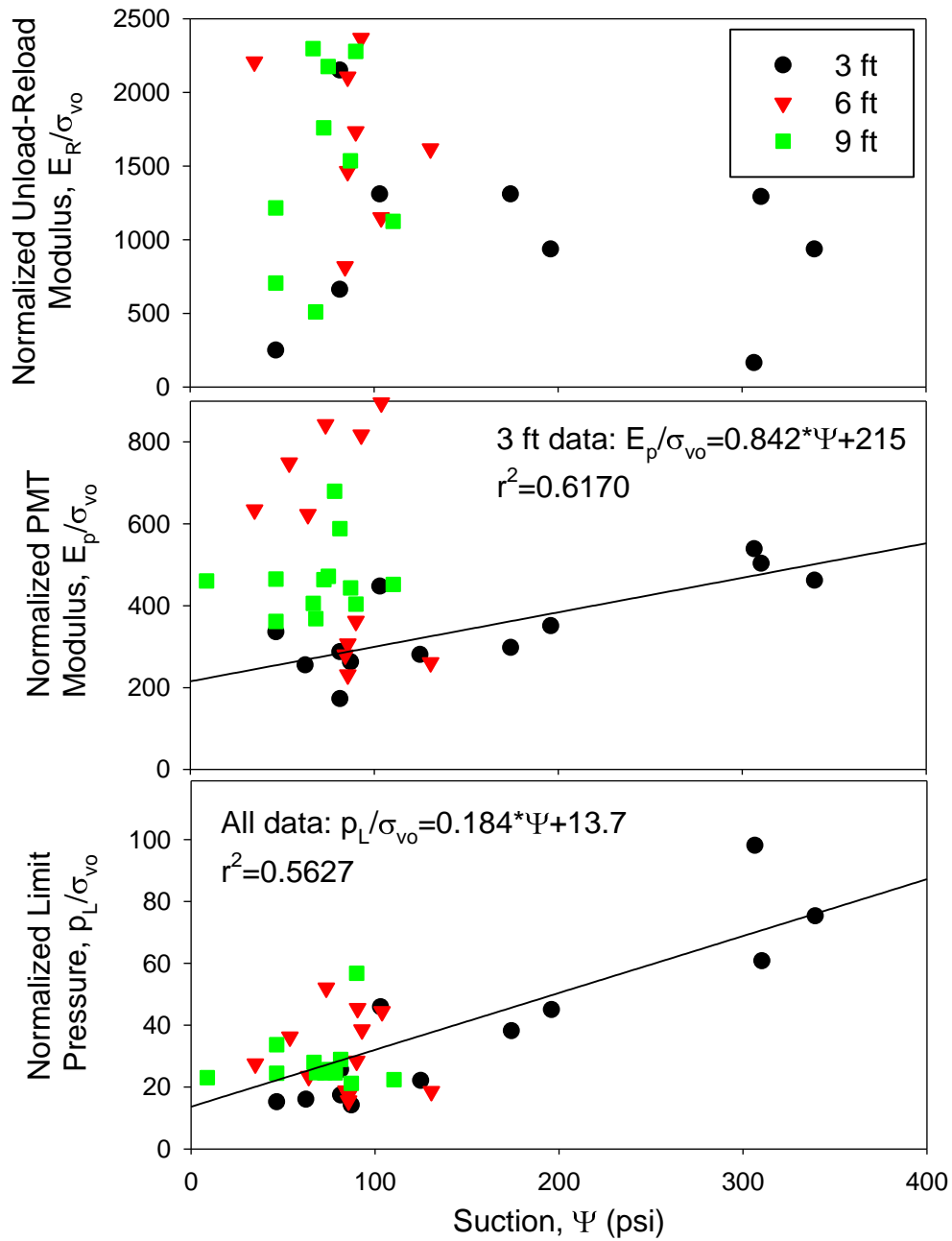


Figure 7. 42. Goldsby: Normalized PMT limit pressure and moduli versus suction.

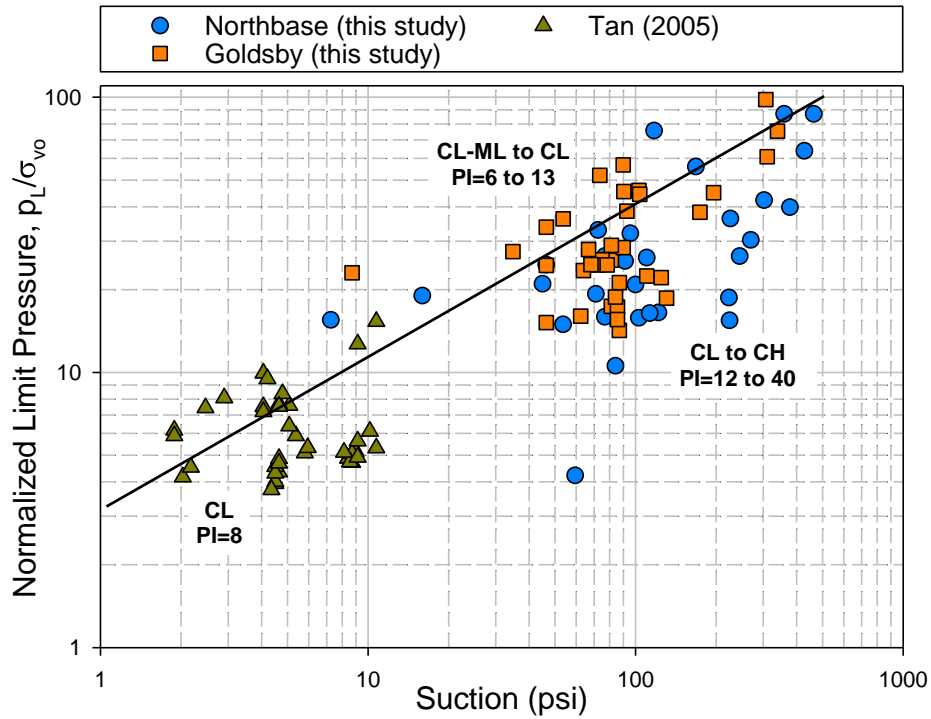


Figure 7. 43. Normalized limit pressure versus suction for North Base and Goldsby test sites and data from Tan (2005).

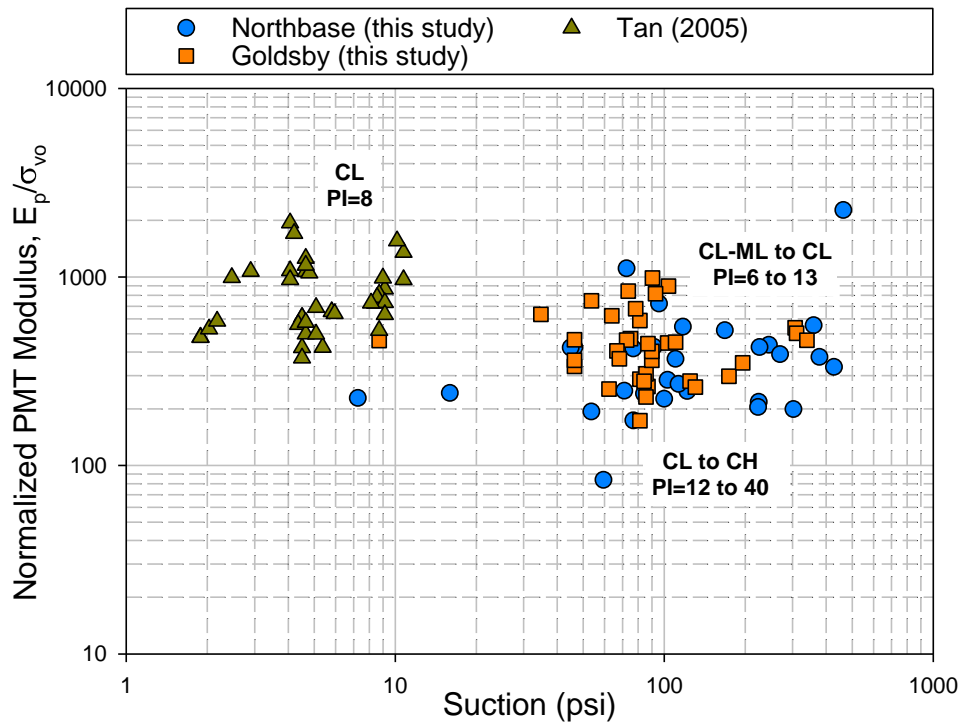


Figure 7. 44. Normalized PMT modulus versus suction for North Base and Goldsby test sites and data from Tan (2005).

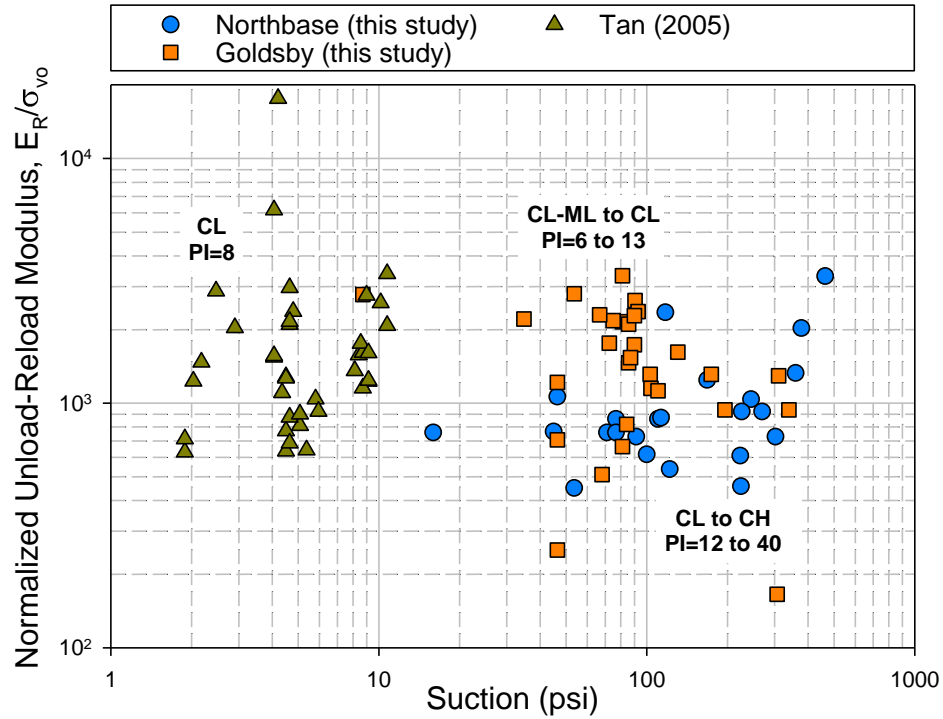


Figure 7. 45. Normalized unload-reload modulus versus suction for North Base and Goldsby test sites and data from Tan (2005).

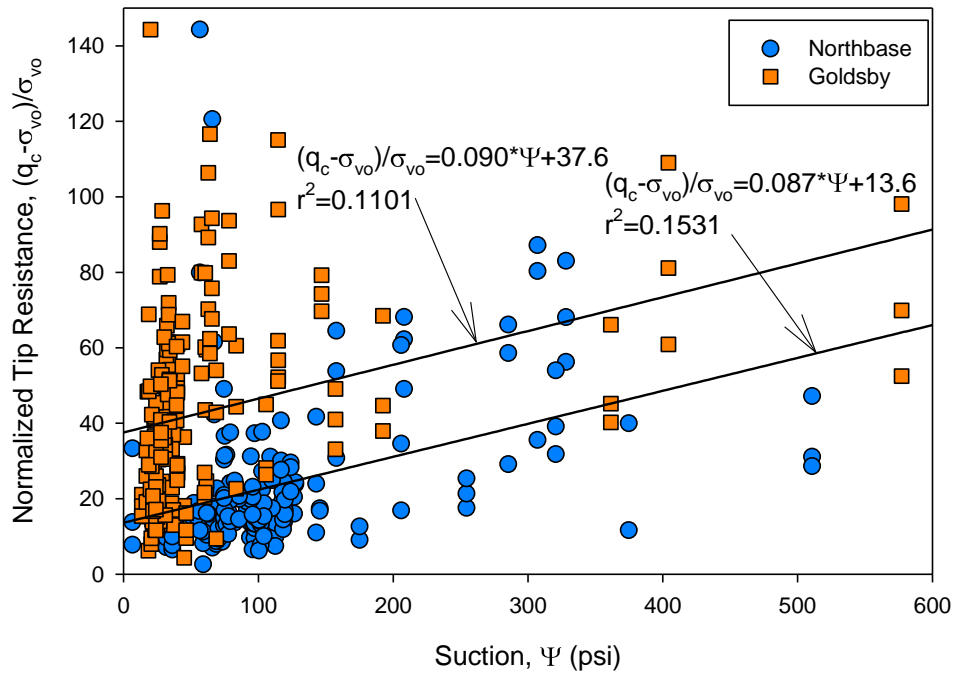


Figure 7. 46. Normalized cone tip resistance versus suction for North Base and Goldsby test sites.

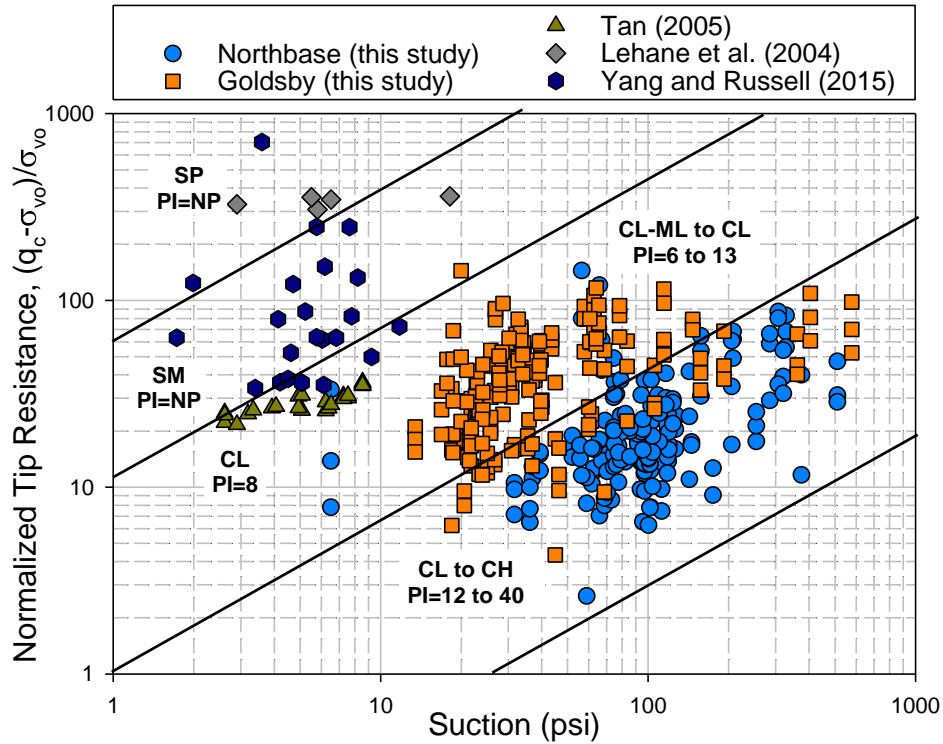


Figure 7. 47. Normalized cone tip resistance versus suction for North Base and Goldsby test sites and data from the literature (Lehane et al. 2004, Tan 2005, Yang and Russell 2015).

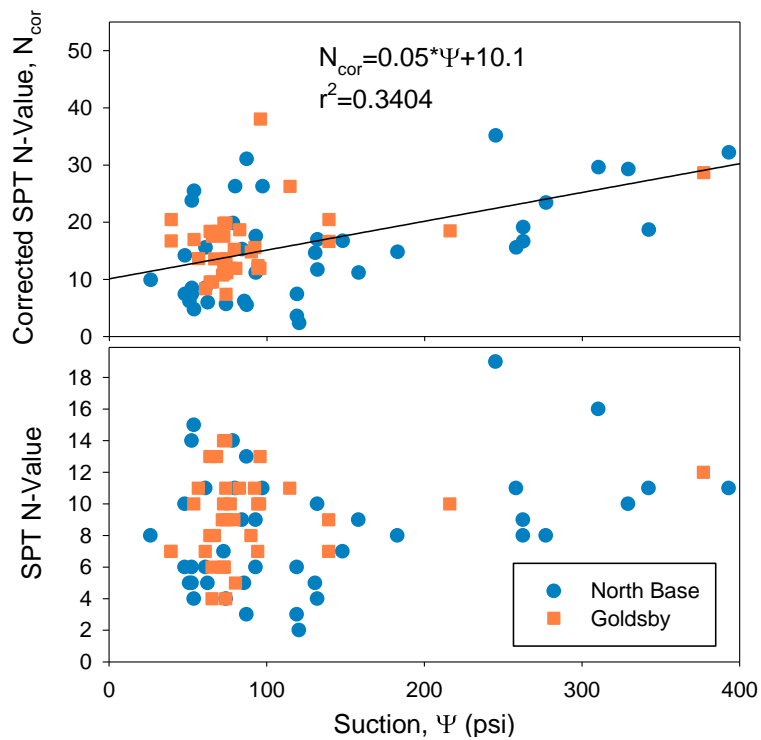


Figure 7. 48. Normalized SPT versus suction.

## **Chapter 8 CONCLUSIONS AND RECOMMENDATIONS**

### **8.1 Summary**

An extensive field investigation was conducted to study the influence of suction on results from the pressuremeter test (PMT), cone penetration test (CPT) and standard penetration test (SPT). A primary goal of this research was to provide recommendations for interpreting these in situ tests in unsaturated soil. To accomplish this, in situ tests were conducted at two field sites with different soil properties over a two-year period. The Goldsby site consists of low plasticity fine grained soil (CL-ML to CL, PI=7-13) while the North Base site contained higher plasticity fine grained soil (CL to CH, PI=12 to 40). The pressuremeter test (PMT), cone penetration test (CPT), and standard penetration test (SPT) were performed in the unsaturated soil profiles at different times of the year when representing different moisture conditions. Measurements of soil suction were taken alongside the in situ test measurements in order to create a database of test results that could be used for interpretation. Soil index property testing and basic strength tests were performed to obtain a complete catalogue of the soil of interest. A review of existing literature was performed to explore possible methods of interpretation that have been used in the past and try to identify useful information that could be used.

The two test sites were instrumented with weather monitoring equipment and sensors capable of measuring variations in the soil moisture content. The variations in soil moisture due to fluctuations in the weather was monitored and modeled using commercially available computer programs, SVFlux and VADOSE/W. Another goal of this project was to evaluate the ability of these programs to predict changes in moisture

content as a function of weather. These programs are basically unsaturated seepage modeling programs that account for weather impacts and groundwater conditions on the moisture flow in the vadose zone.

A simple approach to predicting the influence of suction changes on CPT, PMT and SPT results was presented and based on using empirical correlations developed in this study. Following are some conclusions and recommendations for practice and further study.

## **8.2 Conclusions Regarding Influence of Suction on In Situ Test Results**

The PMT, CPT and SPT parameters determined from standard interpretation of the results were compared to total suction measured at corresponding depths obtained from measurements on samples obtained in the field using a WP4 chilled mirror device. Following are conclusions based on the analysis of the in situ test results in light of suction measurements.

1. At the North Base test site, the measured suctions during the monitoring period varied in the range of 91-463 psi for a depth of 3 feet, 46-168 psi for 5 feet and 7-113 psi for 7 feet. At Goldsby, the measured suctions during the monitoring period varied in the range of 46-339 psi at 3 feet, 35-131 psi at 6 feet, and 9-110 psi at 9 feet. The impact of suction variations on test parameters at both sites was more noticeable for the higher suction ranges at the shallowest 3-foot depth.
2. At both sites, the suction had a profound impact on the PMT limit pressure for total suction in excess of approximately 150 psi, corresponding to a test depth of 3 ft. At both sites for these depths there was a noticeable trend of increasing limit pressure

with increasing suction. For test depths below three feet, where total suction was below 150 psi, a strong trend did not exist. Similar, observations were made with regard to the PMT modulus and unload-reload modulus.

3. There was considerable scatter in the plotted data relating suction to the PMT parameters, particularly for the shallowest depths. It was hypothesized that variations observed in the lower total suction ranges corresponding to depths below 5 feet at both sites may be attributable to variations in osmotic suction since matric suction is likely to be lower. Since variations in osmotic suction may have minimal impact on mechanical behavior, relative to matric suction, this may explain the lack of correlation between suction and test results observed at the lower suction ranges. In addition, the measurement accuracy of the WP4 in the low suction range is more significant.
4. Plots of normalized PMT parameters against suction show expected, albeit weak, correlations for the two test sites. These correlations give a sense of the variation in PMT parameters that might be expected for similar soils under changing suction conditions.
5. Normalized CPT tip resistance was found to correlate with suction particularly for suctions in excess of 150 psi. The scatter is largely attributed to variations in soil characteristics such as % of sand and fines, density, and stress history, as well as the issues related to measuring total suction in the low suction range.
6. Friction ratios were shown to vary considerably at a given depth in response to soil suction variations. For example at a depth of 3 feet at Goldsby, the friction ratio varied from 2% to 6% while for this depth at North Base the friction ratio varied

between 6% and 10%. Such variations will place the soil in different categories using classification schemes based in part on friction ratio. This has implications for using the CPT results for classifying soils based on results in unsaturated soil profiles.

7. Standard penetration test N-values, corrected for overburden were found to correlate reasonably well, particularly for suctions greater than 150 psi. This was similar to the observations for CPT tip resistance and is believed to be affected by the same factors.

It was demonstrated how correlations for PMT, CPT and SPT parameters with suction can be used to roughly predict possible changes in these parameters as a result of suction changes. While these correlations should not be used to determine design parameters, they do allow engineers to develop insight regarding the importance of suction changes. Such information can then be used to decide whether additional lab and/or field testing may be warranted. Or in the case of relatively small projects, more caution can be exercised in develop factors of safety, or load and resistance factors.

### **8.3 Conclusions Regarding Numerical Modeling of Soil Moisture Variations**

This research project studied the ground-atmosphere interaction at two instrumented test sites located at Goldsby and Norman, Oklahoma. Two commercial software packages were used to predict the changes in soil moisture content due to weather conditions over a period of about two years. The volumetric water content values at 3 different depths obtained using VADOSE/W and SVFlux were compared with the recorded field data in order to evaluate the predictive capability of both numerical models. The soil profile at each test site was modeled as a one dimensional soil column

with an element thickness of 1 ft and using hydraulic, thermal (coupled VADOSE/W analysis), and soil-water properties determined from lab tests and estimation functions. Based on the comparison between the measured and predicted volumetric water content (VWC) values, the following conclusions can be drawn:

1. The general trends of the field response to weather changes are reasonably captured by both programs; however, the magnitude of increase or decrease in soil moisture depends upon soil properties, and the numerical model solution.
2. The soil surface layers are strongly affected by any short-term consecutive dry and wet cycles. These layers are also affected by regular rainfall and evaporation events. The predicted VWC fluctuations follow generally the rainfall pattern. The predicted water balance at the soil surface was affected by the way the climate data, such as rainfall precipitation, are utilized in the model, and also by the estimated solar radiation.
3. Allowing water ponding at the surface layer in VADOSE/W gives better volumetric water content predictions.
4. The influence of atmospheric forcing reduces with depth, and this tends to be captured by both models, which provided better predictions at greater depths. In fact, field measurements at depths of 6 ft or lower indicate that the soil displayed reduced moisture content variations. Also, it can be seen that there is a delay of a few days to several weeks in the peaking of soil moisture due to high rainfall as depth increases. This is due to the low hydraulic conductivity of the fine grained soils.

5. Some of the limitations that were encountered while using VADOSE/W and SVFlux, include: the soil-water hysteresis effect was not accounted for, the absence of functions that would account for the presence of desiccation cracks, limitations associated with the ability of modeling several rainfall events at different times in a day and of specifying their intensities.
6. VADOSE/W estimated a greater reduction of soil water storage apparently due to the lack of available built-in functions for determining the leaf area index (LAI) function, as found in SVFlux.
7. For the Goldsby Test site containing a lower plasticity soil profile, SVFlux gave better predictions than VADOSE/W, possibly due to the fact that it uses an adjusted potential evaporation function that matches reasonably with actual field conditions. It also adjusts the time steps and meshing properties when high positive or negative pressure heads develop in the surface layer. However, the moisture variation remains underestimated.
8. For the North Base Test site containing a higher plasticity clayey profile, VADOSE/W gave better predictions than SVFlux, possibly because the latter does not allow water ponding at the surface layer due to high positive gradients.
9. The predictions did not change significantly due to changes in the thermal conductivity and volumetric heat capacity values. However, the saturated conductivity values and soil-water characteristic curves greatly affect the predicted results.
10. The hydraulic conductivity for the materials had the largest impact on predicted values. The unsaturated hydraulic conductivity was defined over several orders of

magnitude while a single or half order magnitude greatly changed the amount of net percolation predicted from a simulation.

11. Neither models predicted percolation accurately. To predict the amount of percolation and infiltration, both programs apply an unsaturated permeability, which depends on the soil suction. This delays the quantity of infiltrated water modeled in unsaturated conditions, where the actual infiltration rate of dry soil is relatively high at the beginning of precipitation and decreases throughout the rainfall event down to soil actual permeability.
12. Generally, the soil at North Base loses and gains water fast during the summer seasons, which contributes to a higher soil water content during the winter. This may be due to the desiccation cracks that develop in the Earth's surface in extreme dry conditions. Goldsby, however, does not show similar significant spatial soil variations compared to North Base, and therefore does not retain a lot of water during the winter.
13. It was noticed that the migration of the wetting front was mostly downward during the summer, and upward during the winter. The upward diffusion of water was generally observed during the winter, where the measured and predicted soil moisture remained high in surface layers, and decreased in deep layers.

#### **8.4 Recommendations**

Following are some general recommendations for interpreting in situ test results in unsaturated soil as well as using unsaturated seepage modeling software for predicting variations in moisture contents in soil profiles.

1. Most importantly, it must be recognized that results of in situ tests in unsaturated soil depend on the moisture and suction conditions at the time the tests are conducted. For example N-values that are routinely used for geotechnical analyses will be higher when dry conditions prevail relative to wetter conditions. One must therefore consider the likelihood of changing moisture conditions in any analyses that involve N-values obtained from unsaturated soils, particularly if conditions are likely to become wetter in the future. The same applies to the interpretation of CPT tip resistance and PMT parameters.
2. Empirical relationships established for the various in situ test parameters provided in this report based on testing at the Goldsby and North Base tests sites can provide some quantitative estimates of what the effect of a change in suction might do to the various test parameters. However, because the data only represent two sites and there is considerable scatter in the data, these relationships should be used with appropriate caution. The data for these test sites encompasses soils that range in classification from low PI clayey silts (CL-ML) to higher PI lean and fat clays (CL, CH) soils. The PI range involved is from about 7 to 32.
3. When in situ tests are conducted in an unsaturated soil profile, it is recommended that soil samples be obtained at various depths to characterize the moisture content and suction in the soil profile. This information can be used to estimate the suction corresponding to particular test depths. In addition, it may be helpful in developing/estimating a soil water characteristic curve (SWCC) in profiles with relatively uniform soil characteristics and variable moisture conditions (and suction). Knowing the suction at the time of testing and using an estimated or measured

SWCC allows for an estimate of the suction change associated with a given change in water content. This can then be used to estimate the impact of the suction change on the in situ test parameters.

4. In cases where it is critical to accurately obtain soil strength and stiffness parameters for design of geotechnical structures over unsaturated soils, it may be necessary to obtain undisturbed samples for additional laboratory testing. This would be especially true if soil conditions were relatively dry when in situ tests were performed and if nearly saturated conditions are possible in the future at the site location. In such a case, the design should consider the fully saturated conditions for design.
5. Predicting future seasonal variations in soil moisture conditions is not trivial. Numerical models provide one possibility; however, in many cases the moisture condition of interest may correspond to the saturated condition. For example, at some sites water tables are known to vary from depths near the surface to 10 or 15 feet below the ground surface. An example is one of the geotechnical test sites on south campus where the water table has been monitored for over 20 years. For most of these years the water table has been below a depth of 10 to 15 feet. However, in about 4 of these 20 years, it has risen to depths of 4 feet or less. Thus, for this site, geotechnical design should be based on saturated conditions since these are likely within the design life of a structure. Faced with an unsaturated soil profile, geotechnical engineers should make the effort to gather information about the water table and potential variations. This would include soil survey available geological information as well as local knowledge of people living and working in an area. If the

potential for a site to become saturated is not known, then the saturated conditions should be the default for design.

6. The use of computer programs to model variations in soil moisture content with depth due to weather variations is a powerful tool for analyzing unsaturated soil profiles. In some cases, such modeling can be useful; however, the models are complex and require numerous input parameters regarding soil and vegetation properties. In addition, the initial soil conditions (moisture content and suction) and expected weather pattern must be established. It is recommended that when these models are used to perform soil moisture predictions based on predicted future weather patterns, they first be calibrated against historical weather patterns and measured soil moisture variations. Such data may not be readily available; however, Oklahoma Mesonet sites are good source of historical weather data and some sites have soil moisture sensors as well. Successful application of these computer programs is highly dependent on use of well-defined soil properties. The models are particularly sensitive to the proper determination of the soil water characteristic curve and unsaturated permeability function. Unfortunately, even if these properties are obtained by carefully conducted testing on high quality samples, some calibration of the models may be needed. This can be attributed to numerous interacting factors, and to the fact that the models do not account for the influence of desiccation cracks and hydraulic hysteresis on the mass flow behavior.

## ACKNOWLEDGEMENTS

The authors are grateful for the financial support of the Oklahoma Department of Transportation and the Oklahoma Transportation Center, and for the logistical support and guidance of ODOT personnel in the Materials and Research Division. In particular, many thanks to Chris Clarke, Stephen Bettis, and John Nicholson from ODOT, for conducting all of the CPT and SPT tests as well as the Shelby tube sampling at the test sites. Thanks is extended to Michael Schmitz from OU for his assistance with manufacturing and maintaining equipment. Graduate students Tommy Bounds and Bo Zhang played a significant role in the field work and laboratory testing near the beginning of the project, for which the authors are grateful. Gratitude is further extended to all of the numerous other graduate and undergraduate students who contributed to the project through laboratory and/or field work.

## REFERENCES

- Benson, C., Bohnhoff, G., Ogorzalek, A., Shackelford, C., Apiwantragoon, P., and Albright, W. (2005): "Field Data and Model Predictions for a Monolithic Alternative Cover Waste Containment and Remediation." ASCE.
- Briaud, J.L. (1992), "The Pressuremeter," A.A. Balkema, Rotterdam, Netherlands.
- Cetin et al. (2004) Standard Penetration Test-Based Probabilistic and Deterministic Assessment of Seismic soil Liquefaction Potential, *Journal of Geotechnical and Geoenvironmental Engineering*
- Chan D Rajeev P., and Kodikara J. (2012): "Grout-Atmosphere Interaction Modeling for Long-term Prediction of Soil Moisture and Temperature." *Canadian Geotechnical Journal*.
- Chao, K., Overton, D. D., and Nelson, J. D. (2010): "Effect of Water Sources on Water Migration in the Vadose Zone. In *Experimental and Applied Modeling of Unsaturated Soils*." ASCE.
- Collins, B.D., Znidarcic, D., (2004): "Stability Analyses of Rainfall Induced landslides." *Journal of Geotechnical and Geoenvironmental Engineering*.
- Cudmani and Osinov 2001 Theoretical investigation of the cavity expansion problem based on a hypoplasticity model *Int. J. Numer. Anal. Meth. Geomech.*, 25 (2001), pp. 473–495

- De Mello, V.F.B. (1971) The standard penetration test. Proc. 4th Pan American Conf. Soil Mechs. Found. Eng., San Juan Puerto Rico, ASCE, v. 1, pp. 1-86.
- Farouki OT., (1982): "Evaluation of Methods for Calculating Soil Thermal Conductivity." CRREL Report.
- Fredlund D.G., Rahardjo H., Soil Mechanics for Unsaturated Soils, John Wiley & Sons, 1993.
- Fredlund, D. G., and Xing (1994): "Equations for the Soil-Water Characteristic Curve." Canadian Geotechnical Journal.
- Fredlund, M.D. Zhang, J.M., Tran, D., and Fredlund, D.G. (2011): "Coupling Heat and Moisture Flow for the Computation of Actual Evaporation" Toronto, Canada.
- Friedman, S. P. (1998): "A saturation Degree-Dependent Composite Spheres Model for Describing the Effective Dielectric Constant of Unsaturated Porous Media", Water Resources.
- GEO-SLOPE International, Ltd. (2007): "GEO-STUDIO VADOSE/W Software Package for Seepage Analysis", Version 7.15, Canada.
- Gitrana, G. Jr., Fredlund, M.D. and Fredlund, D.G. (2006): "Numerical Modeling of Soil-atmosphere Interaction for Unsaturated Surfaces". International Conference on Unsaturated Soils, USA.
- Gofar et al. 2006, Transient Seepage and Slope Stability Analysis for Rainfall-Induced Landslide: A Case Study, Malaysian Journal of Civil Engineering 18 (1): 1-13 (2006)
- Hamilton, J.M., Daniel, D.E., and Olson, R.E. (1981). "Measurement of hydraulic conductivity of partially saturated soils," in *Permeability and Groundwater Contaminant Transport*, ASTM Special Technical Publication No. 746, T.F. Zimmie and C.O. Riggs (Eds.), ASTM, 182-196.
- Hillel (2004) Introduction to environmental Soil Physics. Elsevier Academic Press, Amsterdam, 2004
- Jayarathne, R., Yuen, S. T., Connor, M. A., Pivonka, P., and Pharoah, A. (2012): "A Hydrological Study of On-Site Soil Absorption Systems." ICE-Water Management, USA.
- Johansen, O. (1975): "Thermal Conductivity of Soils." Trondheim, Norway.
- Kang, J. B., Chao, K. C., & Overton, D. D. (2014): "Comparison of 1-D, 2-D, and 3-D Water Migration Study in Expansive Soils", USA.
- Krahn et al. 1989 Effect of soil suction on slope stability at Nothch Hill. Canadian Geotechnical Journal, 26: 269-278
- Kulhawy, F.H. and Mayne, P.W. 1990. Estimating Soil Properties for Foundation Design. EPRI Report EL- 6800, Electric Power Research Institute, Palo Alto: 306 p. www.epri.com
- Lakshmi V, Jackson TJ, Zehrhuhs D (2003): "Soil Moisture–Temperature Relationships: Results from Two Field Experiments." Hydro Process, USA.
- Lehane et al. 2004, Seasonal Dependence of In Situ Test Parameters in Sand Above the Water Table, Geotechnique, 54, No. 3, 215-218
- Liu, C. and Muraleetharan, K.K. (2011a). "A Coupled Hydraulic-Mechanical Elastoplastic Constitutive Model for Unsaturated Sands and Silts. Part I: Formulation," *International Journal of Geomechanics*, ASCE

- Liu, C. and Muraleetharan, K.K. (2011b). "A Coupled Hydraulic-Mechanical Elastoplastic Constitutive Model for Unsaturated Sands and Silts. Part II: Integration, Calibration and Validation," *International Journal of Geomechanics*, ASCE
- Mansell R. S., Liwang, L. R. Ahuja, and Bloom S. A. (2002): "Adaptive Grid Refinement in Numerical Models for Water Flow and Chemical Transport in Soil: A Review", *Vadose Zone Journal*, USA.
- Miller, G.A. 2012 Use of the Yield Pressure to Interpret Pressuremeter Results in Unsaturated soil, *Unsaturated Soils: Research & Applications*, Sydney, 2012
- Miller, G.A. and Muraleetharan, K.K. (1998), "In Situ Testing in Unsaturated Soil," Proc. of UnSat'98, 2nd International Conference on Unsaturated Soils, Beijing, China, Aug. 27-30.
- Miller, G.A. and Muraleetharan, K.K. (2000), "Interpretation of Pressuremeter Tests in Unsaturated Soil," Geotechnical Special Publication No. 99, Geo-Institute of ASCE, pp. 40-53.
- Miller, G.A. and Muraleetharan, K.K. (2000), "Interpretation of Pressuremeter Tests in Unsaturated Soil," Geotechnical Special Publication No. 99, Geo-Institute of ASCE, pp. 40-53.
- Miller, G.A. and Tan, N.K. (2008), "At-rest lateral stress from pressuremeter tests in an unsaturated soil calibration chamber," Proc. of the 3rd International Conference on Site Characterization, Taipei, Taiwan, April 2008, Taylor and Francis Group, p. 621-626.
- Miller, G.A., Muraleetharan, K.K., Tan, N.K. and Lauder, D.A. (2002) "A Calibration Chamber for Unsaturated Soil," Proc. of UNSAT 2002, 3rd International Conference on Unsaturated Soils, Recife, Brazil, March 10-14, A.A. Balkema, Lisse, Netherlands, Vol. 2, pp. 453-457.
- Muraleetharan, K. K., Yang, Y., Salehipour, S. A., and Dhavala, M .D. 1998, "Cavity expansion theories for unsaturated soils", Technical report, School of Civil Engineering and Environmental Science, University of Oklahoma, Norman, 1998.
- Muraleetharan, K.K., Ravichandran, N. and Taylor, L.M. (2003). "TeraDysac: TeraScale Dynamic Soil Analysis Code," *Computer Code*, School of Civil Engineering and Environmental Science, University of Oklahoma, Norman, Oklahoma.
- Muraleetharan, K.K., Ravichandran, N., Miller, G.A. and Tan, N.K. (2003) "Fully Coupled Analyses of Pressuremeter Tests in Unsaturated Soils," Proc. 2nd UNSAT-Asia 2003, Unsaturated Soils – Geotechnical and Geoenvironmental Issues, Osaka, Japan, Published by Organizing Committee of UNSAT-ASIA 2003, pp. 313-318.
- Odorico, P., Laio, F., Ridolfi, L., (2006): "Vegetation Patterns Induced by Random Climatic Fluctuations." *Geophys. Res.*
- Oklahoma Highway Department (OHD) (1969). Engineering Classification of Geologic Materials – Division 3. Prepared by Research and Development Division of OHD in cooperation with U.S. Bureau of Public Roads, 422 p.
- Overton, D.D., Chao, K.-C., and Nelson, J.D. 2006. Time rate of heave prediction for expansive soils. Proceedings of the ASCE Conference GeoCongress 187. pp. 162–168.

- Park, K.D., Fleming, I.R., (2006): "Evaluation of a Geosynthetic Capillary Barrier." Geotextiles and Geomembranes, USA.
- H.L. Penman 1948 Natural evaporation from open water, bare soil, and grass Proc. R. Soc. London. Ser. A, 193 (1032) (1948), pp. 120–146
- Pereira et al. 2003, Numerical Modeling of Unsaturated Soils in a Pressuremeter Test, 16<sup>th</sup> ASCE Engineering Mechanics Conference, July 16-18, 2003, University of Washington, Seattle
- Russell and Khalili 2006 On the Problem of Cavity Expansion in Unsaturated Soils, Computational Mechanics 37: 311-330
- Russell et al. 2011 Development of a New Calibration Chamber for Conducting Cone Penetration Tests in Unsaturated Soils, Canadian Geotechnical Journal, Vol. 48, Issue 2, pp.314-321
- Jayarathne et al. (2012) A Hydrological Study of On-Site Absorption Systems, Water Management Vol. 166 (1), January 2013
- SoilVision Systems Ltd. (2009): "SoilVision Software. Saskatoon, Saskatchewan", Canada.
- Tan, N. 2005 Pressuremeter and Cone Penetrometer Testing in a Calibration Chamber with Unsaturated Minco Silt, Thesis, University of Oklahoma, May 2005
- Tan, N., Miller, G.A., and Muraleetharan, K.K. (2003) "Preliminary Laboratory Calibration of Cone Penetration in Unsaturated Silt," Proc. Soil-Rock America 2003, 12th Pan-American Conference on Soil Mechanics and Geotechnical Engineering/39th U.S. Rock Mechanics Symposium, Cambridge, Mass., June 22-26, VGE, Essen, Germany, pp. 391-396.
- Tan, N.K. and Miller, G.A. (2005), "Pressuremeter Testing in a Calibration Chamber with Unsaturated Minco Silt," Proc. 16th International Conference on Soil Mechanics and Geotechnical Engineering, Osaka, Japan, Sept. 12-16, 2005.
- Tratch, D., (1996): "Moisture Uptake within the Root Zone." M.S. Thesis, University of Saskatchewan, Saskatchewan, Canada.
- United States Department of Agriculture (USDA). [Web Soil Survey](http://websoilsurvey.sc.egov.usda.gov), <http://websoilsurvey.sc.egov.usda.gov>, via the National Resources Conservation Service (NRCS).
- Van Genuchten, M. (1980): "A Closed-Form Equation for Predicting the Hydraulic Conductivity of Unsaturated Soils." Soil Science Society of America Journal, USA.
- Vanapalli, S., and Adem, H. 2013. A simple modeling approach for estimation of soil deformation behaviour of natural expansive soils using the modulus of elasticity as a tool. Poromechanics V, pp. 1695–1704. doi:10.1061/9780784412992.
- Vanapalli SK and Oh WT (2010): "A Model for Predicting the Modulus of Elasticity of Unsaturated Soils Using the Soil-Water Characteristic Curve." International Journal of Geotechnical Engineering, USA.
- Verseghy 1991 Class—A Canadian land surface scheme for GCMS. I. Soil model, International Journal of Climatology, Vol. 11 (2), March 1991
- Vesic, A.S. (1972). "Expansion of Cavities in Infinite Soil Mass." Journal of the Soil Mechanics and Foundation Division, ASCE, 98(3), 265-290.
- Vesic, A.S. (1972). "Expansion of Cavities in Infinite Soil Mass." Journal of the Soil Mechanics and Foundation Division, ASCE, 98(3), 265-290.

- White, Harlon E., Wolf, Dale D. (1995): "Controlled Grazing of Virginia's Pasture."  
Virginia Tech, USA.
- Whitman, R. V., and Liao, S. (1985). "Seismic design of gravity retaining walls." Proc.  
8th World Conf. on Earthquake Engrg., San Francisco, Vol. III, 533–540
- Wilson et al. 1994 Coupled soil-atmosphere modelling for soil evaporation, Canadian  
Geotech Journal, 1994, 31(2): 151-161
- Wilson, G.W., (1990): "Soil Evaporative Fluxes for Geotechnical Engineering Problems".  
Ph.D. Thesis, University of Saskatchewan, Canada
- Yu, H. S., and Mitchell, J. K. (1998). "Analysis of cone resistance: Review of methods."  
Journal of Geotechnical. And Geoenvironmental. Engineering. ASCE, 124(2),  
140–149.
- Zamara, K.A. (2013): "In situ Performance and Numerical Analysis of Lining Systems for  
Waste Containment." Doctor of Engineering Thesis, Loughborough University,  
England.